國立臺灣大學生命科學院生化科學研究所
博士論文

Graduate Institute of Biochemical Sciences

College of Life Science

National Taiwan University

Doctoral Dissertation

雙專一性磷酸水解酶對於血管內皮細胞發炎反應的調控
The Role of Inducible Dual-Specificity Phosphatases in
Vascular Endothelial Inflammation

許淑芳
Shu-Fang Hsu

指導教授：孟子青 博士
Advisor: Tzu-Ching Meng, Ph.D.

中華民國104年7月
July, 2015

誌謝

　　終於所有的努力在這一刻化為實現，本論文得以完成要感謝許多人的付出。首先感謝指導教授孟子青老師多年來的鼓勵與悉心教導，讓我自研究助理的生活中感受到進行研究的樂趣，進而有勇氣挑戰不可能的任務–完成博士學位訓練。這一路走來，高低起伏，感謝孟老師的從不放棄，訓練我邏輯思考與進行科學研究的能力。所有的教誨我謹記於心，並努力實踐，在此致上最深切的感謝。同時感謝王寧老師、裘正健老師、張鎮東老師以及邱繼輝老師在口試期間對本論文提供寶貴的意見與指導，讓我獲益良多，也讓本論文更趨完善。

　　另外，感謝余榮熾老師在我迷惘的時候，耐心的傾聽與適時的指引，讓我不致半途而廢；感謝鄭敬楓醫師以臨床角度所提供的諸多寶貴意見；感謝張美玲醫師無私地傳授動物實驗以及組織切片染色的種種知識。還要感謝每一位曾經共事的同伴們，儘管在我的研究生涯中留下深淺不一的足跡，但這一步步都陪伴了我的成長。感謝同為開國元老的銘佛、翊偉、英志，很開心大家都有各自的一片天；感謝親密戰友艾伶、鈺斌、信傑與瓔祝，沒有你們本論文無法完成；感謝寒風送暖的瑞霞、李函、紋寧、彥錞與 Abirami；感謝提供各式討論的陳博–怡昀；感謝彥蓉的超齡熟成所提供的心靈交流；感謝書柔給予的叮嚀與關懷。更要感謝 Elfy 的美圖與 Deepa 費心修訂我的英文寫作。要感謝的人太多，無法一一細數，在此一鞠躬感謝所有人對於我的鼓勵與照顧。

　　最後，感謝我親愛家人的支持，無論是原生家庭或是現在的家人。尤其感謝我的另一半 Jack，在我求學的這段期間無怨無悔的付出與包容，身兼數職的幫我完成所有大大小小的事，也是我最重要的支柱。感謝一對可愛兒女–Allen & Ann，有了你們讓我更有動力為了明天而努力。

　　謹以此論文獻給我最敬愛的父親許敏夫先生。

<div align="right">

許淑芳

104 年 7 月於中研院生化所

</div>

摘要

腫瘤壞死因子α (Tumor necrosis factor-α, TNF-α)是一種多功能性的促進炎症細胞激素，在感染所造成的細胞損傷中對於先天免疫系統(innate immune system)有著重要的調控作用。同時 TNF-α刺激血管內皮細胞(vascular endothelial cell)會藉由複雜的細胞內信息調控造成細胞發炎反應甚至是動脈粥狀硬化(atherothrombosis)以及發炎性疾病(inflammatory disease)的發生。在發炎反應過程中，TNF-α啟動一連串細胞激酶(kinase)的訊息傳遞，活化核轉錄因子(nuclear factor κB, NF-κB)，促進細胞表面黏著分子(adhesion molecule)的表現以及後續白血球細胞(leukocyte)的附著。在此過程中，人們對於細胞激酶的功能有相對的了解，目前我們並不清楚蛋白質磷酸水解酶(protein phosphatase)是否同樣參與調控 TNF-α造成的訊息傳遞。在本論文中，我們探討雙專一性磷酸水解酶(dual specificity phosphatases, DUSPs)在 TNF-α調控內皮細胞發炎反應中的角色扮演。藉由偵測基因表現的 mRNA 含量，在人類內皮細胞株 EAhy926 中我們找到一群經 TNF-α誘導表現的 DUSPs。我們也發現 TNF-α誘導表現的細胞黏著分子(intercellular adhesion molecule-1, ICAM-1)在經微小 RNA 干擾(RNAi)造成的 DUSP6 基因剔除實驗中，表現量明顯下降；後續單核球(monocyte)在內皮細胞表面附著的數量也隨之下降，顯示 DUSP6 在調控發炎反應有正向的作用。我們接著利用人類初代臍靜脈內皮細胞(human umbilical vein endothelial cells, HUVECs)來研究調控機制。結果顯示，在 TNF-α刺激的HUVEC 細胞中，DUSP6 藉由抑制細胞外訊號調節激酶 (extracellular signaling-regulated kinase, ERK)的活性而促進 NF-κB 的轉錄活性以及其下游 ICAM-1 的表現。在小鼠的血管組織切片染色(immunohistochemistry, IHC)中，我們也觀察到 ICAM-1 的表現量在 DUSP6 基因剔除($Dusp6^{-/-}$)小鼠低於野生型小鼠，證實 DUSP6 確實扮演促進血管內皮發炎的角色。此外，相較於野生型小鼠的敏感，DUSP6 基因剔除小鼠對於脂多醣內毒素(lipopolysaccharide, LPS)所造成的敗血性肺部損傷有較佳的抵禦能力。這些結果證實了 DUSP6 有促進內皮細胞發炎反應及發炎相關病理過程的新穎角色，顯示其作為治療發炎性疾病藥物開發的新契機。

關鍵詞: 腫瘤壞死因子α、內皮細胞發炎反應、雙專一性磷酸水解酶、細胞表面黏著分子、白血球、敗血症、肺部損傷

ABSTRACT

Tumor necrosis factor alpha (TNF-α) is a proinflammatory cytokine that directs multiple events of the innate immune system during infection of cell injury. Meanwhile, TNF-α activates a diverse array of signaling pathways in vascular endothelial cells (ECs), leading to the inflammatory phenotype that contributes to the pathogenesis of atherothrombosis and inflammatory diseases. In a typical inflammatory response, TNF-α initiates a kinase-dependent signaling cascade, which activates nuclear factor (NF)-κB, leading to inducible expression of adhesion molecules and recruitment of leukocytes. In contrast to the known function of kinases in this context, it is not clear whether protein phosphatases participate in the regulation of TNF-α signaling. In the present study, we have investigated the role of dual specificity phosphatases (DUSPs) in TNF-α-induced inflammatory response. Using human endothelia, EAhy926, for screening of mRNA levels, we identified a group of DUSPs to be inducibly expressed under the TNF-α stimulation. Among them, DUSP6 functioned as a prominent positive regulator of the inflammatory response, evidenced by a clear decrease of TNF-α-induced expression of intercellular adhesion molecule-1 (ICAM-1) and a drastic reduction of monocyte adhesion on the surface of endothelia when DUSP6 was ablated via RNAi. We further examined the underlying mechanism controlled by DUSP6 using primary human umbilical vein endothelial cells (HUVECs). Our data showed that inducible DUSP6 promoted canonical NF-κB-dependent increase of adhesion molecules exclusively through inhibition of extracellular signaling-regulated kinase (ERK) in TNF-α-stimulated human ECs. The role that DUSP6 plays in facilitating endothelial inflammation in aorta and vein was confirmed by in vivo experiments using *Dusp6*$^{-/-}$ mice. Furthermore, genetic deletion of Dusp6 significantly reduced the susceptibility to inflammatory responses in a mouse model of lung sepsis. These results are the first to demonstrate a novel function of DUSP6 in the regulation of vascular inflammatory response and the underlying mechanism through which DUSP6 promotes endothelial inflammation-mediated pathological process. Our findings suggest that inhibition of DUSP6 holds great potential for the treatment of inflammatory diseases.

Keywords: tumor necrosis factor-α (TNF-α), endothelial inflammation, dual specificity phosphatases 6 (DUSP6), intercellular adhesion molecule-1 (ICAM-1), neutrophil, sepsis, lung injury
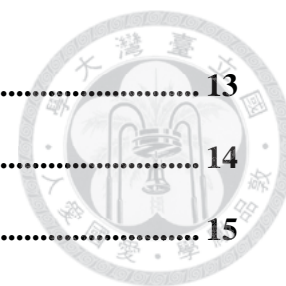
ABBREVIATIONS

CD	cluster of differentiation
DUSPs	dual specificity phosphatases
ECs	endothelial cells
ERK	extracellular signaling-regulated kinase
HUVECs	human umbilical vein endothelial cells
ICAM-1	intercellular adhesion molecules 1
IHC	immunohistochemistry
IκB-α	inhibitor of κB α
IKK	IκB kinase
IVC	inferior vena cava
JNK	*c-jun* N-terminal kinase
KIM	kinase interacting motif
LPS	lipopolysaccharide
MAPKs	mitogen-activated protein kinases
MEK	MAP kinase/ERK kinase
MKP	MAP kinase phosphatase
MPO	myeloperoxidase
NF-κB	nuclear factor κB
p38 MAPK	p38 MAP kinase
PP4	protein phosphatase 4
TBP	TATA-binding protein
TNF-α	tumor necrosis factor α
VCAM-1	vascular cell adhesion molecule 1

TABLE OF CONTENTS

List of identified phosphoproteins altered in DUSP6-ablated HUVECs

LIST OF FIGURES

LIST OF SCHEME

LIST OF TABLES

CHAPTER 1: INTRODUCTION

1.1 The endothelium function and endothelial inflammation

As a semipermeable barrier lining on the internal surface of blood vessels, the endothelium regulates vascular tone as well as the exchange of fluids and solutes between the blood and interstitial space, thus maintaining physiological homeostasis.[1] Vascular endothelium also exerts anticoagulant, antiplatelet, antiproliferation of smooth muscle cells and fibrinolytic properties. Therefore, a healthy endothelium not only controls vasodilation, but also suppresses vascular inflammation, thrombosis, and hypertrophy.[2]

In addition, the endothelium is an integral component of host innate immune response. Vascular endothelia are uniquely situated to detect the presence of pathogens within the vasculature as they are in direct and constant contact with the circulating blood.[3, 4] When microbial infections or tissue injury occurs, a large amount of damage-associated molecular patterns (DAMPs) are released and they stimulate the pattern-recognition receptors (PRRs) on immune cells. The activated immune cells release excessive amount of pro-inflammatory cytokines to induce nearby endothelial cells inflammation, causing the up regulation of cell adhesion molecules on endothelial cell surface to recruit and activate leukocytes at sites of inflammation.[5] Although the leukocyte adhesion cascade ultimately helps to clear the infectious agents and to repair damaged tissues, during disseminated infections or inflammatory disorders the

activation of the endothelium at sites remote from the inciting source can lead to the dysregulation of a variety of microvascular functions, causing organ failure and subsequent death.[6, 7]
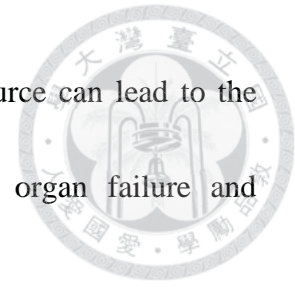
Tumor necrosis factor (TNF)-α is a pro-inflammatory cytokine, which is synthesized primarily by immune cells such as macrophages, dendritic cells, monocytes and T lymphocytes, to induce endothelial inflammation.[8] Accumulating evidence suggests that TNF-α plays a pivotal role in disrupting macrovascular and microvascular circulation both in vivo and in vitro, which causes endothelial inflammation and vascular dysfunction and eventually contributes to pathogenesis of many chronic inflammatory disease.[9] Anti-TNF-α treatment has been applied to a range of inflammatory conditions, including rheumatoid arthritis, ankylosing spondylitis, inflammatory bowel disease and psoriasis, highlighted the role of TNF-α in infectious diseases.[10] Understanding the molecular machine in how TNF-α regulates endothelial inflammatory response may provide further opportunity to treat inflammatory diseases.

1.2 TNF-α signaling in regulating endothelial inflammation

1.2.1 TNF-α induces cell adhesion molecules expression on endothelium

TNF-α is a pleiotropic cytokine which initiates a wide range of diverse cellular responses including cell survival, activation, differentiation and proliferation, and cell

death.[8] Upon interaction with receptors on the endothelium, TNF-α induced signal transduction initiates pro-inflammatory changes, including expression of adhesion molecules and increase of leukocyte adhesion for transendothelial migration.[8, 10] Endothelial cells respond to TNF by releasing chemokines and displaying in a distinct temporal, spatial and anatomical pattern adhesion molecules, including E-selectin, intercellular adhesion molecule-1 (ICAM-1) and vascular cell adhesion molecule-1 (VCAM-1). It has been well-characterized that endothelial ICAM-1 plays an essential role in neutrophil recruitment at the site of acute inflammation.[11-14] ICAM-1 is a cell surface glycoprotein of 505 amino acids with a molecular weight ranging from 76 to 114 kDa, depending upon extent of tissue-specific glycosylation.[15, 16] It belongs to immunoglobulin superfamily and is characterized by the presence of five extracellular Ig-like domains, a hydrophobic transmembrane domain and a short cytoplasmic domain of 28 amino acids.[17] ICAM-1 functions as a ligand for β2 (CD11/CD18)-integrin and associates with lymphocyte function-associated antigen 1 (LFA-1, CD11a/CD18) and macrophage-1 antigen (Mac-1, CD11b/CD18) on neutrophils through Ig-like domain1 and 3 respectively.[18, 19] Due to a strong bond between ICAM-1 and β2-integrin, TNF-α-induced ICAM-1 facilitates neutrophil forming firm adhesion to the endothelium and further migrate across the endothelial barrier.[20]

1.2.2 TNF-α activates canonical NF-κB pathway to regulate ICAM-1 expression

TNF-α regulates ICAM-1 expression mainly through activating canonical nuclear factor (NF)-κB-dependent transcriptional pathway.[21] The NF-κB family of transcription factors consists of RelA (p65), c-Rel, RelB, NF-κB1, and NF-κB2. Activation of the canonical NF-κB pathway results in the degradation of bound inhibitor of NF-κB (IκB)-α, IκB-β, or IκB-ε in the cytoplasm, which leads to the translocation of NF-κB to the nucleus to mediate transcriptional events.[22] Analysis of the 5' flanking region of *ICAM-1* gene revealed two NF-κB binding sites (upstream, -533 bp and downstream, -223 bp).[23] Site-directed mutagenesis and gel supershift assays demonstrated that ICAM-1 expression requires NF-κB p65 (RelA) binding to the downstream NF-κB site of the *ICAM-1* promoter.[24, 25] These findings were further supported by the identification of consensus motifs on the promoter regions of *ICAM-1* gene that is specifically targeted by the NF-κB dimers.[26]

1.2.3 TNF-α-induced MAPKs activation in endothelial inflammation

Except activating of NF-κB pathway, TNF-α stimulation also activates mitogen-activated protein kinases (MAPKs) pathway in vascular endothelium.[27] The MAPKs family includes the p38 MAPK, c-Jun N-terminal kinase (JNK) and the extracellular signaling-regulated kinase (ERK). It has been proposed that crosstalk
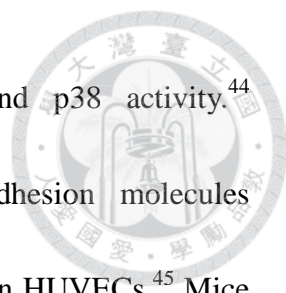
between individual MAPK and NF-κB pathways may play a key role in TNF-α-dependent pro-inflammatory responses.[27, 28] Some studies have implicated a role of p38 MAPK and JNK in regulating TNF-α-induced ICAM-1 expression.[29-31] However, ERK seems to function as negative regulator in NF-κB mediated ICAM-1 expression. One report showed that constitutively active ERK pathway inhibited NF-κB-driven transcription, suggesting a negative role of ERK in regulating NF-κB activity.[32] A subsequent study demonstrated that suppression of ERK signaling enhanced NF-κB-dependent transcription,[33] further suggesting that ERK inactivates NF-κB pathway. Importantly, experiments using human endothelium have identified an anti-inflammatory function of ERK, one in which it suppresses the expression of ICAM-1 by inhibiting NF-κB activity in TNF-α signaling.[34] Collectively, these findings indicate that inhibitory effect of ERK on NF-κB-directed transcriptional activation would be essential in the context of TNF-α-mediated endothelial inflammation, as evidenced by inducible ICAM-1 expression and neutrophil recruitment. Therefore, we assume that under TNF-α signaling there should have some phosphatases activate to inhibit ERK activity, thus promoting TNF-α-induced endothelial inflammation.

1.3 Role of DUSPs in regulating MAP kinase and cell inflammation

MAP kinases activation requires phosphorylation on a threonine and tyrosine residue at TXY motif located on the activation loop of kinase domain. Dual specificity phosphatases (DUSPs) is a subclass of the protein tyrosine phosphatase (PTP) superfamily,[35] which dephosphorylate the critical phosphotyrosine and phosphothreonine residues within MAP kinase.[36] The expression of DUSPs is induced by growth factors and cellular stress, and is restricted to a subset of tissue types and localized to different subcellular compartments.[37] Due to the catalytic activation of DUSPs after tight binding of its amino-terminal to the target MAP kinase, some DUSPs have high selective for inactivating distinct MAP kinase isoforms and hence are also referred to as MAP kinase phosphatase (MKPs).[38] DUSPs regulate activity of MAPK through TXY motif dephosphorylation as well as represent particularly important negative regulators.[39] In addition to their dephosphorylating capacity, DUSPs serve to anchor or shuttle MAP Kinases and control their subcellular localization.[40, 41]

Some members of DUSPs have been reported to regulate MAP kinase as well as cell inflammatory response. In study of macrophages, DUSP1/MKP1 serves to limit the inflammatory reaction by inactivating JNK and p38, thus preventing multiorgan failure caused by exaggerated inflammatory responses.[42, 43] DUSP2 is a positive regulator of inflammatory cell signaling and cytokines functions. DUSP2 deficiency in macrophages

leads to increased JNK activity but impairment of ERK and p38 activity.[44] Overexpression of DUSP4/MKP2 enhances TNF-α-induced adhesion molecules expression (ICAM-1 and VCAM-1) and protects against apoptosis in HUVECs.[45] Mice lacking the DUSP4/MKP2 gene had a survival advantage over wild-type mice when challenged with intraperitoneal lipopolysaccharide (LPS) or a polymicrobial infection via cecal ligation and puncture.[46] DUSP10/MKP5 protects mice from sepsis-induced acute lung injury.[47] Mice lacking DUSP10/MKP5 displayed severe lung tissue damage following LPS challenge, characterized with increased neutrophil infiltration and edema compared with wild-type (WT) controls. Phosphorylation of p38 MAPK, JNK, and ERK were enhanced in DUSP10/MKP5-deficient macrophages upon LPS stimulation.
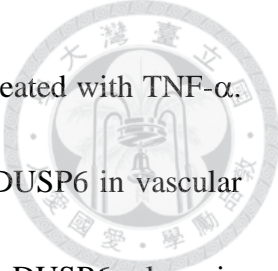
Collectively, above findings suggest that DUSPs may participate in regulating cell inflammation and immune response by controlling MAP kinase intensity and duration. Therefore, DUSPs are promising drug targets for manipulating MAPK-dependent immune response, to suppress infectious diseases or inflammatory disorders.[48] However, except DUSP4 (MKP2) which was performed in HUVECs, most of functional characterizations were performed in macrophages not in endothelium. We need further studies to know the function of DUSPs in regulating endothelial inflammation.

1.4 Study the role of DUSPs targeting on ERK to regulate endothelial inflammation
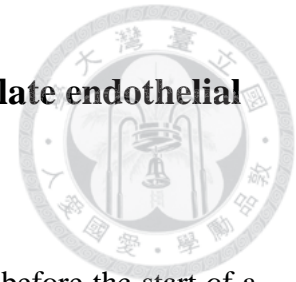
It was found that transiently activated ERK is down-regulated before the start of a relatively slow process of NF-κB-dependent ICAM-1 expression in endothelium stimulated with TNF-α.[49] These results suggest that the immediate response of ERK signaling must be switched off in order to promote vascular inflammation through the canonical NF-κB pathway. We hypothesize that DUSPs, in particular ERK-specific cytoplasmic phosphatase DUSP6/MKP-3,[38] might target the TEY motif in the activation loop of ERK and dephosphorylate both Thr and Tyr residues, hence down-regulating ERK activity in endothelium undergoing pro-inflammatory reaction. In fact, DUSP6 has been identified as an early response gene whose expression is rapidly induced by various extracellular stimuli or stresses.[50, 51] Therefore, it is likely that DUSP6 is transiently expressed in endothelium exposed to TNF-α. If the initial ERK activity could be terminated by endothelial DUSP6, NF-κB-dependent transcription for ICAM-1 expression could be switched on, allowing TNF-α-induced neutrophil adhesion to commence.

This study investigated whether and how DUSP6 might promote expression of ICAM-1 on the surface of endothelium under pro-inflammatory stimulation. We examined the mechanism through which DUSP6 controls the crosstalk between ERK

and NF-κB signaling pathways in primary human endothelial cells treated with TNF-α.

Using knockout mice, we inspected further the *in vivo* function of DUSP6 in vascular

inflammation, and explored the regulatory role that endothelial DUSP6 plays in

pulmonary neutrophil recruitment during experimental sepsis induced by LPS, a process

depending on the interaction between ICAM-1 and β2 (CD11/CD18)-integrin.[52, 53]

CHAPTER 2: MATERIALS AND METHODS
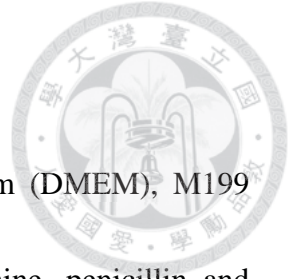
2.1 Reagents
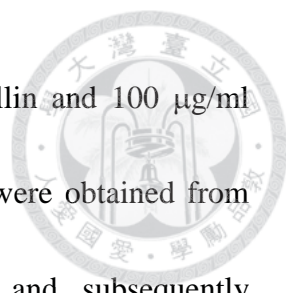
Collagenase, Low glucose Dulbecco's modified Eagle's medium (DMEM), M199 medium, RPMI-1640 medium, fetal bovine serum (FBS), glutamine, penicillin and streptomycin were purchased from Gibco. Endothelial cell growth supplements (ECGS) and Neon Transfection System was purchased from Invitrogen. Heparin, gelatin, actinomycin D, cycloheximide and LPS (from E. coli serotype O55:B5) were purchased from Sigma. TNF-α was purchased from R&D system. PD184352 was purchased from Biovision. PD98059 and U0126 were purchased from Cell signaling. BAY-117082 was purchased from Calbiochem. Small interfering RNA oligonucleotides (siRNA) were purchased from Dharmacon Thermo Scientific.

For stable isotope labeling by amino acids in cell culture (SILAC): SILAC DMEM medium was from Gibico. Sequence grade trypsin and Lys-C protease were from Promega. TiO$_2$ bead was from GL Sciences, Japen. L-^{13}C$_6$^{15}N$_4$-arginine (Arg10), L-^{13}C$_6$-lysine (Lys6), iodoacetamide (IAM) and PT66 antibody were from sigma. 4G10 agarose bead was from Millipore. C$_{18}$StageTip was from PROXEON.

2.2 Cell culture and transient transfection

2.2.1 Culture conditions for each cell line
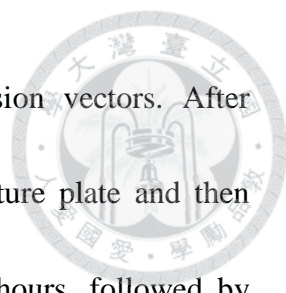
The EAhy926 endothelial cells (ATCC) were maintained in low glucose DMEM,

supplemented with 10% FBS, 2 mM glutamine, 100 U/ml penicillin and 100 μg/ml

streptomycin. Human umbilical vein endothelial cells (HUVECs) were obtained from

collagenase-digested umbilical veins as described previously[2] and subsequently

maintained in M199 medium, supplemented with 20% FBS, 25 U/ml heparin and 30

μg/ml ECGS, 2 mM glutamine, 100 U/ml penicillin and 100 μg/ml streptomycin in

gelatin-coated plates. HUVECs between the third and the fifth passage were used for

experiments. U937 cells (ATCC) were cultured in RPMI-1640 medium, supplemented

with 10% FBS.

2.2.2 Transient cell transfection
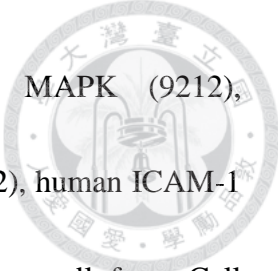
For direct exposure to TNF-α or co-treatment with chemical inhibitors (actinomycin

D, cycloheximide, PD184352, PD98059, U0126, BAY-117082), ECs were plated in

medium containing FBS for 16 hours and then serum-starved for 6 hours before

treatment. Small interfering RNA oligonucleotides (siRNA) or expression plasmids

were delivered to ECs by electroporation using Neon Transfection System (Invitrogen)

according to manufacturer's instructions. Briefly, ECs ($2x10^5$ cells per reaction for

siRNA transfection or $3.5x10^5$ cells per reaction for expression vector transfection) were

suspended in the Resuspension Buffer R (included with Neon Kits) together with the

siRNA duplexes targeting DUSPs (siRAN oligonucleotides obtained from Dharmacon,

and their sequences are shown in Table 2) or DUSP6 expression vectors. After

electroporation, cells were seeded in a single well of 12-well culture plate and then

incubated in normal culture condition without antibiotics for 16 hours, followed by

serum deprivation for an additional 6 hours prior to stimulation with inhibitor and/or

TNF-α. For re-expression of the wild type form, C/S mutant form or KIM mutant form

of DUSP6 in HUVECs in which endogenous DUSP6 was ablated, shRNA constructs

bearing 3'-UTR sequence of DUSP6 (from the National RNAi Core Facility, Academia

Sinica, Taiwan) were tested initially by lentivirus-mediated infection. According to the

knockdown efficiency of DUSP6 by shRNA constructs, a specific clone

(TRCN0000355536) was chosen. Due to the poor viability of virus-infected HUVECs,

an alternative approach of transfection was established. The sequence of selected

shRNA clone targeting the DUSP6 3'-UTR was used as a template for synthesis of

siRNA duplexes (Dharmacon), which were ultimately applied to

electroporation-mediated transient transfection for knocking down only endogenous

DUSP6 but not re-expressed DUSP6.

2.3 Immunoblotting and antibodies

Aliquots of total lysates (15-20 μg) were subjected to SDS-PAGE and transferred to

nitrocellulose membranes, and then incubated with antibodies recognizing caspase8

(9746), caspase3 (9662), phospho-p38 MAPK (9211), p38 MAPK (9212), phospho-JNK (9251), JNK (9525), phospho-ERK (9101), ERK (9102), human ICAM-1 (4915), phospho-NF-κB (3033), NF-κB (3034), IκB-α (9242) above all from Cell Signaling; VCAM-1 (sc-13160) and ERK5 (sc-1284) from Santa Cruz; Tubulin (T5168), Flag (F3165) both from Sigma and DUSP6 (a gift from Stephen Keyse and described previously[54]). The specific signals were visualized by ECL Reagents (GE Healthcare).

2.4 RNA extraction and quantitative real-time PCR

Total RNA was isolated from EAhy926 cells or HUVECs using High Pure RNA Isolation Kit (Roche) according to manufacturer's instructions. The cDNA was synthesized from total RNA with Transcriptor reverse transcriptase (Roche) using oligo(dT)15 primer (Promega) according to manufacturer's instructions. The mRNA expression levels were quantified by real-time PCR using a LightCycler instrument (Roche) with the SYBR Green PCR Master Mix (Qiagen) in a one-step reaction according to manufacturer's instructions. Primers (sequences are shown in Table 1) were designed as described previously.[55] The sequences for the house keeping gene, hydroxymethylbilane synthase (HMBS), were 5'-AGTATTCGGGGAAACCT-3' (forward) and, 5'-AAGCAGAGTCTCGGGA-3' (reverse). The mRNA levels of target genes were normalized to the relative amounts of HMBS.
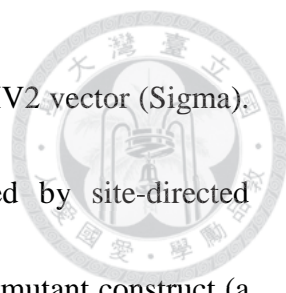
2.5 Monocyte adhesion assay

Endothelial-monocyte adhesion assay was performed following the protocol described previously.[56] HUVECs (2×10^5 cells per reaction for siRNA transfection or 3.5×10^5 cells per reaction for expression vector transfection) were transiently transfected with siRNA or expression vectors by electroporation, and then subsequently seeded on a 24-well plate for overnight. Once reaching to confluence, cells were treated with TNF-α (10 ng/ml) for 4 hours. At the meantime, monocytic U937 (4.5×10^5) were labeled with 10 μg/ml of BCECF-AM (Invitrogen) at 37 ℃ for 30 minutes in dark, subsequently washed twice with PBS to remove free dye, and then suspended in HUVEC culture medium ready for use. Fluorescence dye-labeled U937 cells were added onto a monolayer of TNF-α-treated HUVECs and then incubated for 1 hour. Non-adherent U937 cells were removed by two gentle washes with penol-red free M199 medium (Gibco). The fraction of HUVEC-associated U937 cells was quantified by a fluorescence analyzer (Infinite F200, Tecan) using excitation and emission wavelength at 485 and 535 nm, respectively. The images of adherent U937 cells on HUVEC monolayer were captured using a fluorescence microscope (BX50, Olympus).

2.6 DUSP6 expression plasmids and luciferase reporter constructs
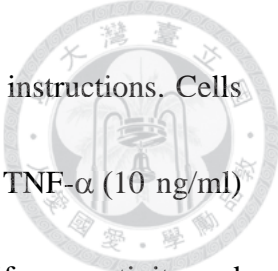
The full-length DUSP6 cDNA was obtained by reverse transcription of total mRNA

isolated from HUVECs and subcloned into an N-terminal pFlag-CMV2 vector (Sigma).

The phosphatase dead C293S mutant of DUSP6 was generated by site-directed

mutagenesis according to the standard procedure. The DUSP6 KIM mutant construct (a

gift from Stephen Keyse) was generated as described previously[41] and then subcloned

into an N-terminal pFlag-CMV2 vector. The ICAM-1 and VCAM-1-luciferase reporter

construct were generated by insertion of NF-κB binding element to a pGL4.27

[luc2P/minP/Hygro] firefly luciferase vector (Promega), which contains a multiple

cloning region for insertion of a response element of interest upstream of a minimal

promoter and the luciferase reporter gene luc2P. The DNA duplex sequences

5'-TGGAAATTCC-3' located at -187 bp of the *ICAM-1* promoter, and

5'-GGGTTTCCCCTTGAAGGGATTTCCC-3' located at -72 bp of the *VCAM-1*

promoter, were synthesized with a flanking restriction enzyme site KpnI/BglII. The

KpnI/BglII digested-DNA duplex was then inserted into KpnI/BglII digested-pGL4.27

vector. All expression clones were verified by sequencing.

2.7 NF-κB reporter assay

HUVECs (3.5×10^5 cells per reaction in a single well of 12-well culture plate) were

transiently transfected with 0.5 μg of the reporter plasmid and 0.025 μg of the pRL-null

vector (Renilla internal control reporter vector, Promega) by electroporation using the

Neon Transfection System (Invitrogen) according to manufacturer's instructions. Cells were seeded on a 12-well plate for overnight and then treated with TNF-α (10 ng/ml) for 4 hours. An aliquot of total lysates was subjected to specific luciferase activity and was analyzed using the Dual-Luciferase Reporter Assay System (Promega) with a luminometer (Luminoskan Ascent, Thermo Scientific).
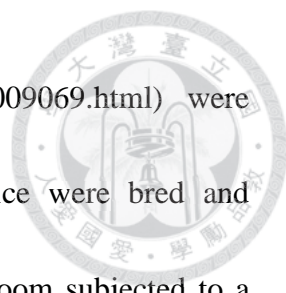
2.8 RNA extraction and Gene expression profiling

Total RNA was isolated from HUVECs using High Pure RNA Isolation Kit (Roche) according to manufacturer's instructions. 300 ng total RNA were used for cDNA synthesis, labeled by in vitro transcription followed by fragmentation according to the manufacturer's suggestion (GeneChip Expression Analysis Technical Manual rev5, Affymetrix). 11 μg labeled samples were hybridized to Human Genome U133 Plus 2.0 Array (Affymetrix) at 45℃ for 16.5 hours. The wash and staining were performed by Fluidic Station-450 and the array were scanned with Affymetrix GeneChip Scanner 7G.

2.9 Animal studies

2.9.1 Mice housing

DUSP6-null mice (B6;129X1-$Dusp6^{tm1Jmol}$/J,[57] stock number 009069, backcrosses number=1) and their appropriate control mice (B6129SF2/J, stock number 101045,

recommended by the manufacture http://jaxmice.jax.org/strain/009069.html) were

purchased from The Jackson Laboratory (Bar Harbor, ME). Mice were bred and

maintained in a specific pathogen-free (SPF) animal facility in a room subjected to a

12-hours light/dark cycle and maintained at constant temperature (22℃) and humidity

(55%). Mice received normal rodent chow and water ad libitum. All experimental

procedures were performed in accordance with the guidelines of the Institutional

Animal Care and Utilization Committee (IACUC) of Academia Sinica.

2.9.2 Genotyping

The genomic DNA was extracted from the tail tissue of mouse by the KAPA Express

Extract kit (KAPK Biosystem) according to the manufacturer's instructions. A common

forward primer A (5'-CCT TCT CCT GCA GCT CGA C-3', #12227), the wild type

mouse reverse primer B (5'-ATG GCA GAT TCG ATG TGT GA-3', #12226) and

$Dusp6^{-/-}$ mouse reverse primer C (5'-CCG CTT CAG TGA CAA CGT C-3', #12228,

catalog numbers provided by The Jackson Laboratory) were used for standard PCR in a

mixture of the KAPA2G Robust HotStart reagent (KAPK Biosystem) according to

manufacturer's instruction.

2.9.3 Tail vein injection with TNF-α

In order to induce endothelium inflammatory response, male mice (10-12 weeks old) were injected with 5 μg/kg of TNF-α (diluted in PBS (Sigma) to a total volume of 100 μl) into the lateral tail vein. Control mice were injected with an equal volume of PBS. After 16 hours, mice were sacrificed. Vessels (containing aorta and inferior vena cava (IVC)) were removed and processed for immunohistochemical staining.

2.9.4 Immunohistochemstry staining and image quantification

Organs from TNF-α-, LPS- or PBS-treated mice were harvested, rinsed in ice-cold PBS, fixed in 4% paraformaldehyde and then embedded in paraffin. For immnunohistochemistry staining, tissue sections were blocked with 10% goat serum (005-000-001, Jackson Immunoresearch) for 2 hours and then incubated for overnight with anti-mouse ICAM-1 antibodies (14-0542) or isotype control (14-4321, both from eBioscience) at a dilution of 1:50. After three washes in PBS, the samples were treated with goat anti-rat IgG secondary antibody (A9037, Sigma) at a dilution of 1:200 for 1.5 hours at room temperature. Bound antibody was detected using a DAB kit (Vector Laboratories). Sections were counterstained with hematoxylin and eosin (H & E, both from Sigma-Aldrich), dehydrated, treated with xylene substitute (Fluka) and subsequently mounted with entellan (Merck). Images of the whole aorta and IVC were

captured using a microscope (BX50, Olympus) with 60x magnification, and images of

lung were captured with 40x magnification. For quantification, images were processed

and analyzed using software Image-Pro Plus 6.0 (Media Cybernetics).
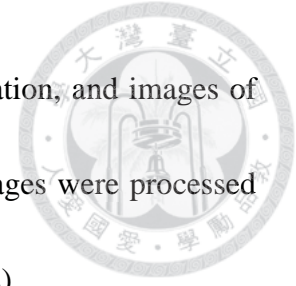
2.9.5 LPS-induced experimental sepsis and neutrophil adoptive transfer

For induction of the experimental sepsis, male mice (5-8 weeks old) were injected

intraperitoneally with 0.1 mg/kg of TNF-α or 10 mg/kg of LPS in a total volume of 200

μl. After 24 hours, mice were sacrificed. Lung were isolated and processed for

myeloperoxidase (MPO) determination by MPO-specific enzyme-linked

immunosorbent assay (ELISA; HyCult Biotechnology) according to manufacturer's

instruction. For neutrophil adoptive transfer, male mice (10-12 weeks old) were utilized.

The endogenous polymorphonuclear leukocytes (PMNs, mainly neutrophils) of

recipient mice were removed by irradiation (9 Gy) exposure. After recovery for 24

hours, 1×10^7 purified neutrophils in PBS (total volume 200 μl) were adoptively

transferred to recipient mice by intravenous injection, followed by intraperitoneal

injection with 10 mg/kg of LPS in a total volume of 200 μl. After 4 hours, mice were

sacrificed. Lung were isolated and processed for H&E staining, immunohistochemistry

staining with anti-ICAM-1 antibody and MPO assay.

2.9.6 Neutrophil isolation from mouse blood

The procedure of neutrophil isolation was performed according to the protocol described previously.[58] In brief, whole blood from adult donor mouse was collected in tubes containing EDTA and then mixed with an equal volume of PBS. The cells were separated onto a three-layer Percoll gradient of 78, 69, and 52% Percoll diluted in PBS through centrifugation at 1500x *g* for 35 min at room temperature. The fraction of neutrophils at the 69/78% interface were harvested and washed with PBS containing 1% BSA once. The residual red blood cells were then eliminated by RBC Lysis Buffer (Becton Dickinson) at 37℃ for 3 min. After two times of wash with PBS containing 1% BSA, the purified neutrophils were suspended in PBS and used immediately. The purity and viability of purified neutrophils was confirmed by Ly6G/CD11b double staining and trypan blue (Sigma) exclusion, respectively.

2.9.7 Flow cytometry analysis

Cells were incubated with Ly6G-FITC (11-5931), CD11b-PerCP-Cyanine5.5 (45-0112) or isotype control antibodies (11-4031 and 45-4031, all from eBioscience) against cell surface antigens in the dark for one hour on ice. Cytofluorimetry was performed with a BD Calibur cytometer (Becton Dickinson) equipped with FL1 (533/30), FL3 (650LP) filters. Neutrophils were identified by characteristic forward/side

scatter and Ly6G/CD11b positivity. Data were analyzed and presented using the BD

CellQuest Pro software (Becton Dickinson).

2.10 Exploring DUSP6-mediated phosphorylation network in TNF-α-activated HUVECs by MS analysis

2.10.1 Sample preparation for MS/MS analysis

HUVECs were cultured in ready-to-use SILAC DMEM medium containing ^{13}C labeled arginine (L-$^{13}C_6$$^{15}N_4$-arginine, Arg10) and lysine (L-$^{13}C_6$-lysine, Lys6) amino acids for five cell division cycles before performing DUSP6 knockdown. 24 hours after knocking down, cells were treated with TNF-α for 1.5 hours then harvested and lysed in 1% NP40 buffer.

2.10.2 In-solution protein digestion

Equal amount (3 mg) of total cell lysates from normal (light) and DUSP6-KD (heavy) HUVECs were combined into one pool. Lysate mixture was reduced with 1 mM dithiothreitol (DTT) for 1 hour at room temperature (RT) and alkylated with 5.5 mM iodoacetamide (IAM) for 1 hour at RT in the dark. Excess detergent, DTT, and IAM were removed by Amicon Ultra-4 10K centrifugal filter unit, and buffer was exchanged to 8 M urea. Proteins were digested for 3 hours with the protease Lys-C (1:100

enzyme/substrate) at 37°C. Sample was diluted with 50 mM ammonium bicarbonate to reduce urea concentration less than 2 M, and trypsin (1:100) was added for further digestion at 37°C overnight. The peptide mixture was acidified by adding trifluoroacetic acid (TFA) to a final concentration of 2.5%.

2.10.3 TiO$_2$ beads enrichment

Twenty percent of digested peptide pool was mixed with loading buffer (1:6 v/v, 30 mg/ml 2,5 dihydrobenzoic acid and 80% acetonitrile in water) and incubated with 5 mg TiO$_2$ beads for 30 minutes at RT for twice. TiO$_2$ beads were washed with washing solution I (30% acetonitrile/3% TFA) and II (80% acetonitrile/0.1% TFA). Phosphopeptides were eluted 2 times with 100 μl elution solution I (1% of NH$_4$OH in 20% acetonitrile) and 1 time with 100 μl elution solution II (1% of NH$_4$OH in 40% acetonitrile). Eluates were dried and then resuspended in 1% acetonitrile/0.5% TFA.

2.10.4 Immunoprecipitation for phosphotyrsine peptide enrichment

Eighty percent of digested peptide pool was dried and resuspended in IP buffer (50 mM MOPS pH 7.2, 10 mM sodium phosphate, 50 mM NaCl). Peptide mixture was incubated with PT66 and 4G10 agarose beads at 4°C overnight. Beads were washed 3 times with IP buffer, followed by 2 washes with water. Phosphotyrsine peptides were

eluted by adding two times 50 µl of 0.15% TFA for 10 min at room temperature. Eluted

peptides were then desalted and concentrated on C_{18}StageTip and resuspended in 1%

acetonitrile/0.5% TFA.
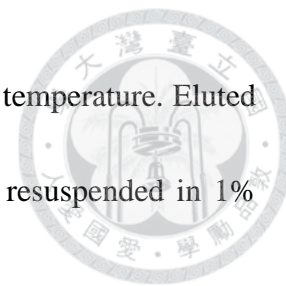
2.10.5 Shotgun proteomic identifications

NanoLC−nanoESi-MS/MS analysis was performed on a nanoAcquity system (Waters,

Milford, MA) connected to an LTQ-Orbitrap XL hybrid mass spectrometer (Thermo

Fisher Scientific, Bremen, Germany) equipped with a nanospray interface (Proxeon,

Odense, Denmark). Peptide mixtures were loaded onto a 75 µm ID, 25 cm length C18

BEH column (Waters, Milford, MA) packed with 1.7 µm particles with a pore width of

130 Å and were separated using a segmented gradient in 120 min from 5% to 40%

solvent B (acetonitrile with 0.1% formic acid) at a flow rate of 300 nl/min and a column

temperature of 35°C. Solvent A was 0.1% formic acid in water. The mass spectrometer

was operated in the data-dependent mode. Briefly, survey full scan MS spectra were

acquired in the orbitrap (*m/z* 350–1600) with the resolution set to 60,000 at *m/z* 400 and

automatic gain control (AGC) target at 10^6. The 10 most intense ions were sequentially

isolated for CID MS/MS fragmentation and detection in the linear ion trap (AGC target

at 7000) with previously selected ions dynamically excluded for 90 s. Ions with singly

and unrecognized charge state were also excluded. For TiO_2 enriched samples,

"multistage activation" at 97.97, 48.99, and 32.66 Thomson (Th) relative to the precursor ion was enabled in all MS/MS events to improve the fragmentation spectra of the phosphopeptides. All the measurements in the orbitrap were performed with the lock mass option for internal calibration.

2.10.6 Data analysis

Phosphopeptides with false discovery rate under 1% were identified and quantified by MaxQuant (version 1.2.2.5). Only high confident phosphopeptides with the localization probability of phosphorylation (pSTY) greater than 0.75 from the two enrichment methods were retained and a list of phosphoproteins from the phosphopeptide results was generated for functional annotation. The proteomics data analyzed by LTQ-Orbitrap XL hybrid mass spectrometer were performed by the Academia Sinica Common Mass Spectrometry Facilities located at the Institute of Biological Chemistry.

2.11 Statistical analysis

Values were expressed as means ± SD. Statistical significance was determined using a Student's t-test. A P-value <0.05 was considered significant.

CHAPTER 3: RESULTS

3.1 TNF-α treatment triggers MAPKs transient activation rather than cell apoptosis in endothelial EAhy926 cells

Before studying the signaling pathway between DUSPs and MAPKs in TNF-α stimulated endothelium, we first eliminated cell apoptosis as the consequence of TNF-α stimulation in endothelial EAhy926 cells, which were established by fusing primary human umbilical vein endothelial cells (HUVECs) with a thioguanine-resistant clone of A549 epithelia. We first checked caspase 8 (initiator caspase) and caspase3 (effector caspase) activation in EAhy926 cells exposed to TNF-α. The protein level of pro-caspase 8 and 3 maintained intact and no cleaved form of caspases has been observed in 13 hours of TNF-α treatment (Fig. 1A). We also performed flow cytometry analysis to check the cell cycle in TNF-α-treated EAhy926 cells and there was no obvious apoptotic cells appeared in sub-G1 group (Fig. 1B). These preliminary tests removed the possibility that TNF-α triggers the cell death signaling in endothelial EAhy926 cells.

Then we checked mitogen-activated protein kinases (MAPKs) activity changes by monitoring phosphorylation levels of MAPKs in TNF-α-treated EAhy926 cells. Exposed to TNF-α, p38 MAPK and JNK were transiently activated whereas the activity of ERK activity was not significantly changed in EAhy926 cells (Fig. 2). At resting state, p38 MAPK and JNK were not activated whereas ERK has basal level activity.

Upon stimulation with TNF-α, p38 MAPK was activated at 5 minutes and then the phosphorylation level of p38 decreased gradually with the time course. JNK activity was peaked at 15 minutes and then diminished to basal level.

In order to know the mechanism by which TNF-α regulates MAPKs activity, we next applied actinomycin D (transcription inhibitor) and cycloheximide (translation inhibitor) to investigate the underling mechanism of MAPKs inactivation. As shown in Fig. 3, actinomycin D and cycloheximide pretreatment sustained the phosphorylation level of all MAPKs in TNF-α-treated EAhy926 cells, indicating that TNF-α regulates the activity of MAPKs through transcriptional and translational regulation mechanisms.

3.2 DUSPs are inducibly expressed in endothelial cells exposed to TNF-α and function as MKPs

In order to know whether some DUSPs were inducibly expressed as negative feedback regulators to down regulate MAPKs signaling in endothelial cell exposed to TNF-α, the mRNA levels of 12 DUSP genes, characterized as MKPs, were measured by quantitative real-time PCR over a course of five hours after TNF-α stimulation. These 12 DUSPs were assigned to three groups based upon the magnitude and pattern of inducible mRNA expression. Phosphatases in the first group, including DUSP6, DUSP8 and DUSP16, were rapidly induced in a transient manner and peaked at 1-2 hours of

29
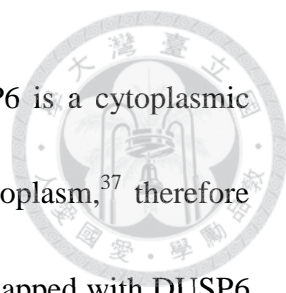
TNF-α exposure (Fig. 4A). DUSP10 was the only phosphatase in the second group whose mRNA levels gradually accumulated and remained at high levels for 5 hours after stimulation (Fig. 4B). The DUSPs in these two groups showed at least a 5-fold induction after treatment, and were, therefore, classified as genes with significant up-regulation in response to TNF-α. In contrast, the mRNA levels of the remaining eight DUSPs, which were listed in the third group, did not change or were only marginally increased (<3.5-fold) after treatment (Fig. 4C). Additional runs of real-time PCR further confirmed the induction of four DUSPs (DUSP6, 8, 10 and 16) in cells exposed to TNF-α (Fig. 4D).

Next we investigated whether these four TNF-α-induced DUSPs function as MKP. So we examined the phosphorylation levels of MAPKs in response to RNAi-mediated knockdown of each DUSP separately. Sufficient knockdown effect of specific siRNA targeting on DUSP6, 10 and 16 were confirmed by quantitative real-time PCR to check the residual mRNA level of each DUSP (Fig. 5A). Although DUSP8 knockdown by RNAi was not complete, the effect on regulating JNK and ERK dephosphorylation by DUSP8 was confirmed (Fig. 5C). Through RNA interference technique, DUSP6 and DUSP8 were identified as JNK and ERK phosphatases in EAhy926 cells stimulated with TNF-α, while DUSP16 showed a marginal effect and DUSP10 was not involved in MAPKs regulation (Fig. 5B-5E).

3.3 DUSP6 is involved in TNF-α-induced endothelial inflammation by regulating intercellular adhesion molecules 1 (ICAM-1) expression

Inflammation is a dominant physiological consequence of endothelia exposed to TNF-α. TNF-α induces endothelial inflammatory response by regulating cell adhesion molecules, such as ICAM-1, VCAM-1 and E-selectin, expression on cell surface through NF-κB pathway. Previous studies reported that ERK may function as a negative regulator in cell adhesion molecules expression by inactivating NF-κB pathway. We next examined whether TNF-α-induced DUSPs may also participate in regulation of endothelial inflammation through targeting ERK activity. For this, ICAM-1 expression in TNF-α-treated EAhy926 cell has been checked by immunoblotting (Fig. 6A). In EAhy926 cells, ICAM-1 expression was induced at 2 hours post TNF-α stimulation and the protein was gradually accumulated with the time progression. In order to investigate the role of inducible DUSPs in regulating inflammatory response, we examined the levels of TNF-α-induced ICAM-1 in response to RNAi-mediated knockdown of each DUSP separately. Interestingly, ablation of DUSP6 led to a decrease of ICAM-1 (Figure 6B), whereas knockdowns of DUSP8, 10, or 16 did not (Figure 6C-6E). These results suggest DUSP6 may regulate ICAM-1 expression through down-regulating ERK activity. Although DUSP8 can function as ERK phosphatase (Figure 5C), knockdown of DUSP8 did not affect ICAM-1 expression. The different regulation of ICAM-1 maybe

due to the different subcellular localization of phosphatase, DUSP6 is a cytoplasmic phosphatase and DUSP8 is found in both the cell nucleus and cytoplasm,[37] therefore DUSP8 may regulate different population of ERK which is not overlapped with DUSP6 regulated ERK population.

3.4 Inducible DUSP6 regulates TNF-α-directed inflammatory responses in primary endothelial HUVECs
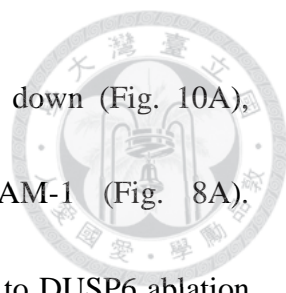
Focusing on the potential role of inducible DUSP6 in TNF-α-induced inflammation, we used primary human umbilical vein endothelial cells (HUVECs) as a physiologically relevant model for further investigations. The induction of DUSP6 was first confirmed with quantitative real-time PCR by monitoring mRNA level of Dusp6 gene in TNF-α-stimulated HUVECs (Fig. 7A). We observed that the mRNA level of Dusp6 was increased and peaked at 1 hour of TNF-α exposure. The protein levels of DUSP6 and ICAM-1 were also checked in parallel by immunoblotting. Upon stimulation, DUSP6 was obviously increased in 1 hour after TNF-α treatment and then ICAM-1 started to express at 2 hours of TNF-α exposure (Fig. 7B).

To evaluate the role of DUSP6 in regulating inflammatory response, we next examined the levels of TNF-α-induced ICAM-1 in HUVECs transfected with DUSP6 siRNA. Interestingly, ablation of DUSP6 led to significant suppression of ICAM-1,

which was otherwise robustly expressed between 4 and 6 hours of TNF-α treatment

(Figure 8A). To validate the specific function of DUSP6 in TNF-α signaling, we

performed a rescue experiment by ectopically expressing a phosphatase-active, wild

type (WT) form of DUSP6 in HUVECs, in which endogenous DUSP6 had been

knocked down. As depicted in Figure 8B, when the WT form of DUSP6 was

re-expressed in RNAi-ablated HUVECs, there was a significant increase in the level of

ICAM-1 in response to TNF-α stimulation. Previously, phosphatase activity of DUSP6

has been found to be required for inhibition of ERK.[59] To further investigate the

importance of DUSP6 enzymatic activity in regulating TNF-α-induced ICAM-1

expression, we re-expressed the phosphatase-dead mutant form of DUSP6 (catalytic

Cys293 replaced by Ser, the C/S mutant) in DUSP6 ablated HUVECs and checked

ICAM-1 level. As shown in Fig. 9, in contrast to restoration of TNF-α signaling by the

WT form of DUSP6, the C/S mutant form of DUSP6, which was robustly accumulated

in cells leading to increased activity of endogenous ERK, did not promote the

expression of ICAM-1. These results suggest that DUSP6-promoted inflammatory

response in HUVECs depends on its catalytic activity.

We further examined whether endothelial leukocyte interaction, which is primarily

mediated by the accumulation of adhesion molecules on the surface of endothelium,[60] is

regulated by DUSP6. Clearly, the binding of U937 monocytes to TNF-α-exposed

HUVECs was inhibited when DUSP6 in HUVECs was knocked down (Fig. 10A), presumably due to the decreased levels of endothelial ICAM-1 (Fig. 8A). Consistently, a loss of endothelial leukocyte interaction in response to DUSP6 ablation was restored by re-expression of the WT form of DUSP6 (Fig. 10B). Together these findings suggested that inducible DUSP6 might play a key role in TNF-α-induced endothelial inflammation.

3.5 DUSP6-mediated termination of ERK activity is essential for TNF-α-induced inflammatory response in endothelium

Having demonstrated the involvement of DUSP6 in TNF-α-stimulated ICAM-1 expression, we next investigated whether down-regulation of ERK, the primary function of DUSP6 thus far identified,[36] is essential for this process. We first examined the detailed time-dependent regulation of ERK by DUSP6 in HUVECs exposed to TNF-α. As shown in Fig. 11A, the immediate activation of ERK was terminated at 1 hour post stimulation in control cells. However, ERK activation was sustained over the duration of 1-6 hours after TNF-α treatment in DUSP6-ablated cells (Fig. 11A). We further evaluated whether DUSP6 also regulates JNK or p38 MAPKs in HUVECs exposed to TNF-α. Surprisingly, unlike in TNF-α-treated EAhy926 that DUSP6 may also regulate JNK activity. In contrast to the knockdown effect on ERK phosphorylation, ablation of

34

DUSP6 did not cause a detectable change of TNF-α-dependent transient activation of either JNK (Fig. 11B) or p38 (Fig. 11C), consistent with the current knowledge that DUSP6 is a specific ERK phosphatase. These results suggested that termination of ERK activity by inducible DUSP6 might promote the subsequent signaling essential for ICAM-1 expression.

To test this hypothesis, we first elucidated the natural instincts of ERK to suppress the expression of ICAM-1 in HUVECs stimulated with TNF-α. The conventional ERK inhibitors, PD184352, U0126 and PD98059 were used to pretreat cells before exposure to TNF-α. As shown in Fig. 12, all three chemical inhibitor pretreatment increased TNF-α-induced ICAM-1 expression. We also performed another approach by knocking down ERK with siRNA to verify this result. Data shown in Fig. 13 demonstrated that ablation of ERK leads to enhanced ICAM-1 expression in HUVECs response to TNF-α stimulation. Furthermore, forced inhibition of ERK via treatment with the chemical inhibitors led to restoration of ICAM-1 levels in DUSP6 RNAi-ablated HUVECs (Fig. 14). Such findings supported the notion that ERK-caused negative constraint on ICAM-1 expression may be lifted by inducible DUSP6. We tested this hypothesis by examining the knockdown effect of ERK on TNF-α-promoted ICAM-1 levels in DUSP6 RNAi-ablated HUVECs. Clearly, DUSP6 deficiency-caused low levels of ICAM-1 were partially restored when ERK expression was suppressed by the siRNA

specifically targeting ERK1 and ERK2 (Fig. 15). These results together suggest a

functional role in termination of ERK activity that DUSP6 plays during promotion of

endothelial inflammation.

3.6 Inhibition of ERK by DUSP6 promotes NF-κB transcriptional activation in endothelium exposed to TNF-α

In order to figure out the underlining mechanism that DUSP6 increased ICAM-1

expression, mRNA level of ICAM-1 was checked by quantitative real-time PCR in

DUSP6 ablated HUVECs. As shown in Fig. 16, Dusp6 knockdown by siRNA decreased

ICAM-1 mRNA level, indicting Dudp6 regulate ICAM-1 in a transcriptional-dependent

manner. It was suggested previously that activation of NF-κB is essential for expression

of adhesion molecules in endothelium under inflammatory response.[49] Upon TNF-α

treatment, upstream kinase activation mediates inhibitor of NF-κB (IκB)

phosphorylation and proteasome-dependent degradation, therefore releases free form of

NF-κB to direct downstream inflammatory gene expression. We first examined NF-κB

signaling in HUVECs exposed to TNF-α stimulation. As shown in Fig. 17A,

degradation of IκB-α happened in 5 minutes of TNF-α treatment and newly synthesized

IκB-α appeared at 45 minutes of stimulation. Meanwhile the increased phosphorylation

level of NF-κB indicates TNF-α-induced activation. We further elucidate the role of
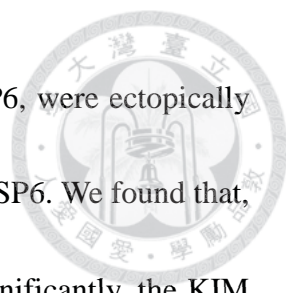
NF-κB in regulating ICAM-1 expression in TNF-α-treated HUVECs. Using a specific inhibitor BAY-117082 to pretreat cells, we showed intact IκB-α level in TNF-α treated sample which demonstrates sufficient inhibition of NF-κB signaling, and TNF-α-induced ICAM-1 expression was blocked completely (Fig. 17B). This result suggests a critical role of NF-κB in TNF-α-mediated induction of ICAM-1 protein in HUVECs. We wonder whether inducible DUSP6 would promote the expression of ICAM-1 through its up-regulation of NF-κB signaling. To test this hypothesis, we first examined the dynamic change of IκB-α levels over the duration of TNF-α stimulation and investigated whether ablation of DUSP6 could affect this process. Interestingly, the immediate degradation of IκB within the first 15 minutes post treatment occurred independent of endogenous levels of DUSP6 (Fig. 17C), indicating that release of NF-κB from its inhibitor IκB was not influenced by DUSP6. Consistently, NF-κB was rapidly phosphorylated soon after TNF-α treatment even though DUSP6 was knocked down (Fig.17C), further eliminating the possible involvement of DUSP6 at the initial phase of NF-κB pathway. In contrast, during the course of IκB re-synthesis, a NF-κB-dependent process[61] that became evident between 1-6 hours after TNF-α stimulation (Fig. 17C); we observed that DUSP6 played a clear role. Specifically, the accumulated levels of re-synthesized IκB at 4-6 hours post treatment were significantly suppressed when endogenous DUSP6 was ablated (Fig. 17C). Together, these results

suggest that transcriptional activation of NF-κB, which is essential for re-synthesis of

IκB and also inducible expression of ICAM-1, might be regulated by DUSP6 in

endothelium under TNF-α stimulation.
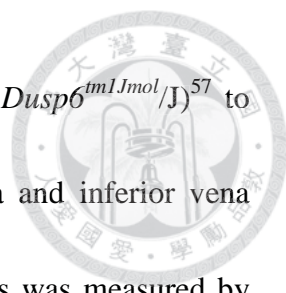
This finding led us to wonder whether inducible DUSP6 would promote the

expression of ICAM-1 through its up-regulation of NF-κB transcriptional activity; and

if this is the case, whether the underlying mechanism of such process is determined by

DUSP6-dependent inactivation of ERK. To test this hypothesis, we examined the role of

DUSP6 in NF-κB-directed transcription of *ICAM-1* gene. For this, luciferase reporter

assay was conducted in TNF-α-treated HUVECs. One unique NF-κB binding element

in the promoter region of *ICAM-1* gene[26] was selected for characterization (Fig. 18A).

The pilot test demonstrated that NF-κB-mediated transcription of *ICAM-1* gradually

increased after TNF-α treatment, and that the robust enhancement of luciferase activity

occurred at 4 hours post stimulation (Fig. 18A). This led us to examine a role that

DUSP6 plays in regulating NF-κB at this time. Clearly, upon the ablation of DUSP6,

NF-κB-mediated transcription of *ICAM-1* promoter was significantly suppressed (Fig.

18B). We further investigated whether inactivation of ERK is essential for

DUSP6-mediated activation of NF-κB. To do this, a mutant form of DUSP6 in which

the kinase interacting motif (KIM) was disrupted thereby losing its interaction with

ERK (termed KIM mutant thereafter),[62] and the WT form of DUSP6, were ectopically

expressed in HUVECs treated with siRNA to ablate endogenous DUSP6. We found that,

unlike the WT form of DUSP6 that restored the NF-κB activity significantly, the KIM

mutant form of DUSP6 was unable to do so (Fig. 18C). In addition, the KIM mutant

form of DUSP6 was incapable of restoring TNF-α-induced expression of ICAM-1

protein (Fig. 19). We thus concluded that DUSP6 promotes canonical NF-κB signaling

through its inactivation of ERK for inducible expression of ICAM-1 during endothelial

inflammation.

3.7 TNF-α-induced ICAM-1expression on the endothelial layer of aorta and vein is attenuated in *Dusp6*^{-/-} mice

Having demonstrated the mechanism that illustrates how DUSP6 promotes inducible

expression of ICAM-1 during initial six hours of TNF-α exposure, we further examined

the role of DUSP6 in endothelium with prolonged inflammatory response. As shown in

Fig. 20, the induction of ICAM-1 in HUVECs peaked at 12-hour of TNF-α treatment,

and then sustained up to 24 hours. Importantly, RNAi ablation of DUSP6 led to a

significant decrease of ICAM-1 levels during the period of 12 to 24 hours after

stimulation (Fig. 20), suggesting that the maximal expression of ICAM-1 in the

inflamed endothelium is DUSP6-dependent. This hypothesis was subsequently tested *in*
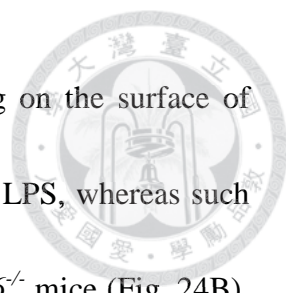
vivo. For this, we used DUSP6 null mice (*Dusp6*$^{-/-}$ strain B6;129-*Dusp6*^{tm1Jmol}/J)[57] to study whether DUSP6 regulates endothelial inflammation in aorta and inferior vena cava (IVC). The degree of inflammatory response in animal tissues was measured by the immunohistochemistry (IHC) staining with anti-ICAM-1 antibody. First, we checked the mice knockout background by genotyping and the absence of DUSP6 expression in tissues also shown in Fig. 21. Then we challenged mice with TNF-α (5 μg/kg) to examine ICAM-1 level on vascular endothelia of aorta and IVC. After injection with TNF-α for 16 hours, there was significant increase in levels of ICAM-1 on the endothelial layer of both aorta and IVC isolated from the WT control mice (B6129SF2/J) (Fig. 22A). Pairs of WT and *Dusp6*$^{-/-}$ mice were then examined under various conditions. Basal expression of endothelial ICAM-1 was low regardless of the presence or absence of *Dusp6* gene (Fig. 22B). Furthermore, TNF-α-induced ICAM-1 expression on the surface of aorta and IVC was visualized by the specific anti-ICAM-1 antibody but not by the isotype IgG (Fig. 22C). This data confirmed the reliability of IHC staining. Interestingly, although endothelial ICAM-1 expression on the surface of aorta and IVC was robustly enhanced in the WT mice exposed to TNF-α, its level in the *Dusp6*$^{-/-}$ mice remained low (Fig. 23). Quantitative results from multiple animals revealed a significant difference in ICAM-1 levels on endothelial layer of aorta (Fig. 23A) and IVC (Fig. 23B) between the WT and *Dusp6*$^{-/-}$ mice under TNF-α stimulation.

3.8 Deficiency of DUSP6 protects mice from acute lung injuries during experimental sepsis

We investigated whether DUSP6 regulates the pathological process of sepsis, which is a severe medical condition characterized by a systemic inflammatory response to infection.[63] We particularly focused on the potential role of DUSP6 involved in inflammatory consequence of sepsis within the pulmonary circulation, as the lung is continuously exposed to circulating pathogen-associated molecular patterns such as endotoxin lipopolysaccharide (LPS).[14, 63] In addition, human pulmonary microvascular endothelial cells and HUVECs respond to TNF-α and LPS similarly in terms of NF-κB activation and surface ICAM-1 expression,[64] suggesting that a DUSP6-dependent regulatory mechanism might be adopted by two types of endothelia. This hypothesis was tested by intraperitoneal injection of WT and $Dusp6^{-/-}$ mice with TNF-α (0.1 mg/kg) or LPS (10 mg/kg); the latter stimulates the expression of ICAM-1 and thus promoting neutrophil infiltration-dependent pulmonary injury through release of TNF-α.[65] After 24 hours of treatment, lung sections taken from the mice were subjected to staining with hematoxylin and eosin (H&E) or anti-ICAM-1 antibody. As shown in Fig. 24A, a significant degree of histologic lung injury, as indicated by notable inflammatory cells infiltration and inter-alveolar septal thickening, was observed in the WT mice exposed to TNF-α or LPS. Interestingly, these tissue damages were attenuated in TNF-α or
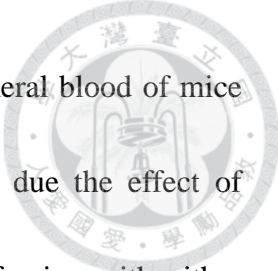
LPS-treated *Dusp6*$^{-/-}$ mice (Fig. 24A). Moreover, ICAM-1 staining on the surface of

alveolar walls was increased in the WT mice exposed to TNF-α or LPS, whereas such

stimulation-induced ICAM-1 expression was alleviated in the *Dusp6*$^{-/-}$ mice (Fig. 24B).

We further assessed pulmonary neutrophil infiltration by measuring myeloperoxidase

(MPO) activity in the lung tissues. As expected, the basal levels of lung MPO activity

were low and comparable between the WT and *Dusp6*$^{-/-}$ mice (Fig. 24C). Importantly,

although the MPO activity was increased 3-fold or 5-fold in the WT mice receiving

TNF-α or LPS treatment respectively, such change was significantly lower in the

Dusp6$^{-/-}$ mice (Fig. 24C). These results collectively suggest that *Dusp6*$^{-/-}$ mice were

protected from pulmonary neutrophil infiltration and subsequent lung injury in the

mouse model of experimental sepsis.
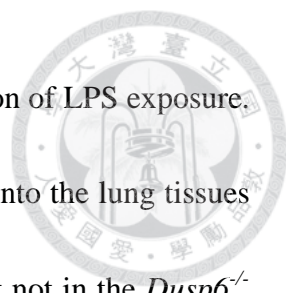
3.9 Pulmonary endothelial DUSP6 is essential for LPS-induced neutrophil recruitment in mice

To confirm that the decreased susceptibility to lung injury in the knockout mice (Fig.

24) is caused by the deficiency of endothelial DUSP6, we adoptively transferred

neutrophils from the WT mice into the irradiated WT or *Dusp6*$^{-/-}$ recipient mice, and

subsequently induced experimental sepsis in the recipient mice (Fig. 27A). For

experimental condition setting, both WT and *Dusp6*$^{-/-}$ mice were exposed to whole body

irradiation (9 Gy). After 24 hours recovery, the leukocytes in peripheral blood of mice

were collected and analyzed by flow cytometry. We noticed that, due the effect of

irradiation, the number of total leukocytes in peripheral blood of mice with either

genotype was diminished significantly (Fig. 25), indicating an effective removal of

intrinsic neutrophils in recipient mice by this treatment. We next established neutrophil

adoptive transfer condition in WT mice. The whole blood from the WT donor mice was

drawn by submandibular-bleeding, and polymorphonuclear leukocytes (PMNs) were

isolated from total leukocytes by density gradient centrifugation in Percoll. Purified

PMNs were subjected to flow cytometry analysis and the enriched fraction of

neutrophils was confirmed by double staining with specific markers Ly-6G and CD11b

(Fig. 26A). Purified PMNs were adoptively transferred to the irradiated recipient WT

mice, followed by intraperitoneal injection with LPS (10 mg/kg) into the recipient mice

for 4 hours. The neutrophil infiltration into lung was analyzed by the ELISA-based

detection of myeloperoxidase (MPO) activity. Compare to control mice without

neutrophil transfer, recipient mice with adopted transfer developed higher degrees of

neutrophil infiltration into lung (Fig. 26B). These pilot studies suggested that the

experimental design illustrated in Fig. 27A is suitable for examining the potential role of

pulmonary endothelial DUSP6 in the neutrophil recruitment response to LPS

stimulation. Following this protocol, we measured the MPO activity in lung tissues
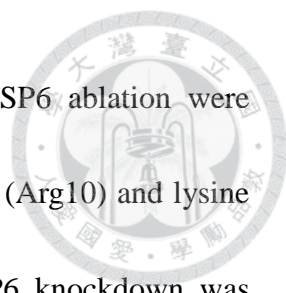
harvested from the WT or *Dusp6*^{-/-} recipient mice upon the completion of LPS exposure.

As shown in Fig. 27B, the increased level of neutrophil infiltration into the lung tissues

by the adoptive transfer of PMNs was observed only in the WT, but not in the *Dusp6*^{-/-}

recipient mice. Data collectively suggested that endothelial DUSP6 plays a key role in

neutrophil recruitment during acute pulmonary inflammation.
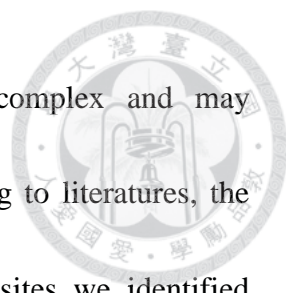
3.10 Exploring DUSP6-mediated phosphorylation network in TNF-α-activated HUVECs by MS analysis

In this study we found that Dusp6 up regulated ICAM-1 expression through

inhibition of ERK activity therefore activating NF-κB transcriptional activity in

TNF-α-treated HUVECs. However suppression of ERK activity by either chemical drug

inhibition or by siRNA influence could not fully restore ICAM-1 expression as well as

NF-κB transcriptional activity under DUSP6 knockdown background (Fig. 14, 15 and

18C). These results let us wonder whether other proteins, except ERK, also affected by

DUSP6 to coordinate endothelial inflammation. And we also want to know whether

DUSP6 may regulate other potential functions involved in endothelial inflammation.

For this purpose, we adopted stable isotope labeling by amino acids in cell culture

(SILAC) of control and DUSP6-ablated cells to explore DUSP6-mediated

phosphorylation network in TNF-α-activated HUVECs. The workflow of SILAC

44

experiment was outlined in Scheme1. Briefly, HUVECs for DUSP6 ablation were cultured in SILAC DMEM medium containing ^{13}C labeled arginine (Arg10) and lysine (Lys6) amino acids for five cell division cycles and then DUSP6 knockdown was performed. Cell lysates from normal (light) HUVECs without isotope labeling and DUSP6-KD (heavy) HUVECs labeled with ^{13}C were harvested and mixed by 1:1 ratio and then digested by Lys-C and Trypsin proteases. Phosphorylated peptides enriched by TiO2 and anti-phoshotyrsine antibody were analyzed by MS/MS and quantified by MaxQuant.
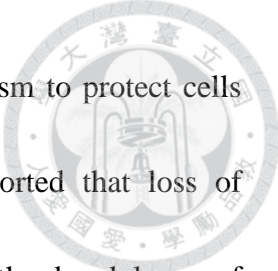
From the two repeats of SILAC analysis, we identified total 183 phosphopeptides (145 phosphoproteins) which have altered ratio between heavy and light samples (as shown in appendix). In which, 47 proteins showed increased phosphorylation level (Table 3) and 103 proteins showed decreased phosphorylation level. 5 out of 145 phoshoproteins have both up and down phosphorylation levels in different residues. For exploring DUSP6-mediated phosphorylation networks, we first focused on the up-regulated proteins. In which, we found several proteins function in cell junctions or focal adhesion complex, including PECAM-1 (pY663, pY686), connexin 43 (pS365), p120 catenin (pS269), caveolin-1 (pY14), paxillin (pS340) and vimentin (pS144). As shown in Fig. 31, we analyzed these up-regulated proteins by ingenuity pathway analysis (IPA) software with connection and growth algorithm. The result indicates

these proteins forming connected network with VE-cadherin complex and may functioning in regulating endothelial junctional integrity. According to literatures, the enhanced phosphorylation of PECAM-1[66] and connexin 43[67] at sites we identified showed correlation with enhanced cell junction integrity, therefore we speculate they may be targeted by DUSP6 to regulate endothelial inflammation.

PECAM-1 is a cellular adhesion and signaling receptor and functions as a regulator in maintenance of endothelial cell junctional integrity.[66] It has been published, the phosphorylation on Y663 and Y686 of PECAM-1 help to recruit SHP-2 phosphatase. PECAM-1/SHP-2 complexes have been proposed to dephosphorylate β-catenin and thereby stabilize β-catenin/VE-cadherin complexes.[68] In SILAC analysis, both pY663 and pY686 of PECAM-1 were increased clearly (refer to Table 3) in DUSP6-ablated HUVECs, this make the hypothesis that DUSP6 may target on PECAM-1 tyrosine dephosphorylation to perturb β-catenin be dephosphorylated by SHP-2 and increase HUVECs permeability through dissociation of VE-cadherin complex under TNF-α stimulation. Eventually the DUSP6-mediated increasing of permeability facilitates leukocyte transmigration and endothelial inflammation.

Connexin 43 is a gap junction proteins forms hydrophilic membrane channels that allow direct communication between neighboring cells via diffusion of ions, metabolites, and small cell signaling molecules.[69] The phosphorylation on Ser365 of connexin 43

functions in maintaining protein structure and represents a mechanism to protect cells from down-regulation of channel conductance.[67] It has been reported that loss of connexin 43 destabilizes intercellular junctions, contributing to the breakdown of endothelial barrier function and inhibition of angiogenesis.[70] In endothelial-smooth muscle interaction mold, connexin 43 mediates β-catenin Tyr142-phosphorylation and the Tyr142-phosphorylated β-catenin stimulates VCAM-1 expression to increase EC-monocytic adhesion.[71] Our SILAC analysis observed enhanced phosphorylation on Ser365 of connexin 43, suggesting another possibility that DUSP6 through dephosphorylating connexin 43 Ser365 to influence gap junction as well as adherens junction, disrupt vascular integrity therefor promoting endothelial inflammation.

Although the proteins list above from SILAC analysis all have increased phosphorylation level, not every phosphorylation site has been reported as regulating site in maintain cell junction integrity. Maybe they are yet-to-be-identified critical sites targeted by DUSP6. Whether these phosphoproteins are direct or indirect inferenced by DUSP6 needs further validations. These results suggest that DUSP6 promoting endothelial inflammation and leukocyte transmigration not only dependent on regulating ICAM-1 expression but also increasing endothelial permeability by down regulating cell junction integrity. This direction of study will promisingly unravel the other roles of DUSP6 which is critical for further investigations.
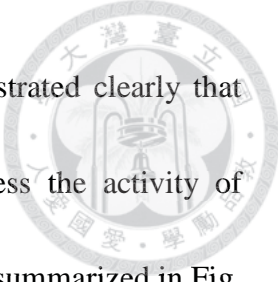
CHAPTER 4: DISCUSSION
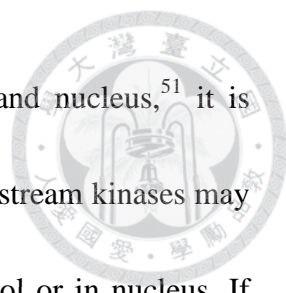
The present work discovered that DUSP6 promotes endothelial inflammatory response and delineated the underlying molecular mechanism (Fig. 30). DUSP6 has been identified as a MKP that specifically inactivates ERK in signaling response to physiological stimuli.[72, 73] However, it has remained unclear whether DUSP6 participates in the progression of disease conditions. The present study highlights the role of DUSP6 as an ERK phosphatase, one that is not only critical for correct cell specification and differentiation during ligand-guided embryonic development as proposed previously,[72, 73] but also one that is important for cytokine-stimulated endothelial inflammation in adult animals.

TNF-α-induced ERK activation peaked at 15 minutes and was then brought back to a sub-basal level by inducible DUSP6 one hour later in HUVECs (Fig. 11A). Once ERK activity was terminated, transcriptional initiation of NF-κB became obvious on the ICAM-1 promoter (Fig. 18). These findings reveal the stepwise signaling events that coordinate to achieve TNF-α-induced inflammatory response in endothelium. It was shown more than two decades ago that ERK could be activated by TNF-α stimulation.[74] Although such an event might be important for cell survival,[50] to date the exact function of immediately activated ERK in the context of TNF-α signaling remained elusive. On the other hand it was known that subsequent NF-κB-dependent inflammatory response required inhibition of ERK.[32-34] Therefore, identification of the DUSP6-ERK signaling

axis to activate NF-κB by the present study is critical. We demonstrated clearly that

NF-κB cannot drive functional transcription on *ICAM-1*gene unless the activity of

cellular ERK has been terminated by inducible DUSP6 (Fig. 18, and summarized in Fig.

30).

We observed a residual level of ICAM-1 in DUSP6-ablated HUVECs when exposed

to TNF-α (Fig. 8, 15 and 20). Similarly, mice with DUSP6 deficiency still showed

response to TNF-α or LPS treatment, although the degree of neutrophil recruitment by

lung in *Dusp6⁻/⁻* mice was much lower than the WT counterparts (Fig. 24 and 27). These

results suggest that, in addition to DUSP6, other ERK phosphatases might be involved

in the promotion of endothelial inflammation. Focusing on members within the DUSP

family, we analyzed microarray data obtained from HUVECs exposed to TNF-α.

Interestingly, among four ERK-specific DUSPs detected in this assay (DUSP1, 4, 6 and

9),[36] DUSP6 was the only one that showed TNF-α-dependent mRNA expression (Fig.

28). This finding suggests that inducible DUSP6 might be the primary MKP responsible

for down-regulation of ERK activity, thus highlighting an indispensable role of DUSP6

in endothelium under inflammatory stimulation. Further studies are required to define

whether and how other types of phosphatases, including atypical DUSPs, classical

Tyr-specific and Ser/Thr-specific phosphatases, might coordinate with DUSP6 to

terminate ERK signaling for a robust inflammatory response in endothelial cells.

Because the active form of ERK can shuttle between cytosol and nucleus,[51] it is possible that once activated by TNF-α stimulation, ERK or its downstream kinases may phosphorylate Ser/Thr residues of the NF-κB dimer either in cytosol or in nucleus. If this is the case, ERK-mediated phosphorylation may ensure that NF-κB stays in the "switch-off" mode. Subsequently, upon accumulation of inducible DUSP6 in cells, ERK is dephosphorylated and inactivated, rendering NF-κB susceptible to Ser/Thr phosphatase-mediated activation. One such candidate may be protein phosphatase 4 (PP4), a nuclear Ser/Thr phosphatase that directly interacts with and activates NF-κB.[75, 76] It has been recently shown that pharmacological inhibition of MEK-ERK pathway enhances the cellular level of PP4, leading to dephosphorylation and activation of NF-κB.[33] Considering these studies and our findings together, we propose that inducible DUSP6-mediated inhibition of ERK might promote NF-κB activity via a PP4-dependent process in endothelium response to TNF-α stimulation. In addition, a recent investigation proposed that the active form of ERK might suppress endothelial inflammation through inhibition of IκB kinase (IKK), a key upstream kinase to enhance NF-κB transcriptional activity.[34] Although experimental evidence is unavailable, we cannot rule out the possibility that inducible DUSP6 might activate IKK indirectly via inhibiting ERK. More studies are required to clarify whether DUSP6 coordinates with PP4 or other yet-to-be-confirmed regulators to promote NF-κB-dependent expression of

51
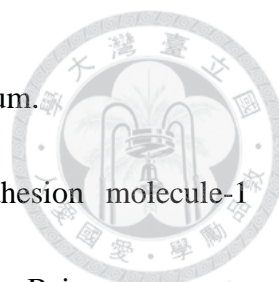
ICAM-1 during TNF-α-induced inflammatory response in endothelium.
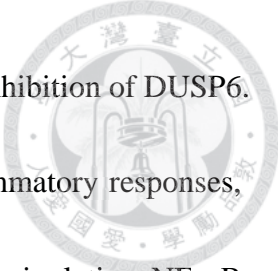
In addition to ICAM-1, the expression of vascular cell adhesion molecule-1 (VCAM-1) on endothelial surface is also under the control of NF-κB in response to TNF-α stimulation.[49] We investigated whether NF-κB-dependent transcription of *VCAM-1* gene is regulated by the signaling axis of DUSP6-ERK in HUVECs. Interestingly, inducible DUSP6 appeared to be critical for TNF-α-driven expression of endothelial VCAM-1 (Fig 29). Moreover, inactivation of ERK was a key step in DUSP6-promoted NF-κB transcription on the *VCAM-1* promoter in endothelium exposed to TNF-α (Fig. 29). Together, our results illustrated an important role that DUSP6 plays in robust transcriptional activation NF-κB-targeted genes, including *ICAM-1* and *VCAM-1*, involved in vascular inflammation. Nonetheless, we propose that inducible expression of ICAM-1 is the primary downstream effector of endothelial DUSP6 during the pulmonary neutrophil infiltration illustrated by our present study using experimental sepsis (Fig. 24 and 27), as the β2-integrin expressed on the surface of neutrophil interacts specifically with ICAM-1 but not VCAM-1.[60] The inducible expression of VCAM-1, on the other hand, manifests specific ligand for the integrin α4β1 (VLA-4), which appears on the surface of monocyte, B and T lymphocytes but not neutrophil.[60] Further investigations may reveal intriguing function of DUSP6 in regulating VCAM-1-dependent recruitment of leukocytes in the context of vascular

inflammation.

Using the mouse model of experimental sepsis in conjunction with adoptive transfer of neutrophils, we have defined a novel role of DUSP6 in pulmonary circulation response to inflammatory stimulation (Fig. 24 and 27). It has been known clearly that pulmonary infection results in robust emigration of neutrophils from the capillary bed into the alveolar space, leading to acute lung injuries often seen in patients with sepsis.[14] Moreover, previous studies showed that intratracheal exposure of LPS in mice induced a significant increase of ICAM-1 expression on capillary endothelial cells,[13] and that TNF-α-stimulated neutrophil adhesion on human pulmonary capillary endothelial cells was an ICAM-1 dependent process.[77, 78] These previous data together with our current findings suggest a critical function of DUSP6 that drives inducible ICAM-1 expression within pulmonary capillary endothelial cells during acute inflammatory process. We propose that capillary endothelial DUSP6 is particularly important in the development of acute lung injury caused by infection of *Escherichia coli* or *Pseudomonas aeruginosa*, as the endotoxin produced by these bacteria elicits neutrophil emigration via a β2-intergin pathway,[79-81] which acts through ICAM-1 on the endothelial surface for strong binding.[60]

Our study using *Dusp6*^{-/-} mice not only validated the results of cell-based experiments showing DUSP6's role in inflammatory response, they also provided the opportunity to

explore the possibility of subduing inflammatory disorders through inhibition of DUSP6.

From the perspective of drug development for suppression of inflammatory responses, interference of DUSP6 activity may be a feasible strategy for manipulating NF-κB pathway. Due to the ubiquitous expression profiles of NF-κB as well as its involvement in normal cellular physiology, it is expected that application of inhibitors against NF-κB may lead to profound side effects in humans.[82, 83] Still the inducible expression of DUSPs follows a cell-type-specific and disease-context-dependent manner,[48] rendering these phosphatases promising drug targets. The present work suggests that specific inhibitors of DUSP6, for example some lead compounds already identified by recent studies,[84, 85] could be used in novel therapeutic strategies for the treatment of patients with sepsis through the reduction of pulmonary endothelial inflammation.

In summary, we demonstrated how the interplay between ERK and NF-κB pathways is precisely controlled by inducible DUSP6 for the inflammatory response in endothelium exposed to TNF-α. Therefore, our study provides the rationale for future experiments focusing the possibility of targeting DUSP6 in the treatment of inflammatory disorders.
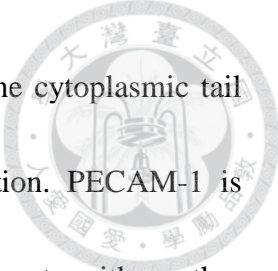
CHAPTER 5: FUTURE PERSPECTIVES

In the current study, we have identified ERK as the DUSP6 downstream target to regulate cell adhesion molecule ICAM-1 expression. However knocking down ERK by siRNA or inhibiting ERK by chemical inhibitors can only partially restore ICAM-1 expression in DUSP6-ablated HUVECs, indicating DUSP6 may also influence some other proteins to coordinate ICAM-1 expression as well as inflammatory response in endothelial cells.
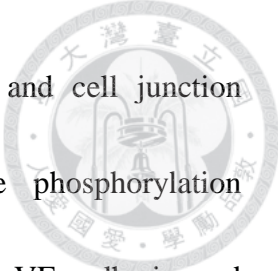
We adopted SILAC analysis for exploring DUSP6-mediated phosphorylation network in TNF-α-activated HUVECs, and found several cell junction or cell adhesion proteins with altered phosphorylation level under DUSP6 knockdown condition. These proteins include p120 catenin (pS269), PECAM-1 (pY663, pY686), connexin 43 (pS365), caveolin-1 (pY14), paxillin (pS340) and vimentin (pS144), which either associated with VE-cadherin complex and function in maintaining adherens junctions (AJs) or belongs to gap junctions or focal adherin complex and function in maintaining vascular integrity. This result suggests that DUSP6 promotes endothelial inflammation and leukocyte transmigration not only through increasing cell adhesion molecules expression but also increasing endothelial permeability by influencing cell junction integrity.

Among these phosphoproteins identified by SILAC analysis, we suspect PECAM-1 as a DUSP6 direct substrate. PECAM-1 is a cellular adhesion and signaling receptor, containing six extracellular immunoglobulin (Ig)-like homology domains, a short

transmembrane domain and a 118 amino acid cytoplasmic tail.[86] The cytoplasmic tail

becomes serine and tyrosine phosphorylated upon cellular activation. PECAM-1 is

highly expressed at endothelial cell intercellular junctions, and interacts with another

PECAM-1 on adjacent endothelial cell by Ig domain 1 in a homophilic manner. Thus

PECAM-1 functions as a regulator in maintaining endothelial cell junctional integrity.[67]

PECAM-1/SHP-2 complexes have been proposed to regulate the phosphorylation state

of β-catenin and thereby β-catenin/VE-cadherin complexes.[87] The Tyr686 and Tyr663

on immunoreceptor tyrosine-based inhibitory motif (ITIM) of PECAM-1 were

sequentially phosphorylated by Src and Csk respectively. Phosphorylated ITIM domain

recruit Src homology 2 domain-containing phosphatase 2 (SHP-2, PTPN11) to

dephosphorylate and stabilize β-catenin in VE-cadherin complex thereby maintaining

endothelial cell junction.[87]

According to our SILAC analysis, the phosphorylation level on both Tyr663 and

Tyr686 of PECAM-1were increased in DUSP6-ablated HUVECs stimulated with

TNF-α (refer to Table 3). Hence, we propose DUSP6 may directly dephosphorylate

Tyr663 and Tyr686 of PECAM-1 to disable SHP-2 recruitment by ITIM domain. By

this way, β-catenin continues remain in phosphorylated form and dissociates from

VE-cadherin complex thus destabilizing VE-cadherin complex. In this situation, cell

adherens junction will remain opening and let leukocyte emigration much easier.

To validate of our hypothesis further, HUVECs permeability and cell junction integrity should be monitored upon TNF-α stimulation. The phosphorylation modification on junction regulating proteins such as PECAM-1, VE-cadherin and β-catanin could be checked by immunoblotting. The PECM-1 Y663F and Y686F mutant, phosphorylation mimic mutant, could be used to rescue DUSP6-mediated junction integrity loss and permeability increase in TNF-α activated HUVECs.

In summary, our findings suggest DUSP6 may regulate endothelial inflammation and leukocyte transmigration through multiple aspects. Inhibition of Dusp6 may serve as a new therapy for the treatment of inflammatory disease.

CHAPTER 6: FIGURES
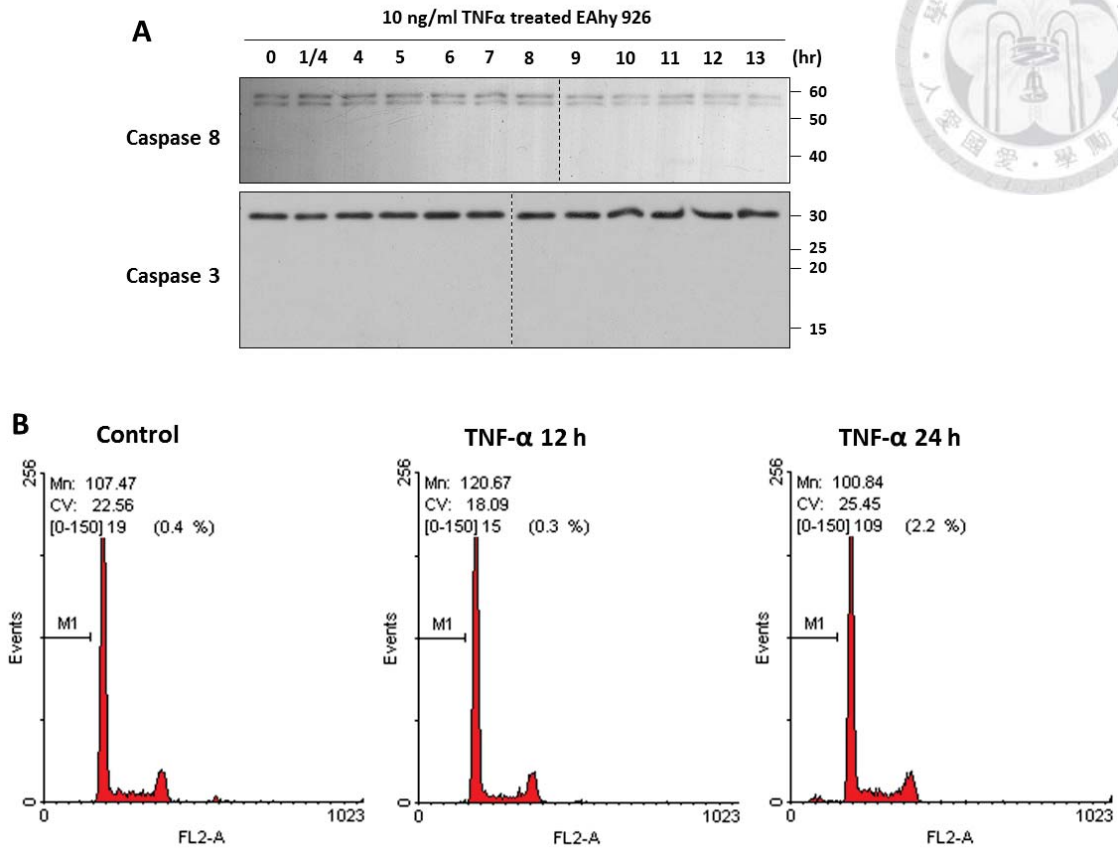
Figure 1. TNF-α treatment in EAhy926 does not trigger caspases activation and cell apoptosis. A to B, EAhy926 cells were serum starved for 16 hours prior to the treatment of TNF-α (10 ng/ml) for indicated time points. A, aliquots of lysates were subjected to immunoblotting with anti-caspase 8 and caspase 3 antibodies. Data shown are the representatives of three independent experiments. B, Cells were harvested, stained with propidium iodide (PI) and subjected to flow cytometry analysis. Data shown are the representatives of two independent experiments.
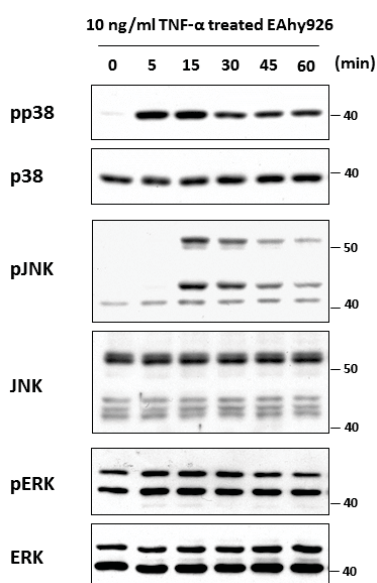
Figure 2. Mitogen-activated kinases (MAPKs) were transiently activated in endothelial EAhy926 cells stimulated with TNF-α. EAhy926 cells were treated with TNF-α (10ng/ml) for indicated time points, aliquots of lysates were subjected to immunoblotting with anti-phosoho-p38 (pp38), p38, phosphor-JNK (pJNK), JNK, phosphor-ERK (pERK) and ERK antibodies. Data shown are the representatives of three independent experiments.
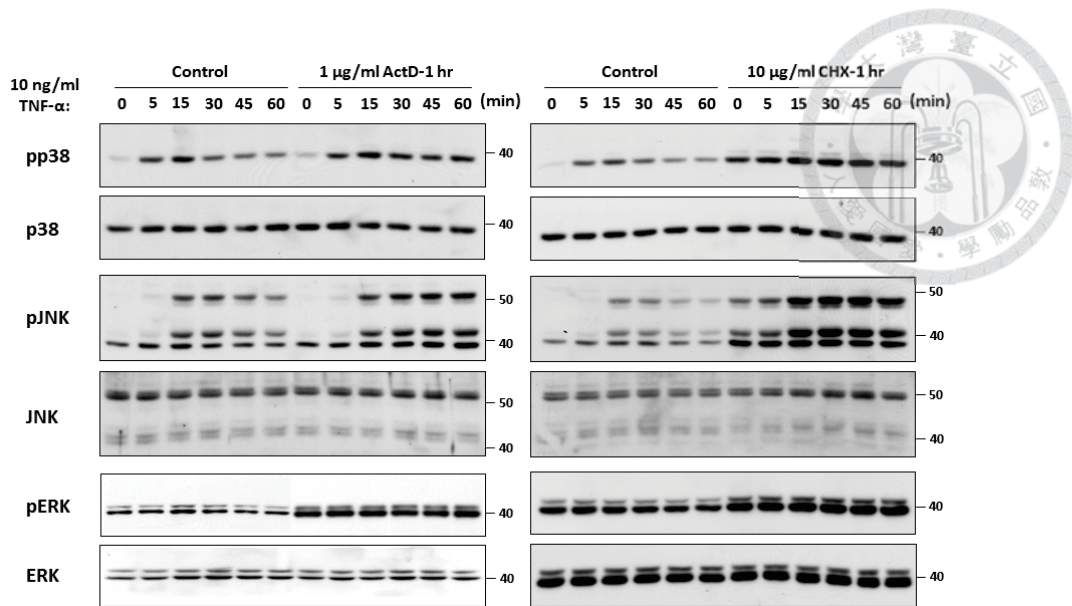
Figure 3. In EAhy926 cells, TNF-α regulates the activity of MAPKs through transcriptional and translational regulation mechanism. EAhy926 cells were left untreated, or pretreated with actinomycin D (ActD, 1 μg/ml, **left panel**) or cycloheximide (CHX, 10 μg/ml, **right panel**) for 1 hour and followed by TNF-α (10 ng/ml) treatment for indicated time points, aliquots of lysates were subjected to immunoblotting with anti-phosoho-p38 (pp38), p38, phosphor-JNK (pJNK), JNK, phosphor-ERK (pERK) and ERK antibodies. Data shown are the representatives of three independent experiments.
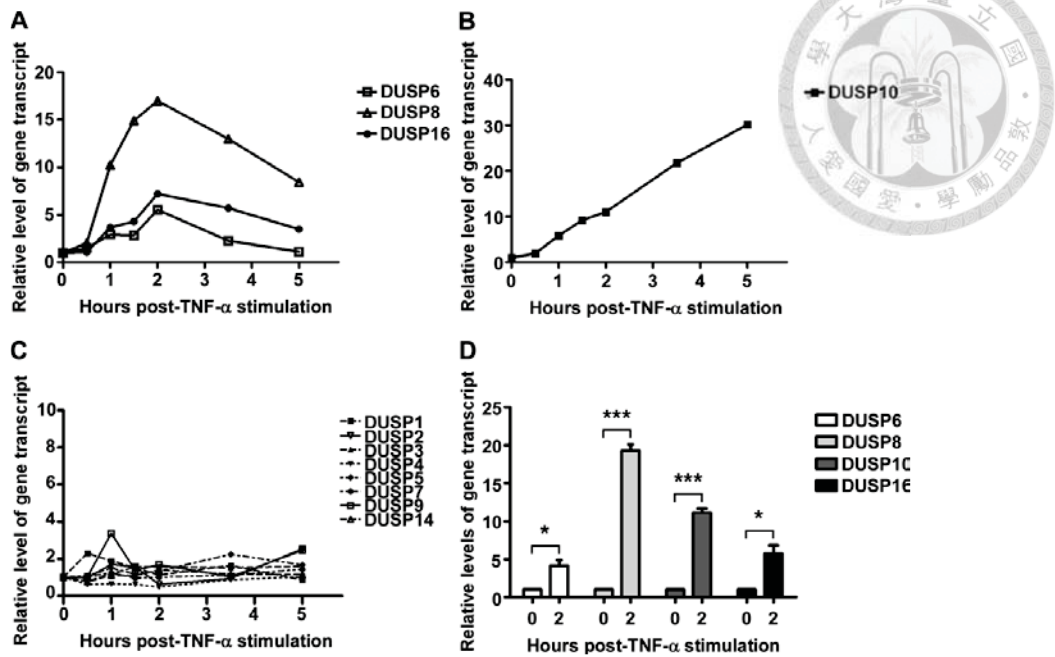
Figure 4. Based on quantitative real-time PCR analysis, 12 DUSPs, typical MKP, were classified to three groups by gene expression pattern upon TNF-α stimulation. **A to D,** EAhy926 cells were treated with TNF-α (10 ng/ml) for indicated time points. Total mRNA were prepared and subjected to real time-PCR analysis that depicted expression profiles of 12 Dusp genes. **A,** Dusp6, Dusp8 and Dusp16 were transiently expressed. **B,** The mRNA level of Dusp10 was steadily increased during the time of treatment. **C,** Eight Dusp genes did not respond to TNF-α stimulation. **D,** Statistic analysis showed significant induction of four Dusp genes. Data are expressed as mean± SD from three independent experiments (n=3; *, P<0.05 and ***, P<0.001).
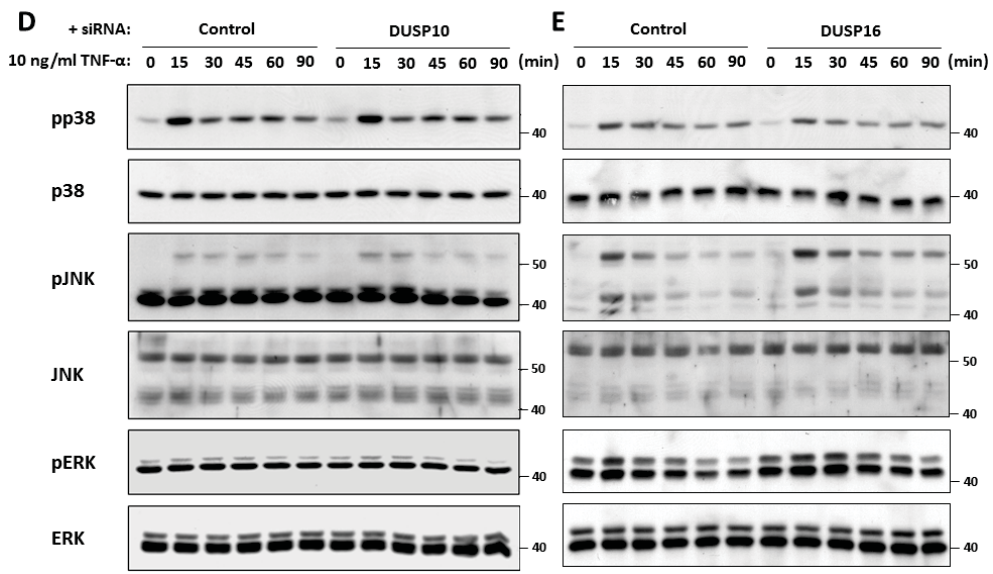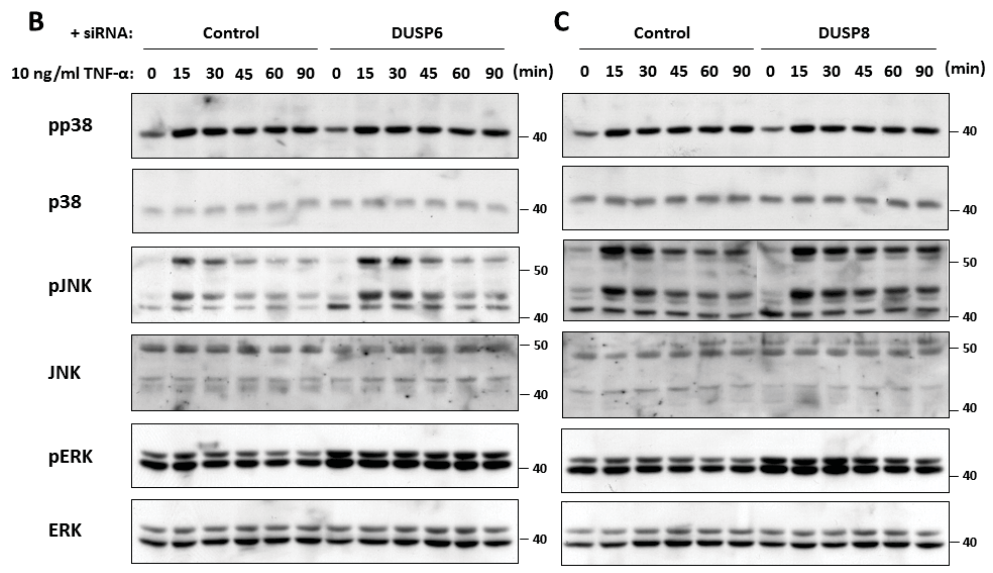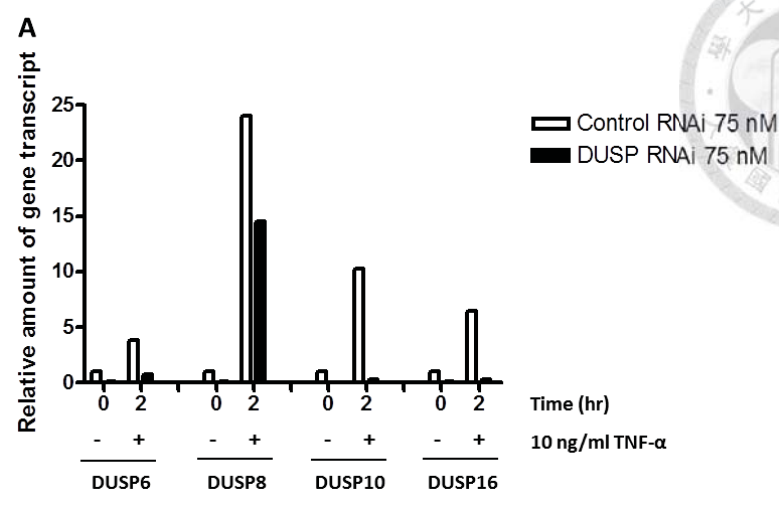
Figure 5. Based on RNA interference knockdown technique, DUSP6, 8, and 16 were identified as both ERK and JNK phosphatases. A to E, EAhy926 cells were transiently transfected with control or individual Dusp siRNA as indicated. After 24 hours, cells were treated with TNF-α (10 ng/ml) for indicated time points. **A,** Total mRNA were prepared and subjected to quantitative real time-PCR analysis that depicted RNA interfering effect of individual Dusp genes expression. **B to E,** Aliquots of lysates were subjected to immunoblotting with anti-phosoho-p38 (pp38), p38, phosphor-JNK (pJNK), JNK, phosphor-ERK (pERK) and ERK antibodies. Data shown are the representatives of three independent experiments.
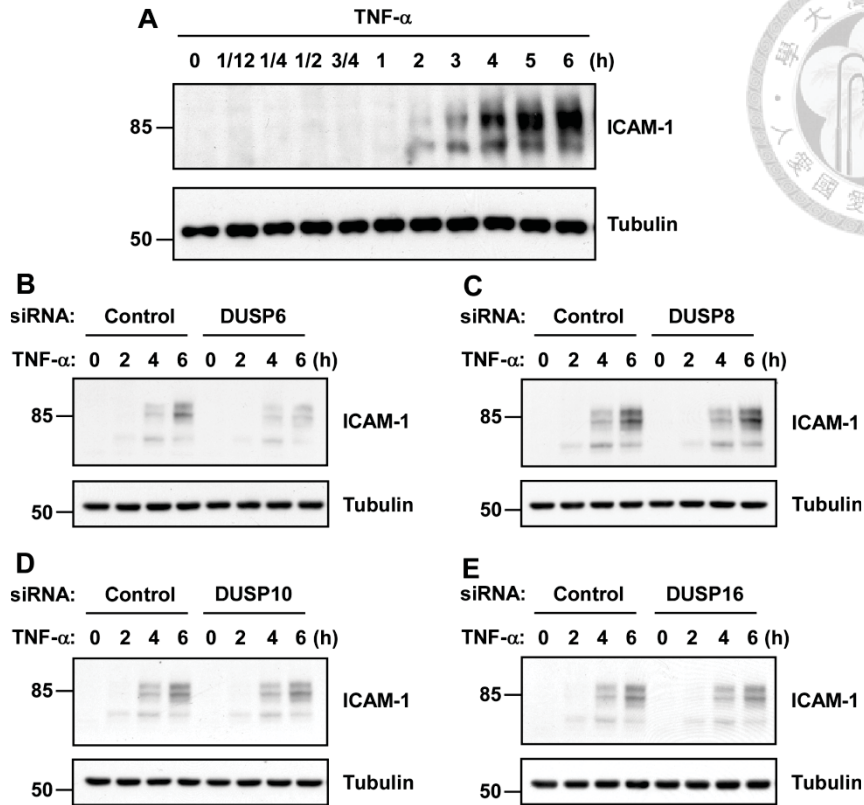
Figure 6. Inducible DUSP6 promotes expression of ICAM-1 in endothelial EAhy926 cells stimulated with TNF-α. A, EAhy926 cells were treated with TNF-α (10 ngl/ml) for indicated time points, aliquots of lysates were subjected to immunoblotting with anti-ICAM-1 and tubulin antibodies. **B to E,** EAhy926 cells were transiently transfected with control or individual Dusp siRNA as indicated. Transfectants were then treated with TNF-α for indicated time points. Aliquots of lysates were subjected to immunoblotting with anti-ICAM-1 and tubulin antibodies. Data shown are the representatives of three independent experiments.
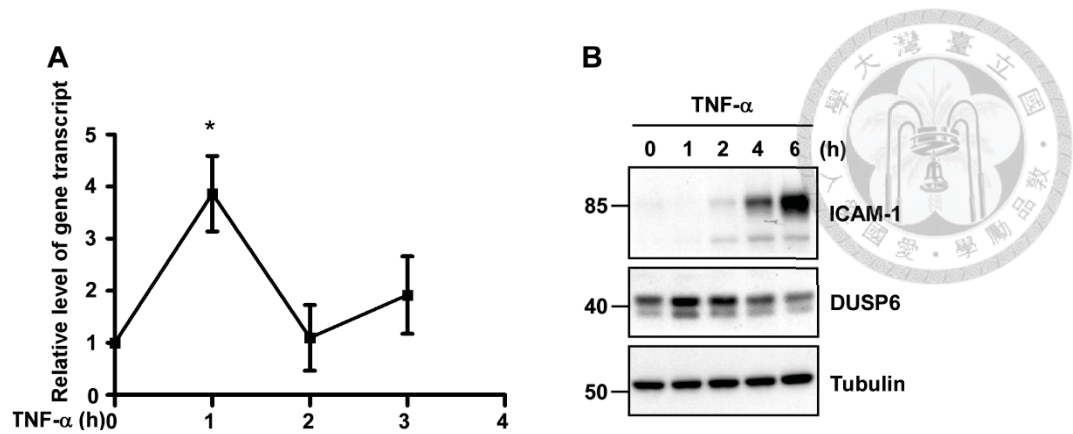
Figure 7. Transient expression of DUSP6 in HUVECs stimulated with TNF-α. A to B, HUVECs were treated with TNF-α (10 ng/ml) for indicated time points, total mRNA were subjected to quantitative real time-PCR analysis that depicted expression of Dusp6 gene (**A**) or aliquots of lysates were subjected to immunoblotting with anti-ICAM-1, DUSP6 and tubulin antibodies (**B**). Data shown in **A** is presented as mean±SD from three independent experiments (n=3; *, P<0.05). Data shown in **B** are the representatives of three independent experiments.
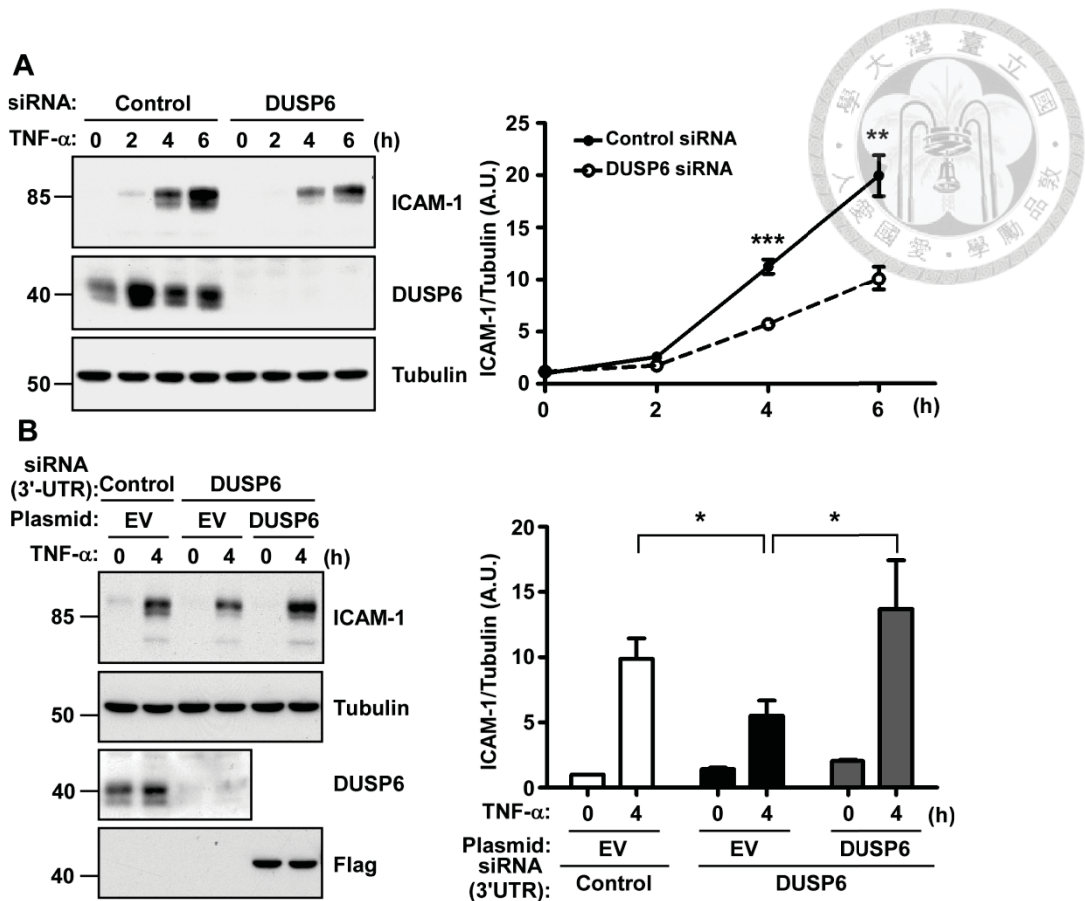
Figure 8. Inducible DUSP6 is essential for expression of ICAM-1 in HUVECs stimulated with TNF-α. A, HUVECs transiently transfected with control siRNA or specific siRNA that targets the coding region of Dusp6 were treated with TNF-α (10 ng/ml) for indicated time points. Aliquots of lysates were subjected to immunoblotting with anti-ICAM-1, DUSP6 and tubulin antibodies indicated. **B,** HUVECs transiently transfected with control siRNA or specific siRNA that targets the 3'-UTR region of Dusp6 were transfected with empty vector (EV) or plasmid encoding the wild type (WT) form of Flag-tagged DUSP6. Transfected HUVECs were exposed to TNF-α for 4 hours. Aliquots of lysates were subjected to immunoblotting with indicated antibodies. The relative ICAM-1 levels were obtained by a densitometric analysis of the gel image as a ratio of ICAM-1 relative to tubulin. A.U., arbitrary unit. Quantitative data shown in the right panels are presented as mean±SD (n=3; *, $P<0.05$, **, $P<0.01$ and ***, $P<0.001$).
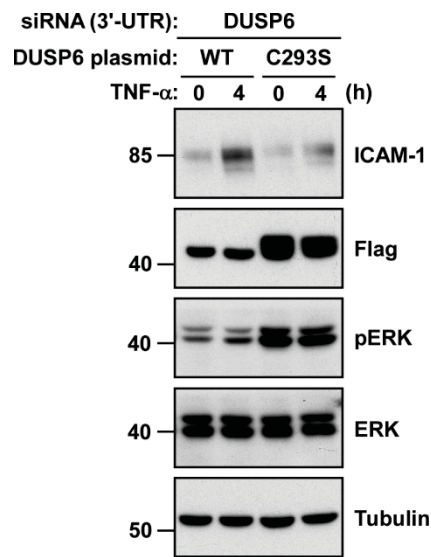
Figure 9. The catalytic activity of DUSP6 is required for inducible ICAM-1 expression in HUVECs stimulated with TNF-α. HUVECs transiently transfected with specific siRNA that targets the 3'-UTR region of *Dusp6* gene were transfected with plasmid encoding the wild type (WT) form or the phosphatase-dead C293S mutant form of Flag-tagged DUSP6. Transfected HUVECs were then stimulated with TNF-α for 4 hours. Aliquots of lysates were subjected to immunoblotting with anti-ICAM-1, Flag, phospho-ERK (pERK), ERK and tubulin antibodies. Data shown are the representatives of two independent experiments.
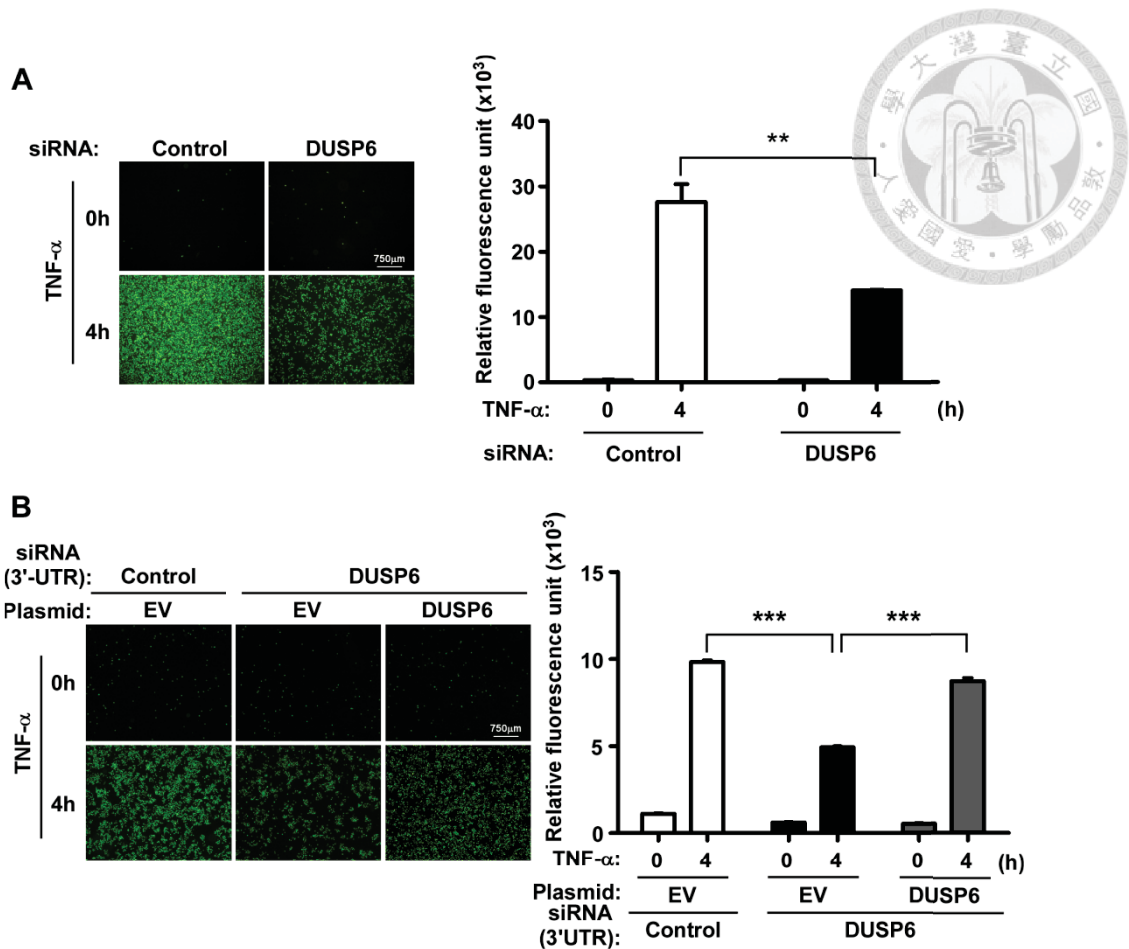
Figure 10. Inducible DUSP6 is essential for endothelial leukocyte interaction in HUVECs stimulated with TNF-α. A, HUVECs transiently transfected with control siRNA or specific siRNA that targets the coding region of Dusp6 were treated with TNF-α (10 ng/ml) for 4 hours. **B,** HUVECs transiently transfected with control siRNA or specific siRNA that targets the 3'-UTR region of Dusp6 were transfected with empty vector (EV) or plasmid encoding the wild type (WT) form of Flag-tagged DUSP6. Transfected HUVECs were exposed to TNF-α for 4 hours. A mono-layer of HUVECs was incubated with fluorescence dye BCECF-AM-labeled monocytic U937 cells. After extensive washes, U973 cells bound to HUVECs were visualized by fluorescence microscopy. The relative quantity of U937 cells attached to HUVECs was measured by a fluorescence analyze. Quantitative data shown in the right panels are presented as mean±SD (n=3; **, $P<0.01$ and ***, $P<0.001$).
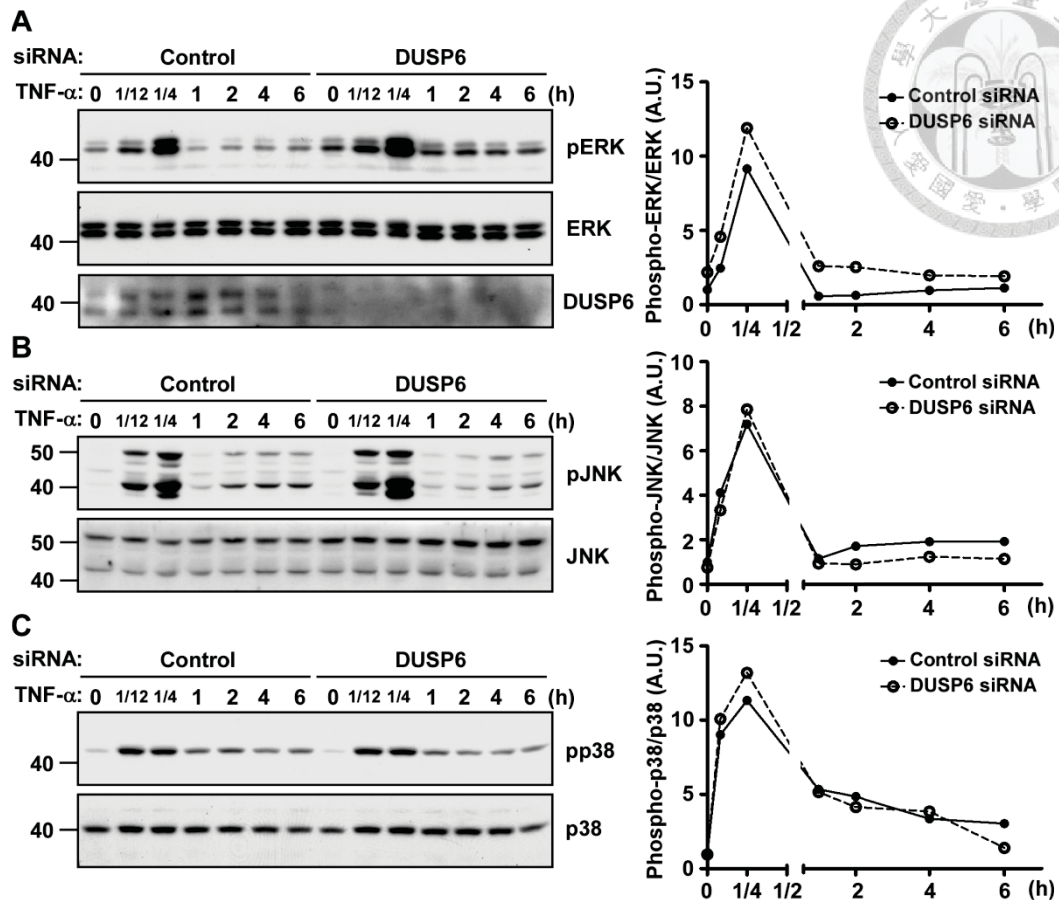
Figure 11. DUSP6 functions as ERK phosphatase in HUVECs stimulated with TNF-α. A to C, HUVECs transiently transfected with control siRNA or specific siRNA targeting Dusp6 were treated with TNF-α (10 ng/ml) for indicated time points. Aliquots of lysates were subjected to immunoblotting with anti-phospho-ERK (pERK), ERK, DUSP6, phosphor-JNK (pJNK), JNK, phosphor-p38 (pp38) and p38 antibodies. The right panels show a densitometric analysis of the gel image as a ratio of phosphorylated ERK (pERK) relative to total ERK (**A**), phosphorylated JNK (pJNK) relative to total JNK (**B**) and phosphorylated p38 (pp38) relative to total p38 (**C**). Data shown are the representatives of two independent experiments.
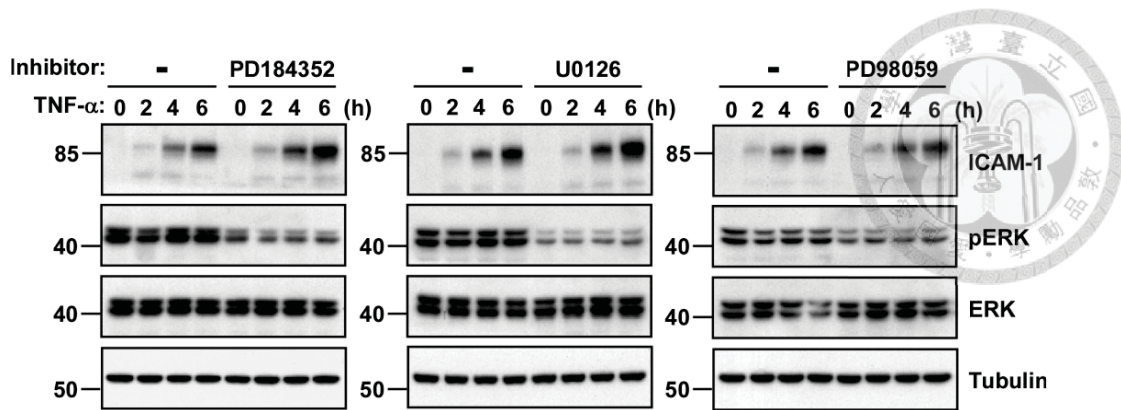
Figure 12. Inactivation of ERK by chemical inhibitors promoted ICAM-1 expression in HUVECs stimulated with TNF-α. HUVECs were left untreated, or treated with PD184352 (2 μmol/L, **left panel**), U0126 (10 μmol/L, **middle panel**) or PD98059 (10 μmol/L, **right panel**) for 1 hour, followed by TNF-α stimulation for indicated time points. Aliquots of lysates were subjected to immunoblotting with anti-ICAM-1, phospho-ERK (pERK), ERK and tubulin antibodies. Data shown are the representatives of three independent experiments.

Figure 13. Ablation of ERK by RNA interference promoted ICAM-1 expression in HUVECs stimulated with TNF-α. A and B, HUVECs were transiently transfected with control siRNA or specific siRNA targeting the coding region of *Dusp6*, followed by treatment with TNF-α (10 ng/ml) for indicated time points. Aliquots of lysates were subjected to immunoblotting with indicated antibodies. Data shown in (**A**) demonstrated that ablation of ERK by siRNA leads to enhanced level of inducible ICAM-1 in HUVECs response to TNF-α stimulation. The right panels show a densitometric analysis of the gel image as a ratio of ICAM-1 relative to tubulin. Data shown in (**B**) demonstrated that ablation of ERK by siRNA does not affect intrinsic expression of MAP kinases such as ERK5, JNK and p38. Similar results (**A**-**B**) were observed in two independent experiments.
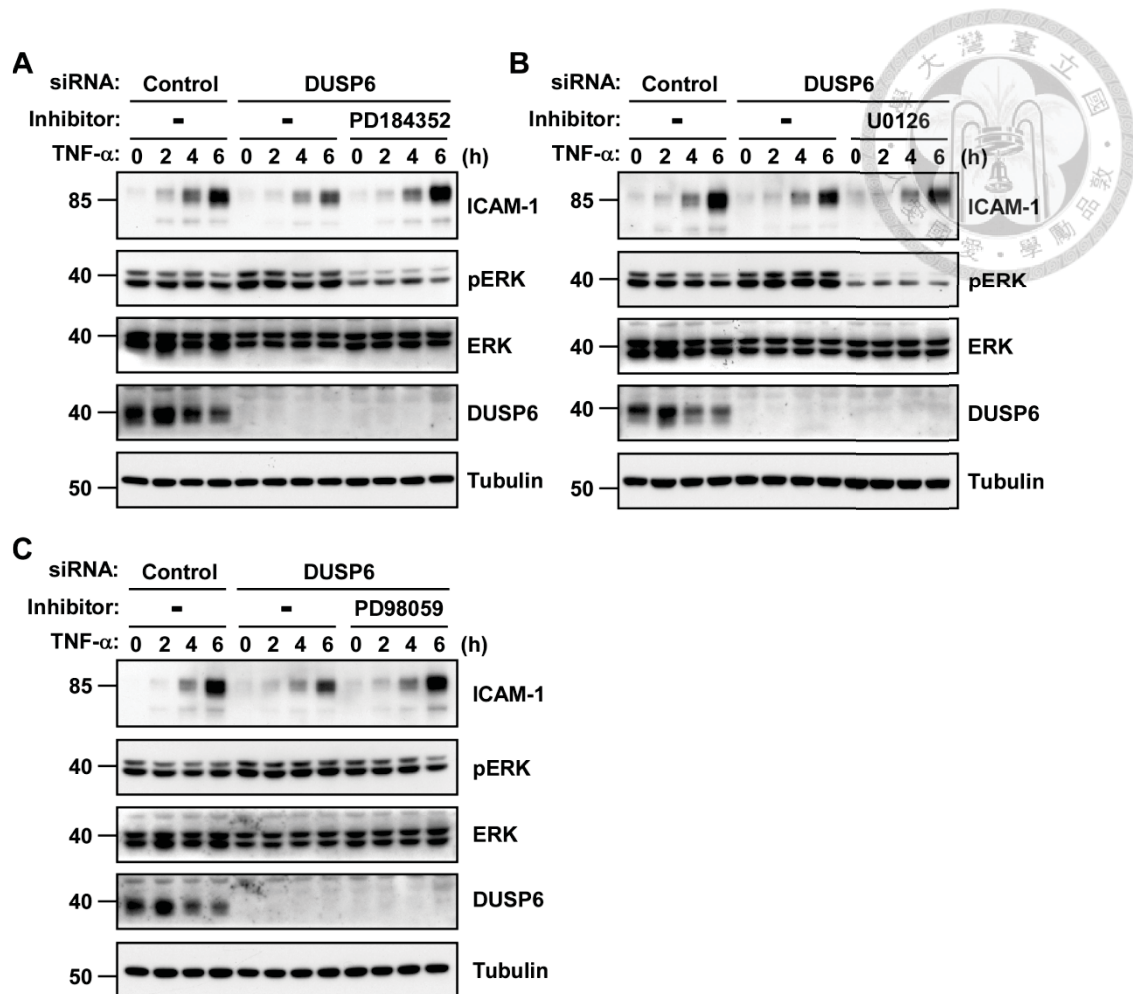
Figure 14. Inactivation of ERK restored ICAM-1 expression in DUSP6 RNAi-ablated HUVECs stimulated with TNF-α. HUVECs transiently transfected with control siRNA or specific siRNA targeting the coding region of *Dusp6* were left untreated, or treated with pharmacological MEK inhibitors PD184352 (2 μmol/L, **left panel**), U0126 (10 μmol/L, **middle panel**) or PD98059 (10 μmol/L, **right panel**) for 1 hour, followed by TNF-α stimulation for indicated time points. Aliquots of lysates were subjected to immunoblotting with anti-ICAM-1, phospho-ERK (pERK), ERK, DUSP6 and tubulin antibodies. Compare to the control cells, DUSP6 ablation led to enhanced pERK level and suppressed ICAM-1 expression. Interestingly, application of pharmacological inhibitors in DUSP6 knockdown HUVECs effectively diminished the phosphorylation level of ERK, leading to restoration of ICAM-1 expression in the context of TNF-α signaling. Data shown are the representatives of two independent experiments.
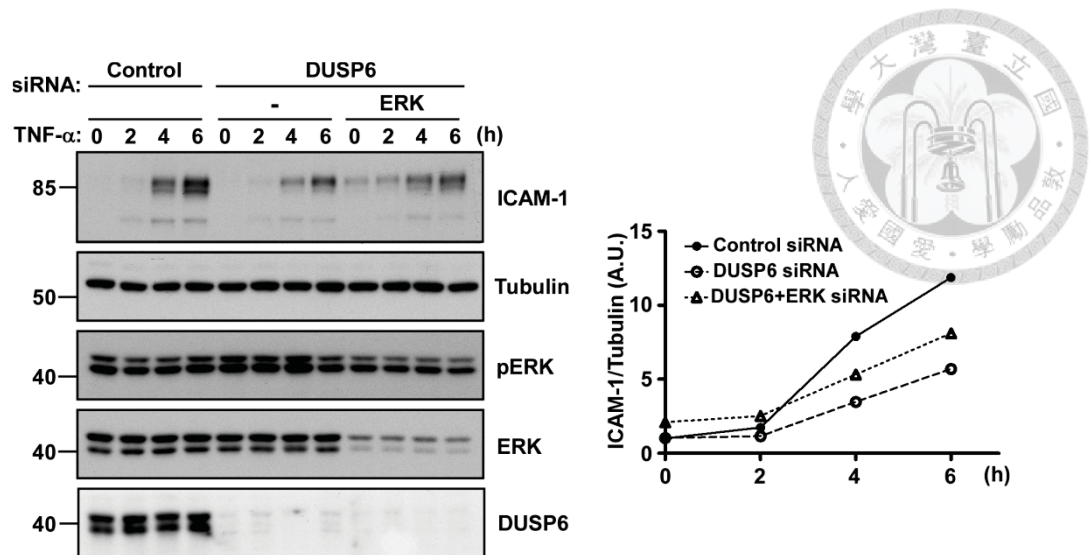
Figure 15. Inactivation of ERK by DUSP6 is required for inducible expression of ICAM-1 in HUVECs stimulated with TNF-α. HUVECs transiently transfected with control siRNA or specific siRNA targeting the coding region of *Dusp6* were left untreated or transfected with specific siRNA targeting *ERK1/2*. Transfected HUVECs were treated with TNF-α (10 ng/ml) for indicated time points. Aliquots of lysates were subjected to immunoblotting with indicated antibodies. The right panels show a densitometric analysis of the gel image as a ratio of ICAM-1 relative to tubulin. Similar results were observed in two independent experiments.
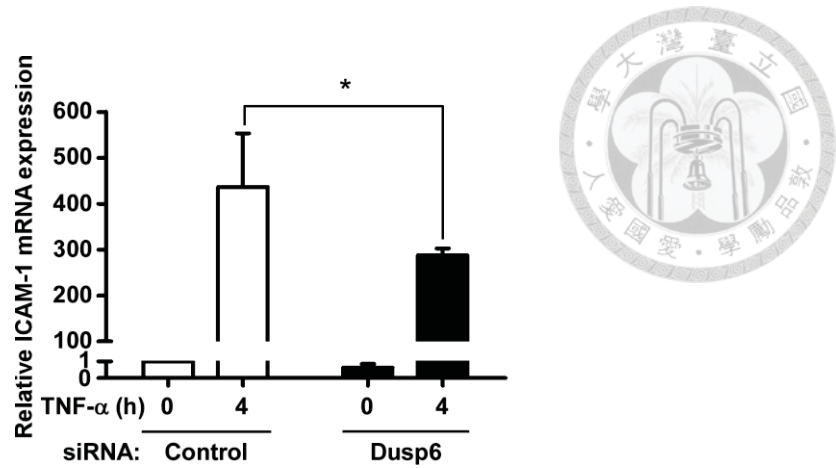
Figure 16. DUSP6 regulates ICAM-1 expression in a transcriptional-dependent manner in HUVECs stimulated with TNF-α. HUVECs were transiently transfected with control or Dusp6 siRNA. After 24 hours, cells were treated with TNF-α (10 ng/ml) for 4 hours. Total mRNA were prepared and subjected to quantitative real time-PCR analysis that depicted Dusp6 interfering effect of ICAM-1 gene expression. Data shown is presented as mean±SD (n=3; *, $P<0.05$).
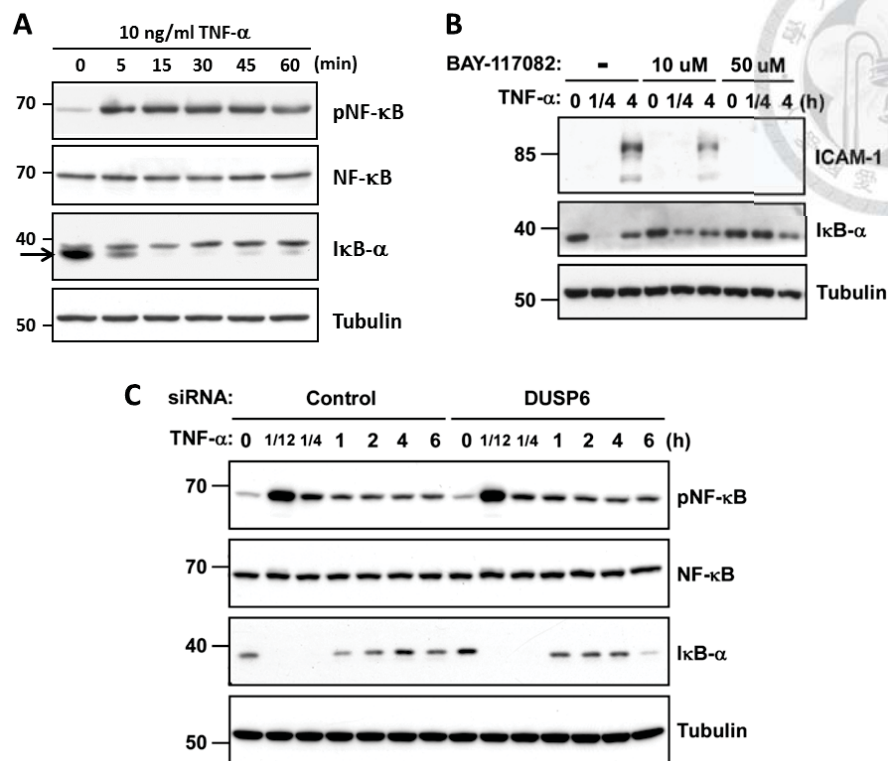
Figure 17. NF-κB is major regulator of ICAM-1 expression and DUSP6 ablation does not affect NF-κB activation in HUVECs stimulated with TNF-α. A, HUVECs were treated with TNF-α (10 ng/ml) for indicated time points. Aliquots of lysates were subjected to immunoblotting with anti-phospho-NF-κB (pNF-κB), NF-κB, IκB-α and tubulin antibodies. **B,** HUVECs were pretreated with BAY-117082 with indicated concentrations for 1 hour then followed by TNF-α (10 ng/ml) stimulation for indicated time points. Aliquots of lysates were subjected to immunoblotting with anti-ICAM-1, IκB-α and tubulin antibodies. **C,** HUVECs were transiently transfected with control or Dusp6 siRNA. After 24 hours, cells were treated with TNF-α (10 ng/ml) for indicated time points. Aliquots of lysates were subjected to immunoblotting with anti-phospho-NF-κB (pNF-κB), NF-κB, IκB-α and tubulin antibodies. Arrow in penal **A** indicates IκB-α banding. Data shown are the representatives of three independent experiments.
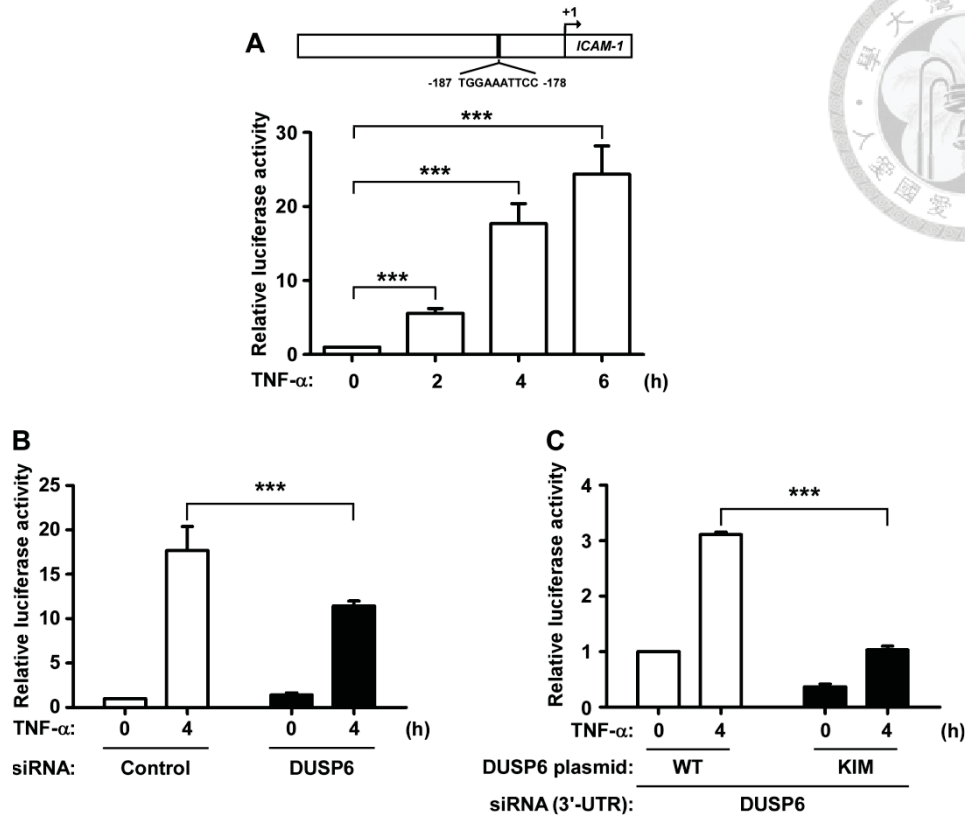
Figure 18. NF-κB-directed transcriptional activation of *ICAM-1* gene depends on termination of ERK signaling by inducible DUSP6 in HUVECs stimulated with TNF-α. A, Specific NF-κB binding motif on *ICAM-1* promoter region[2626] was used to generate the firefly luciferase reporter plasmid. HUVECs were transiently transfected with the *ICAM-1* firefly luciferase reporter plasmid and a control renilla luciferase expression plasmid. After 24 hours, cells were left untreated or stimulated with TNF-α (10 ng/ml) for indicated time points. Aliquots of lysates were subjected to analysis of firefly and renilla luciferase activity. The firefly luciferase activity was normalized with the renilla luciferase activity to eliminate the variation that might be introduced by transfection efficiency. **B,** HUVECs transiently transfected with control siRNA or specific siRNA targeting the coding region of *Dusp6* were co-transfected with firefly luciferase reporter plasmids driven by NF-κB-targeted promoter region of *ICAM-1* gene. Transfected HUVECs were then treated with TNF-α for 4 hours. Aliquots of lysates were subjected to luciferase activity assay. **C,** HUVECs transiently transfected with specific siRNA that targets the 3'-UTR region of *Dusp6* were transfected with plasmids encoding the wild type (WT) form or the kinase interacting motif (KIM) mutant form of DUSP6, and co-transfected with firefly luciferase reporter plasmids driven by NF-κB-targeted promoter region of *ICAM-1* gene. Transfected HUVECs were then treated with TNF-α for 4 hours. Aliquots of lysates were subjected to luciferase activity assay. Data shown are presented as mean±SD (n=3; ***, $P<0.001$).
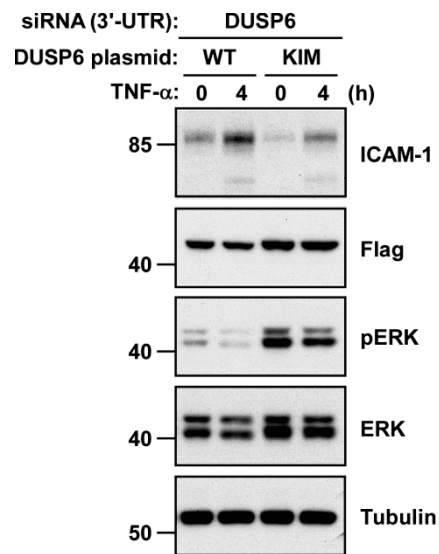
Figure 19. Inactivation of ERK by DUSP6 is required for inducible expression of ICAM-1 in HUVECs stimulated with TNF-α. HUVECs transiently transfected with specific siRNA that targets the 3'-UTR region of *Dusp6* were transfected with plasmids encoding the wild type (WT) form or the kinase interacting motif (KIM) mutant form of Flag-tagged DUSP6, followed by stimulation with TNF-α for 4 hours. Aliquots of lysates were subjected to immunoblotting with anti-ICAM-1, Flag, phospho-ERK (pERK), ERK and Tubulin antibodies. Data shown are the representatives of three independent experiments.
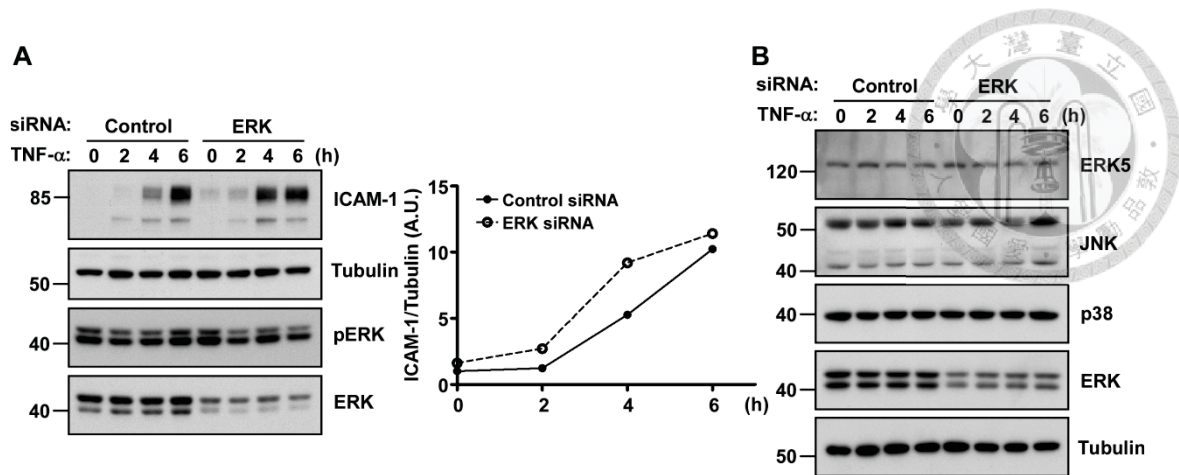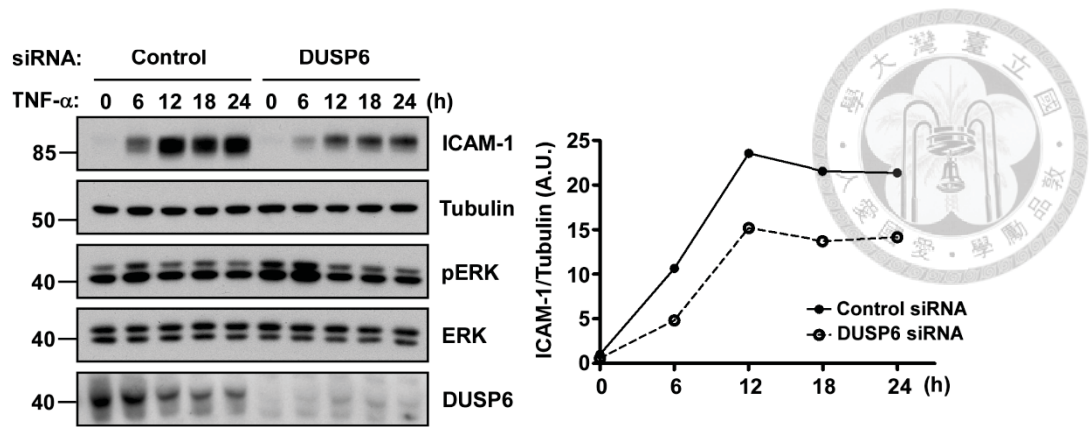
Figure 20. Ablation of DUSP6 reduced endothelial ICAM-1 expression *in vitro* after prolonged TNF-α treatment. HUVECs transiently transfected with control siRNA or specific siRNA targeting the coding region of *Dusp6* were treated with TNF-α (10 ng/ml) for indicated time points. Aliquots of lysates were subjected to immunoblotting with indicated antibodies. The right panels show a densitometric analysis of the gel image as a ratio of ICAM-1 relative to tubulin. Similar results were observed in three independent experiments.
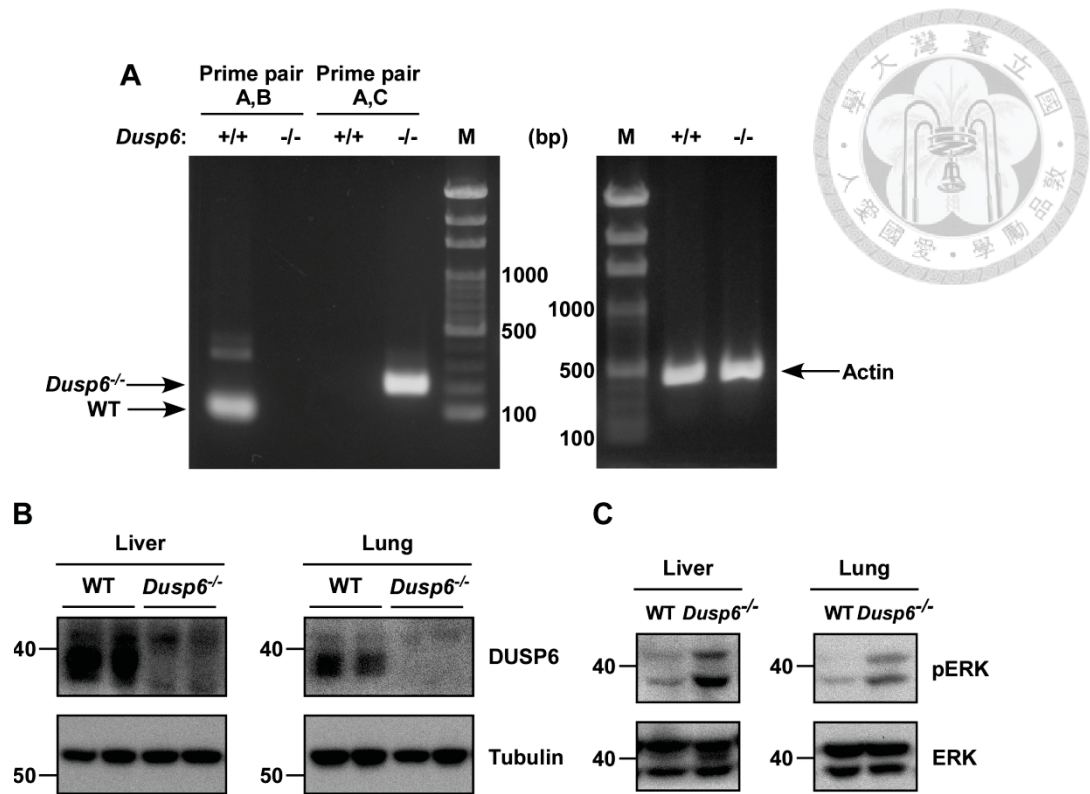
Figure 21. A loss of DUSP6 expression and an increased phosphorylation of ERK in liver and lung isolated from *Dusp6^{-/-}* mice. A, Genotyping was operated following the standard protocol suggested by The Jackson Laboratory. Sequences of specific primers A, B and C were described in the section of Genotyping in Detailed Methods. These results confirmed the genetic background of the *Dusp6* null mice. **B,** Immunoblotting results showed the absence of endogenous DUSP6 expression in liver and lung tissue extracts isolated from *Dusp6^{-/-}* mice, whereas the expression of DUSP6 was obviously detectable in tissue extracts prepared from the wild type (WT) mice. **C,** Immunoblotting results showed that phosphorylation level of endogenous ERK in liver and lung of the *Dusp6^{-/-}* mice was significantly higher compared to the WT mice.
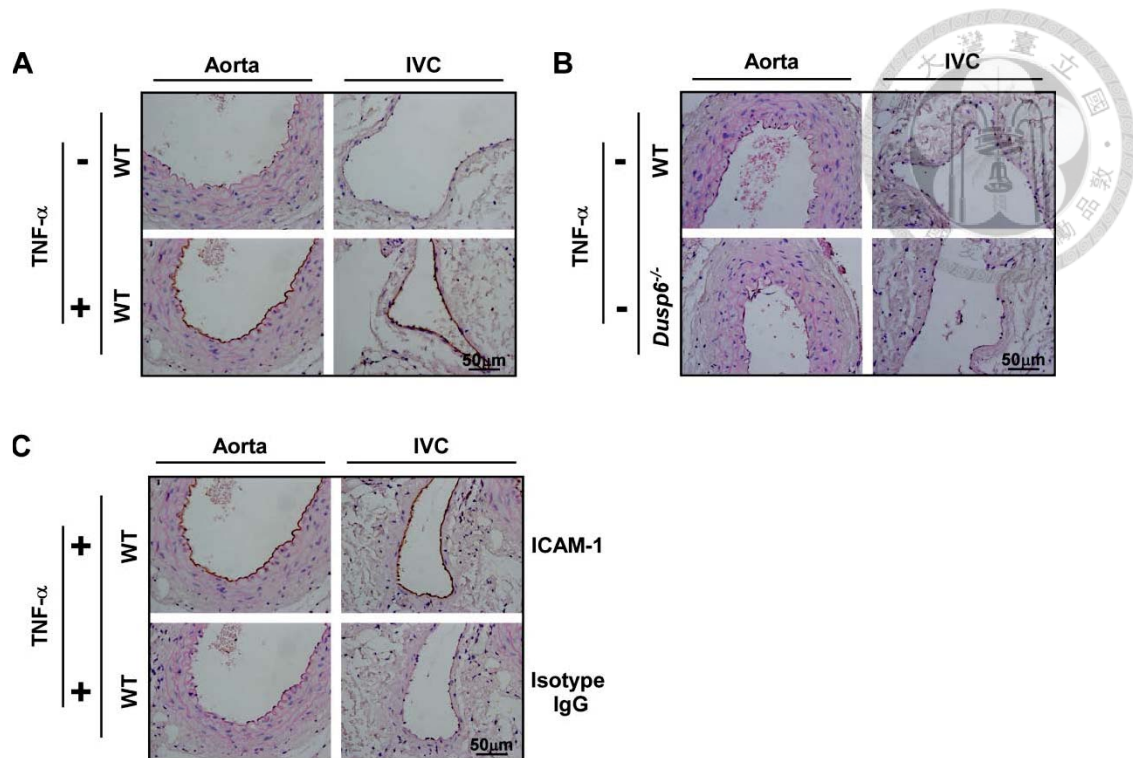
Figure 22. Specific ICAM-1 staining was observed on aorta and inferior vena cava (IVC) in the wild type (WT) mice treated with TNF-α. A to C, Wild type (WT) and *Dusp6⁻/⁻* mice were treated with PBS (-) or 5 μg/kg TNF-α (+) via tail-vein injection for 16 hours. Paraffin-embedded sections of aorta and IVC were subjected to immunohistochemistry (IHC) staining with anti-ICAM-1 antibody or isotype IgG. Representative micrograph images show ICAM-1 staining on the surface of **(A)** aorta and IVC from WT mice with or without TNF-α treatment, and **(B)** aorta and IVC from WT or *Dusp6⁻/⁻* mice without TNF-α treatment. **C,** TNF-α-induced ICAM-1 expression on the surface of aorta and IVC was visualized by the specific anti-ICAM-1 antibody but not by the isotype IgG. Data shown are representatives from two independent set of experiments (n=3 mice in each experiment). Bar in **A**, **B** and **C**, 50 μm.
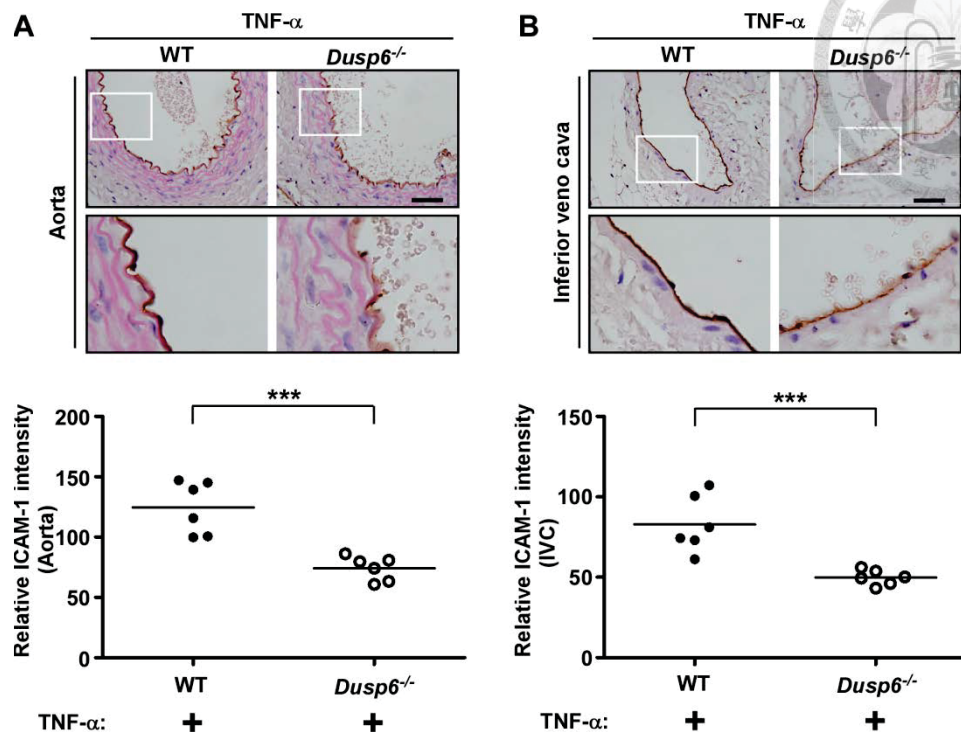
Figure 23. Ablation of DUSP6 reduced endothelial ICAM-1 expression *in vivo* after prolonged TNF-α treatment. A and B, Wild type (WT) and *Dusp6⁻/⁻* mice were treated with TNF-α (5 μg/kg) via tail-vein injection for 16 hours. Paraffin-embedded sections of aorta and inferior vena cava (IVC) were subjected to immunohistochemistry (IHC) staining with anti-ICAM-1 antibody. Representative micrograph images show ICAM-1 staining (brown color) on the surface of aorta **(A)** and IVC **(B)** from mice exposed to TNF-α. Rectangles indicate areas supplied with magnified views. Quantitation of relative ICAM-1 staining was performed by denstometric analysis of the IHC images. Data shown are presented from six mice in each group (bar, the mean of each group; ***, *P*<0.001). Bar in **A** and **B**, 50 μm.
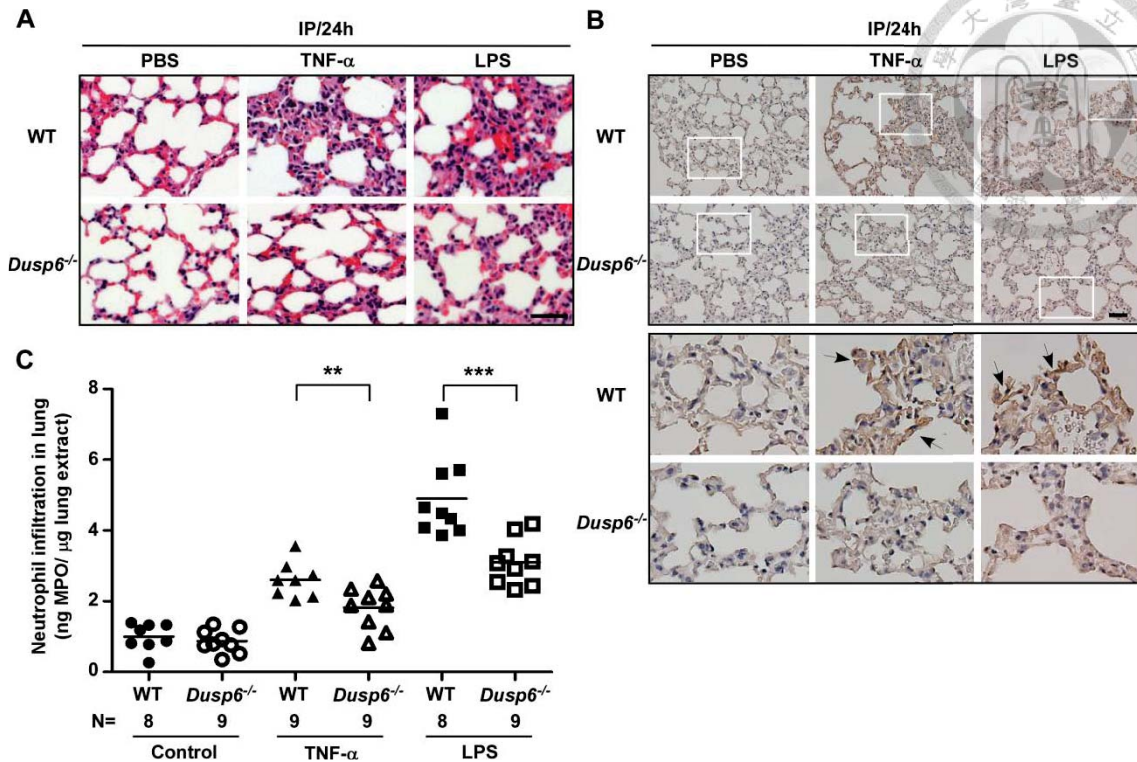
Figure 24. Deficiency of DUSP6 reduced lung injury and pulmonary neutrophil infiltration during experimental sepsis. A through **C,** Wild type (WT) and $Dusp6^{-/-}$ mice were intraperitoneally (IP) injected with TNF-α (0.1 mg/kg), LPS (10 mg/kg) or PBS for 24 hours. Paraffin-embedded lung sections were stained with hematoxylin and eosin (**A**), or subjected to immunohistochemistry staining with anti-ICAM-1 antibody (**B**). Representative micrograph images shown in **B** indicate ICAM-1 expression (brown color, and denoted by **black arrows**) on the alveolar walls from mice exposed to TNF-α or LPS. Rectangles in **B** indicate areas supplied with magnified views. **C,** Lung homogenates were subjected to the activity measurement of neutrophil-specific myeloperoxidase (MPO). Data shown in **C** are presented from 8 or 9 mice in each group (N, the number of mice; bar, the mean of each group; **, $P<0.01$ and ***, $P<0.001$). Bar in **A** and **B**, 50 μm.
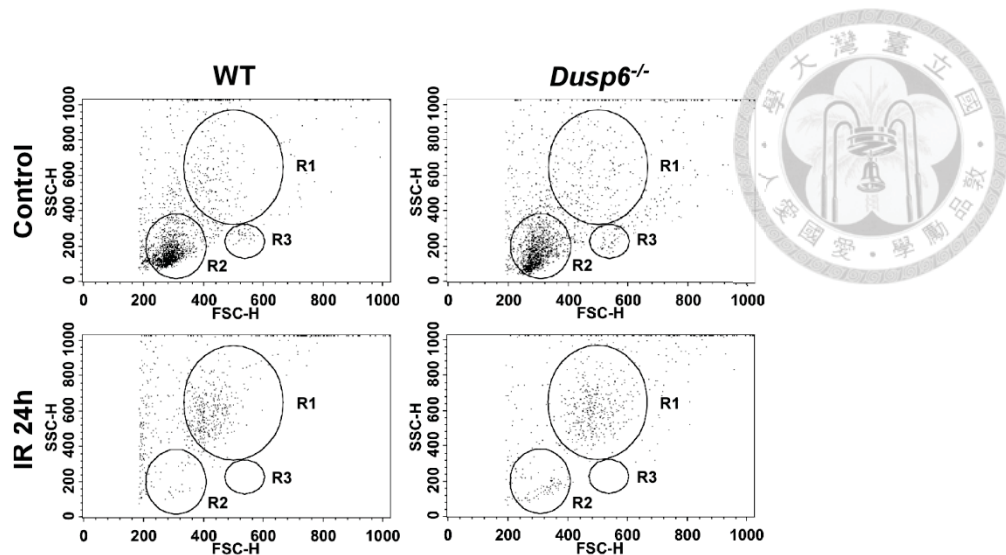
Figure 25. The effect of irradiation on leukocyte removal in mice. Wild type (WT) and *Dusp6*$^{-/-}$ mice were subjected to total body irradiation (9 Gy) or remained untreated. After 24 hours, the whole blood was taken by submandibular-bleeding and total leukocytes were analyzed by flow cytometry. There was no obvious difference in the number of total leukocytes between WT and *Dusp6*$^{-/-}$ mice without irradiation (Control). In contrast, upon irradiation for 24 hours, the number of endogenous leukocytes was significantly diminished in both genotypes of mice. Data shown are the representatives of three independent experiments (n= 3 mice per genotype in each experiment; R1-granulocytes, R2-lymphocytes, R3-monocytes).
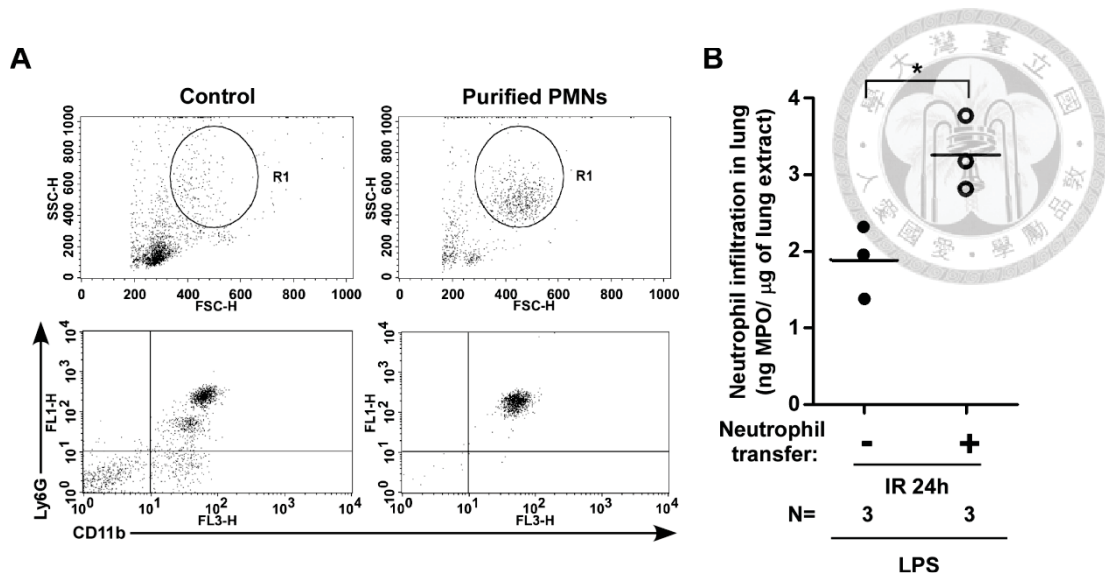
Figure 26. Purification of polymorphonuclear leukocytes (PMNs) for the adoptive transfer of neutrophils in lung during experimental sepsis. A, The whole blood from the wild type (WT) mice were taken by submandibular-bleeding, and PMNs were isolated from total leukocytes by density gradient centrifugation in Percoll. Purified PMNs were subjected to flow cytometry analysis and the enriched fraction of neutrophils (circle R1 in the top panels) was confirmed by double staining with specific markers Ly-6G and CD11b (shown in the lower panels). **B,** Purified PMNs from the WT donor mice were adoptively transferred to the irradiated (9 Gy) recipient WT mice, followed by intraperitoneal injection with LPS (10 mg/kg) into the recipient mice for 4 hours. The neutrophil infiltration into lung was analyzed by the ELISA-based detection of myeloperoxidase (MPO) activity. Compare to control mice without neutrophil transfer, recipient mice with adopted transfer developed higher degrees of neutrophil infiltration into lung. Data shown in **B** are presented from 3 mice in each group (N, the number of mice; bar, the mean of each group; *, $P<0.05$).
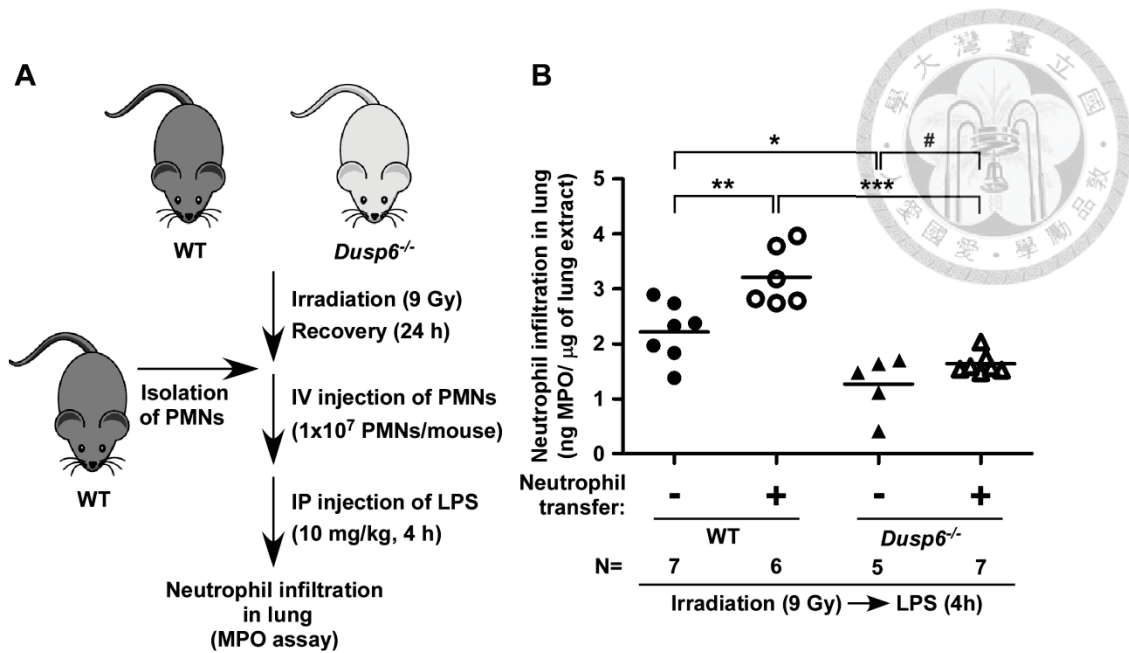
Figure 27. DUSP6 deficiency-reduced neutrophil infiltration in lung is pulmonary endothelium intrinsic. A, Schematic illustration of the workflow to assess the potential function of pulmonary endothelial DUSP6 in LPS-stimulated neutrophil infiltration in the lung tissue. Wild type (WT) and *Dusp6⁻/⁻* mice were subjected to irradiation (9 Gy) for 24 hours. The irradiated recipients were adoptively transferred with purified polymorphonuclear leukocytes (PMNs) from the WT donor mice via intravenous (IV) injection, followed by intraperitoneally (IP) treatment with LPS (10 mg/kg) for 4 hours. **B,** Lung homogenates were subjected to the activity measurement of neutrophil-specific myeloperoxidase (MPO). Data shown in **B** are presented from 5, 6 or 7 mice in each group (N, the number of mice; bar, the mean of each group; *, *P*<0.05, **, *P*<0.01 ; ***, *P*<0.001; #, no significant difference).
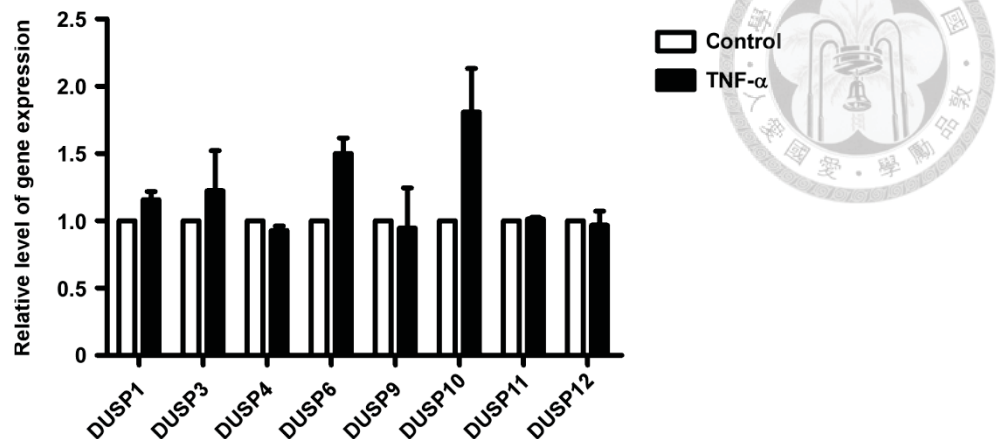
Figure 28. TNF-α-induced mRNA profile of DUSPs in HUVECs by microarray analysis. Total RNA samples were prepared from HUVECs exposed to TNF-α for one hour. Microarray analysis (Human Genome U133 Plus 2.0 Array from Affymetrix) was performed according to the manufacturer's instructions. A subset of DUSPs with implied function of MAP kinase phosphatases was the primary focus. Data are presented as the mean±SE (n=2). According to the data shown in the Figure, we proposed that, among four ERK-specific phosphatases (DUSP1, 4, 6 and 9), DUSP6 was the only one exhibiting significant mRNA induction in endothelium response to TNF-α stimulation.
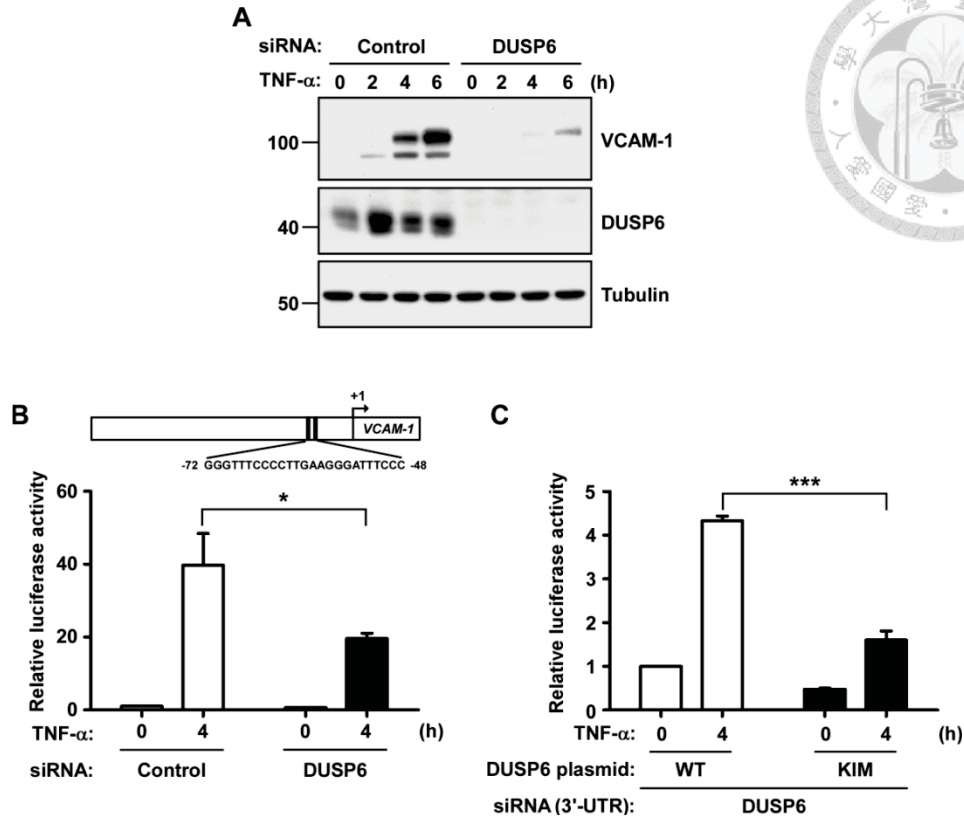
Figure 29. NF-κB-directed transcriptional activation of *VCAM-1* gene depends on termination of ERK signaling by inducible DUSP6 in HUVECs stimulated with TNF-α. A, HUVECs transiently transfected with control siRNA or specific siRNA that targets the coding region of *Dusp6* were treated with TNF-α (10 ng/ml) for indicated time points. Aliquots of lysates were subjected to immunoblotting with anti-VCAM-1, DUSP6 and Tubulin antibodies. Data shown are the representative from three independent experiments. **B,** HUVECs transiently transfected with control siRNA or specific siRNA targeting the coding region of *Dusp6* were co-transfected with firefly luciferase reporter plasmids driven by the NF-κB-targeted promoter region of *VCAM-1* gene (nucleotides -72~-48). Transfected HUVECs were then treated with TNF-α for 4 hours. Aliquots of lysates were subjected to luciferase activity assay. **C,** HUVECs transiently transfected with specific siRNA that targets the 3'-UTR region of *Dusp6* were transfected with plasmids encoding the wild type (WT) form or the kinase interacting motif (KIM) mutant form of DUSP6, and then co-transfected with firefly luciferase reporter plasmids driven by NF-κB-targeted promoter region of *VCAM-1* gene. Transfected HUVECs were subsequently treated with TNF-α for 4 hours. Aliquots of lysates were subjected to luciferase activity assay. Data shown in **B** and **C** are presented as mean±SD (n=3; *, $P<0.05$, ***, $P<0.001$).
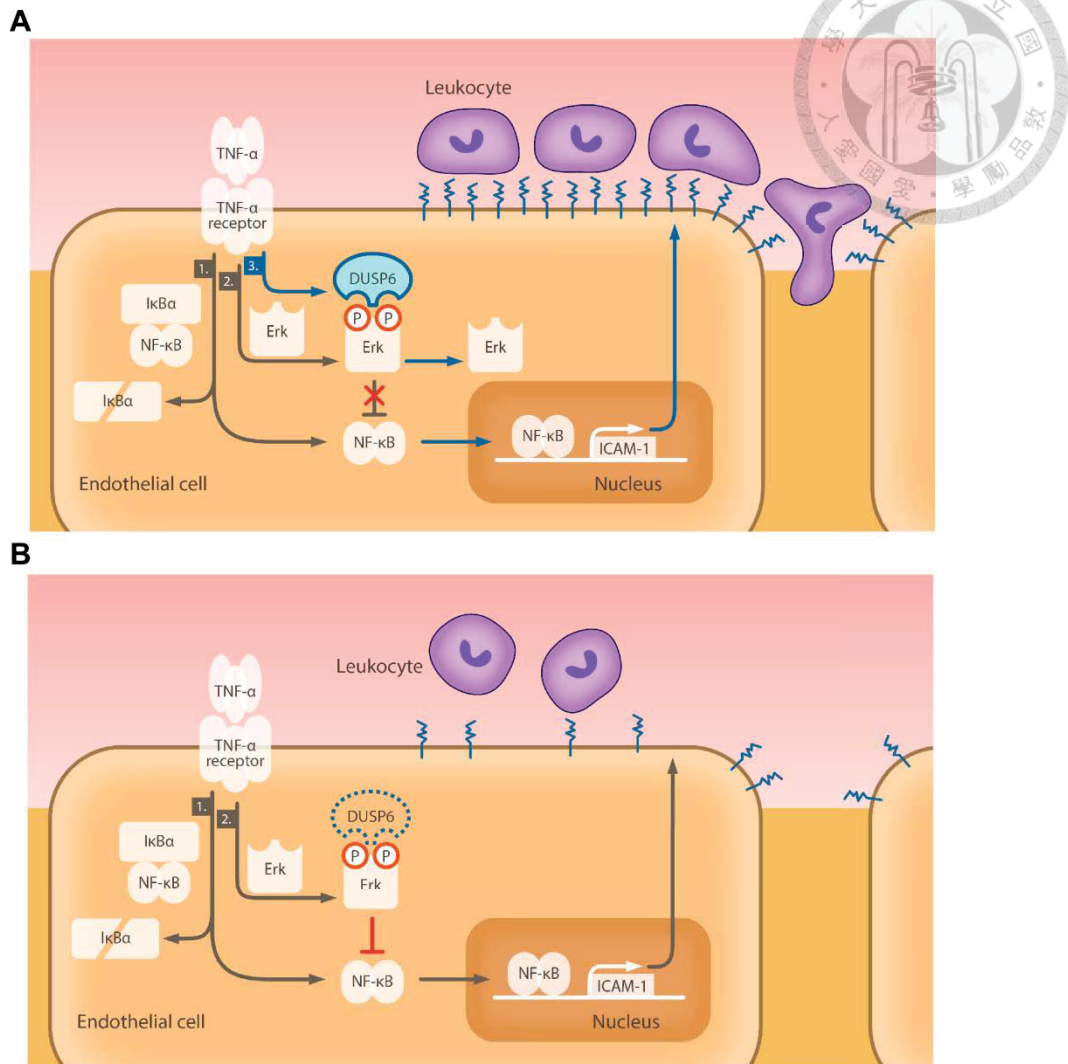
Figure 30. Proposed model for the functional role of endothelial DUSP6 in regulating vascular inflammation. A, Ligand-bound TNF-α receptor drives (1) release of NF-κB dimer from the IκB complex, (2) activation of ERK and (3) inducible expression of DUSP6 in vascular endothelium. Dephosphorylation of ERK by DUSP6 unleashes NF-κB from the inhibitory constraint. Consequently, NF-κB-dependent expression of ICAM-1 leads to recruitment of leukocytes, thus promoting inflammatory response. **B,** Upon gene deletion of *Dusp6* or chemical inhibition of DUSP6, activation of ERK is sustained in TNF-α-stimulated endothelium. Therefore, NF-κB dimer is prevented from transcriptional activation. As a result, low levels of ICAM-1 on endothelial surface decrease inflammatory response.

Flowchart of SILAC-based approach
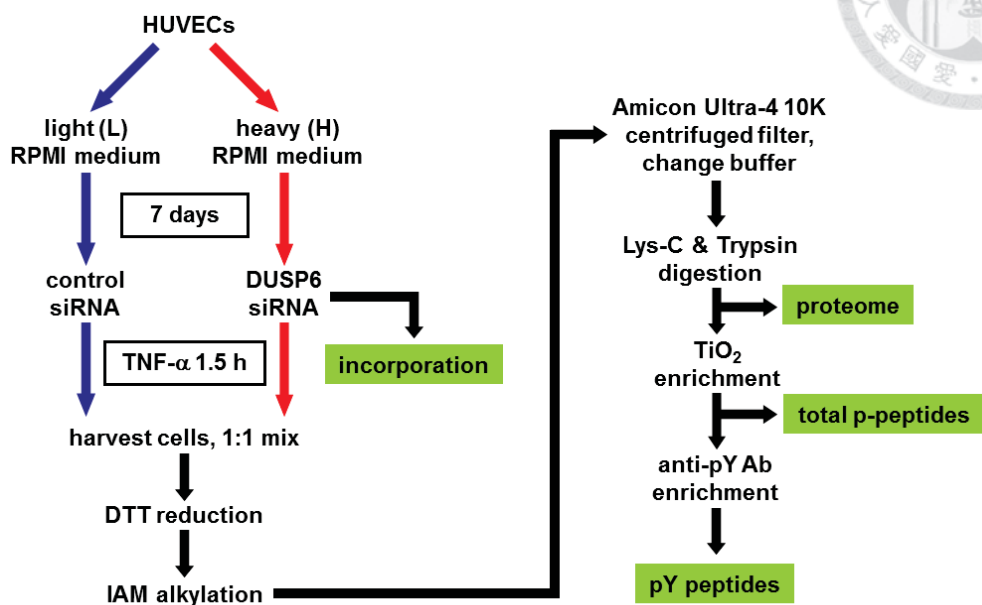
Scheme 1. Quantitative phosphoproteomic workflow. The procedure combines isotopic amino acid incorporation, sample preparation, protein digestion, phosphopeptide enrichment (TiO$_2$), and phosphotyrosine peptides enrichment.
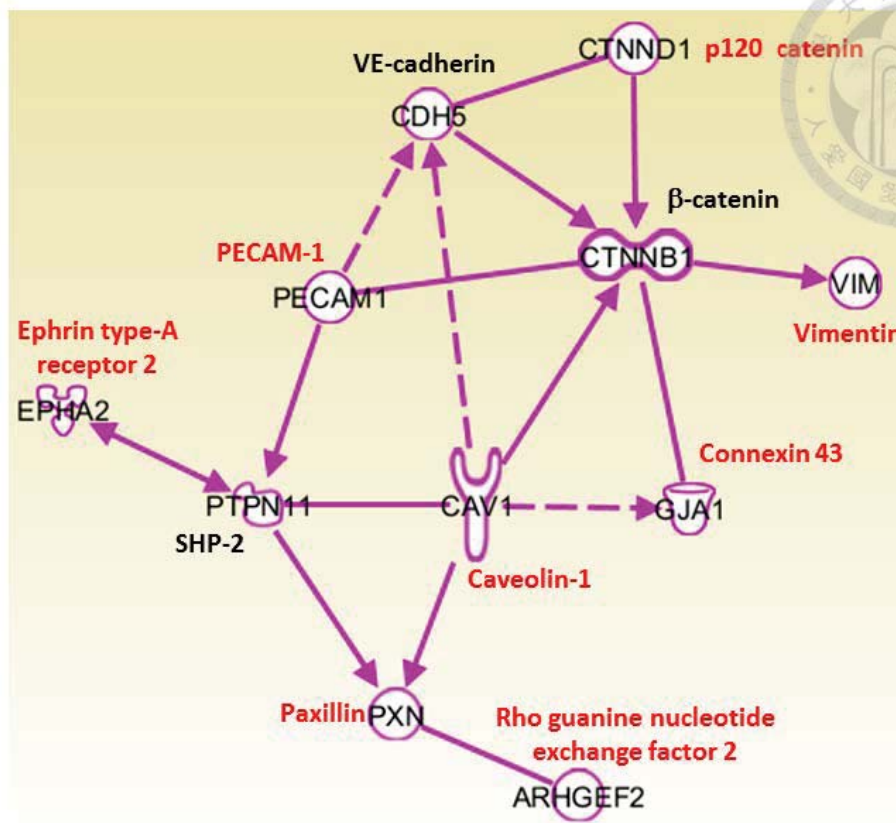
Figure 31. Sub-network indicates proteins involved in cell junction and focal adhesion derived from IPA analysis. The sub-network was drawn using the connection and growth algorithm of the ingenuity pathway analysis (IPA) software. The protein labeled in red indicates up-regulated phosphoproteins in SILAC analysis. The line indicates protein-protein interaction and/or enzymatic regulation of adjacent proteins.

Table 1.

Primers used for quantitative real-time PCR analysis

Gene name	Accession number	Primer sequence
DUSP1	NM_004417	Forward: 5'-**TTTGAGGGTCACTACCAG**-3'
		Reverse: 5'-**GAGATGATGCTTCGCC**-3'
DUSP2	NM_004418	Forward: 5'-**AGTCACTCGTCAGACC**-3'
		Reverse: 5'-**TGTTCTTCACCCAGTCAAT**-3'
DUSP3	NM_004090	Forward: 5'-**ACGTCAACACCAATGC**-3'
		Reverse: 5'-**ATGAGGTAGGCGATAACT**-3'
DUSP4	NM_001394	Forward: 5'-**CAAAGGCGGCTATGAG**-3'
		Reverse: 5'-**GGTTATCTTCCACTGGG**-3'
DUSP5	NM_004419	Forward: 5'-**CTAGGTGTTGCGTGGA**-3'
		Reverse: 5'-**GATCTATTGCTTCTTGAAAGT**-3'
DUSP6	NM_001946	Forward: 5'-**CGAGACCCCAATAGTGC**-3'
		Reverse: 5'-**AATGGCCTCAGGGAAA**-3'
DUSP7	NM_001947	Forward: 5'-**TCATTGACGAAGCCCG**-3'
		Reverse: 5'-**GCGTATTGAGTGGGAACA**-3'
DUSP8	NM_004420	Forward: 5'-**GACGCAAAATGGAATAAGC**-3'
		Reverse: 5'-**CTTCACGAACCTGTAGGC**-3'
DUSP9	NM_001395	Forward: 5'-**ATCCGCTACATCCTCAA**-3'
		Reverse: 5'-**AGGTCATAGGCATCGTT**-3'
DUSP10	NM_007207	Forward: 5'-**CTGAACATCGGCTACG**-3'
		Reverse: 5'-**GGTGTAAGGATTCTCGGT**-3'
DUSP14	NM_007026	Forward: 5'-**CTGCTCACTTAGGACTTTCT**-3'
		Reverse: 5'-**CCTTGGTAGCGTGCTG**-3'
DUSP16	NM_030640	Forward: 5'-**AGAATGGGATTGGTTATGTG**-3'
		Reverse: 5'-**TGTAGGCGATAGCGATG**-3'
ICAM-1	NM_000201	Forward: 5'-**GATACAACCGTCTTGGTCAGCCC**-3'
		Reverse:5'-**CAGTTGAAGGATGCGGGAGTATATG**-3'
VCAM-1	NM_001078	Forward: 5'-**TGCCGAGCTAAATTACACATTG**-3'
		Reverse: 5'-**CCTTGTGGAGGGATGTACAGA**-3'
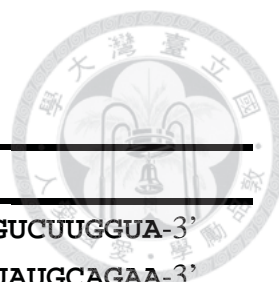
Table 2.

Oligonucleotides of siRNA used for *dusp6* knockdown

Gene name	Catalog number*	siRNA sequence
DUSP6	D-003964-01	5'-**GAACUGUGGUGUCUUGGUA**-3'
	D-003964-03	5'-**UGGCUUACCUUAUGCAGAA**-3'
	D-003964-04	5'-**GACUGUGGCUUACCUUAUG**-3'
	D-003964-05	5'-**GCGACUGGAACGAGAAUAC**-3'
DUSP6 (3'-UTR)	None	5'-**CUGAUACUCCAUUUGAUUAUU**-3'
Non-targeting	D-001810-01	5'-**UGGUUUACAUGUCGACUAA**-3'

* Catalog numbers provided by Dharmacon
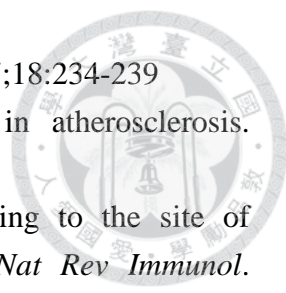
Table 3.
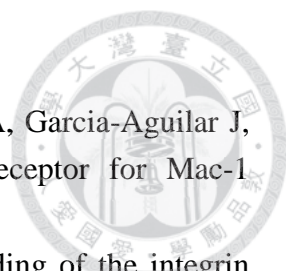
List of the identified up-regulated phosphoproteins in DUSP6-ablated HUVECs

Protein Names	PTM Score	Ratio H/L	PhosphoSTY (STY) Probabilities
Vimentin	78.875	7.9152	S(1)RLGDLYEEEMR
Nestin	70.439	5.1826	S(1)LDQEIARPLENENQEFLK
MAPK3	105.65	3.8955	IADPEHDHTGFLT(0.012)EY(0.986)VAT(0.002)R
MAPK1	95.966	3.8053	VADPDHDHTGFLT(0.002)EY(0.987)VAT(0.011)R
Thymosin beta-10	101.53	3.719	ADKPDMGEIAS(1)FDK
Heme oxygenase 1	69.667	3.5229	DQS(0.954)PS(0.046)RAPGLR
Neuroblast differentiation-associated protein AHNAK	121.34	2.7094	LKS(1)EDGVEGDLGETQSR
Metastasis-associated protein MTA2	82.295	2.5995	GHLSRPEAQS(0.121)LS(0.872)PY(0.003)T(0.003)T(0.001)S(0.001)ANR
WD repeat-containing protein 44	69.159	2.564	S(0.804)NS(0.155)GRELT(0.041)DEEILASVMIK
Adenylyl cyclase-associated protein 1	114.1	2.3664	PFSAPKPQT(0.909)S(0.09)PS(0.001)PK
Cell division protein kinase 3	137.54	2.313	IGEGT(0.001)Y(0.999)GVVYK
Serine/threonine-protein kinase N2	76.09	2.3019	AS(0.123)S(0.877)LGEIDESSELR
Platelet endothelial cell adhesion molecule	81.616	2.2931	DTETVY(0.995)S(0.005)EVRK
Ephrin type-A receptor 2	62.998	2.2448	QS(0.002)PEDVY(0.987)FS(0.011)K
Serine/threonine-protein kinase receptor R3	114.1	2.2057	GLHSELGES(0.948)S(0.052)LILK
Nestin	101.53	2.1597	S(0.104)LRS(0.896)LEEQDQETLR
Eukaryotic translation initiation factor 1	97.956	2.048	S(0.985)AIQNLHS(0.012)FDPFADAS(0.003)K
Ephrin type-A receptor 2	62.998	2.0097	QSPEDVY(0.001)FS(0.999)K
TBC1 domain family member 4	104.43	2.0054	RSLTS(0.001)S(0.999)LENIFSR
Trans-Golgi network integral membrane protein 2	69.159	1.9625	DS(0.115)PS(0.751)KS(0.019)S(0.115)AEAQTPEDTPNK
Sphingosine-1-phosphate phosphatase 1	82.955	1.9245	RNS(0.994)LT(0.006)GEEGQLAR
High mobility group protein HMG-I/HMG-Y	96.484	1.8938	KQPPVSPGT(0.004)ALVGS(0.995)QKEPS(0.001)EVPTPK
Platelet endothelial cell adhesion molecule	62.185	1.8389	EPLNS(0.147)DVQY(0.823)T(0.029)EVQVSSAESHK
Nexilin	80.761	1.7835	RAEQIEDINNT(0.801)GT(0.033)ES(0.158)AS(0.007)EEGDDSLLITVVPVK
Adenylyl cyclase-associated protein 1	114.1	1.7655	PFSAPKPQT(0.003)S(0.968)PS(0.028)PK
Nestin	97.769	1.7339	S(1)LGEEIQESLK
Paxillin	140.37	1.7083	PGSQLDSMLGS(1)LQSDLNK
E3 ubiquitin-protein ligase RAD18	107.9	1.7064	NDLQDTEIS(1)PR
MLN64 N-terminal domain homolog	97.769	1.7036	LLIVQDAS(1)ER
Palladin	104.29	1.7021	IAS(1)DEEIQGTK
Transcription factor AP-1	186.77	1.6877	NSDLLT(0.001)S(0.999)PDVGLLK
Eukaryotic translation initiation factor 1	97.956	1.6859	SAIQNLHS(1)FDPFADASK
LIM domain only protein 7	123.3	1.6371	VTTEIQLPS(0.107)QS(0.893)PVEEQSPASLSSLR
Platelet endothelial cell adhesion molecule	81.616	1.6292	DTETVY(0.94)S(0.06)EVRK
WD repeat-containing protein 44	101.53	1.6248	ELSDQAT(0.005)AS(0.995)PIVAR
Centrosomal protein 170kDa	101.53	1.6106	ARLGEAS(0.992)DS(0.008)ELADADK
Tyrosine-protein kinase SgK269	88.753	1.609	ANTLS(1)PVR
Actin-binding protein anillin	61.011	1.5967	AAS(0.969)PPRPLLS(0.031)NASATPVGR
Nuclear fragile X mental retardation-interacting protein 2	166.57	1.5883	DYEIESQNPLAS(0.996)PT(0.004)NTLLGSAK
Neuron navigator 1	88.268	1.5869	AVALDS(0.003)DNIS(0.997)LK
Cdc42 effector protein 1	110.05	1.5867	RSDS(1)LLSFR
PDZ and LIM domain protein 5	87.563	1.5837	YTEFY(1)HVPTHSDASK
Arginine-glutamic acid dipeptide repeats protein	71.758	1.5777	KQPAS(1)PDGRT(0.874)S(0.127)PINEDIR
Arginine-glutamic acid dipeptide repeats protein	71.758	1.5777	KQPAS(1)PDGRT(0.874)S(0.127)PINEDIR
Phosphatase and actin regulator 2	146.92	1.5769	ASIANSDGPTAGSQT(1)PPFK
Pre-B-cell leukemia transcription factor-interacting protein 1	74.948	1.5752	ALQAPHS(0.995)PS(0.005)K
Nucleolin	88.753	1.5741	VVVS(0.993)PT(0.007)KK
Centrosomal protein 170kDa	80.533	1.5736	LGSLSARS(0.914)DS(0.085)EATISR
Histone H1.4	141.09	1.5599	SETAPAAPAAPAPAEKT(1)PVK
Annexin A2	140.37	1.5485	LSLEGDHSTPPS(0.054)AY(0.946)GSVK
Caveolin-1	73.06	1.5394	YVDS(0.002)EGHLY(0.897)T(0.101)VPIR
Catenin delta-1	74.948	1.5305	VGGS(0.002)S(0.998)VDLHR
Mitochondrial import receptor subunit TOM34	91.202	1.5227	NRVPS(1)AGDVEK
Gap junction alpha-1 protein	64.385	1.5225	LAAGHELQPLAIVDQRPS(0.178)S(0.822)R
DNA ligase 1	86.649	1.5176	RTIQEVLEEQS(1)EDEDREAK
Telomere-associated protein RIF1	94.905	1.51	RSQEDEIS(0.06)S(0.94)PVNK
Rho guanine nucleotide exchange factor 2	78.251	1.5095	ERPS(0.078)S(0.921)AIY(0.001)PSDSFR

CHAPTER7: REFERENCES

1. Jaffe EA. Cell biology of endothelial cells. *Hum Pathol*. 1987;18:234-239

2. Davignon J, Ganz P. Role of endothelial dysfunction in atherosclerosis. *Circulation*. 2004;109:III27-32

3. Ley K, Laudanna C, Cybulsky MI, Nourshargh S. Getting to the site of inflammation: the leukocyte adhesion cascade updated. *Nat Rev Immunol*. 2007;7:678-689

4. Hickey MJ, Kubes P. Intravascular immunity: the host-pathogen encounter in blood vessels. *Nat Rev Immunol*. 2009;9:364-375

5. Rittirsch D, Flierl MA, Ward PA. Harmful molecular mechanisms in sepsis. *Nat Rev Immunol*. 2008;8:776-787

6. Hotchkiss RS, Karl IE. The pathophysiology and treatment of sepsis. *N Engl J Med*. 2003;348:138-150

7. Aird WC. The role of the endothelium in severe sepsis and multiple organ dysfunction syndrome. *Blood*. 2003;101:3765-3777

8. Waters JP, Pober JS, Bradley JR. Tumour necrosis factor in infectious disease. *J Pathol*. 2013;230:132-147

9. Zhang H, Park Y, Wu J, Chen X, Lee S, Yang J, Dellsperger KC, Zhang C. Role of TNF-α in vascular dysfunction. *Clin Sci (Lond)*. 2009;116:219-230

10. Bradley JR. TNF-mediated inflammatory disease. *J Pathol*. 2008;214:149-160

11. Smith CW, Rothlein R, Hughes BJ, Mariscalco MM, Rudloff HE, Schmalstieg FC, Anderson DC. Recognition of an endothelial determinant for CD 18-dependent human neutrophil adherence and transendothelial migration. *J Clin Invest*. 1988;82:1746-1756

12. Smith CW, Marlin SD, Rothlein R, Toman C, Anderson DC. Cooperative interactions of LFA-1 and Mac-1 with intercellular adhesion molecule-1 in facilitating adherence and transendothelial migration of human neutrophils in vitro. *J Clin Invest*. 1989;83:2008-2017

13. Burns AR, Takei F, Doerschuk CM. Quantitation of ICAM-1 expression in mouse lung during pneumonia. *J Immunol*. 1994;153:3189-3198

14. Burns AR, Smith CW, Walker DC. Unique structural features that influence neutrophil emigration into the lung. *Physiol Rev*. 2003;83:309-336

15. Springer TA. Adhesion receptors of the immune system. *Nature*. 1990;346:425-434

16. Staunton DE, Marlin SD, Stratowa C, Dustin ML, Springer TA. Primary structure of ICAM-1 demonstrates interaction between members of the immunoglobulin and integrin supergene families. *Cell*. 1988;52:925-933

17. Staunton DE, Merluzzi VJ, Rothlein R, Barton R, Marlin SD, Springer TA. A cell adhesion molecule, ICAM-1, is the major surface receptor for rhinoviruses.
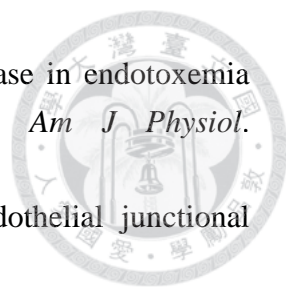
Cell. 1989;56:849-853

18. Diamond MS, Staunton DE, de Fougerolles AR, Stacker SA, Garcia-Aguilar J, Hibbs ML, Springer TA. ICAM-1 (CD54): A counter-receptor for Mac-1 (CD11b/CD18). *J Cell Biol*. 1990;111:3129-3139

19. Diamond MS, Staunton DE, Marlin SD, Springer TA. Binding of the integrin Mac-1 (CD11b/CD18) to the third immunoglobulin-like domain of ICAM-1 (CD54) and its regulation by glycosylation. *Cell*. 1991;65:961-971

20. Rao RM, Yang L, Garcia-Cardena G, Luscinskas FW. Endothelial-dependent mechanisms of leukocyte recruitment to the vascular wall. *Circ Res*. 2007;101:234-247

21. Rahman A, Fazal F. Hug tightly and say goodbye: Role of endothelial ICAM-1 in leukocyte transmigration. *Antioxid Redox Signal*. 2009;11:823-839

22. Scheidereit C. IκB kinase complexes: Gateways to NF-κB activation and transcription. *Oncogene*. 2006;25:6685-6705

23. Voraberger G, Schafer R, Stratowa C. Cloning of the human gene for intercellular adhesion molecule 1 and analysis of its 5'-regulatory region. Induction by cytokines and phorbol ester. *J Immunol*. 1991;147:2777-2786

24. Ledebur HC, Parks TP. Transcriptional regulation of the intercellular adhesion molecule-1 gene by inflammatory cytokines in human endothelial cells. Essential roles of a variant NF-kB site and p65 homodimers. *J Biol Chem*. 1995;270:933-943

25. Rahman A, Anwar KN, True AL, Malik AB. Thrombin-induced p65 homodimer binding to downstream NF-κB site of the promoter mediates endothelial ICAM-1 expression and neutrophil adhesion. *J Immunol*. 1999;162:5466-5476

26. Xue J, Thippegowda PB, Hu G, Bachmaier K, Christman JW, Malik AB, Tiruppathi C. NF-κB regulates thrombin-induced ICAM-1 gene expression in cooperation with NFAT by binding to the intronic NF-κB site in the ICAM-1 gene. *Physiol Genomics*. 2009;38:42-53

27. MacEwan DJ. TNF receptor subtype signalling: Differences and cellular consequences. *Cell Signal*. 2002;14:477-492

28. Schmitz ML, Bacher S, Kracht M. IκB-independent control of NF-κB activity by modulatory phosphorylations. *Trends Biochem Sci*. 2001;26:186-190

29. Jersmann HP, Hii CS, Ferrante JV, Ferrante A. Bacterial lipopolysaccharide and tumor necrosis factor alpha synergistically increase expression of human endothelial adhesion molecules through activation of NF-κB and p38 mitogen-activated protein kinase signaling pathways. *Infect Immun*. 2001;69:1273-1279

30. Lin SJ, Shyue SK, Hung YY, Chen YH, Ku HH, Chen JW, Tam KB, Chen YL.

Superoxide dismutase inhibits the expression of vascular cell adhesion molecule-1 and intracellular cell adhesion molecule-1 induced by tumor necrosis factor-α in human endothelial cells through the JNK/p38 pathways. *Arterioscler Thromb Vasc Biol*. 2005;25:334-340

31. Yoshizumi M, Fujita Y, Izawa Y, Suzaki Y, Kyaw M, Ali N, Tsuchiya K, Kagami S, Yano S, Sone S, Tamaki T. Ebselen inhibits tumor necrosis factor-α-induced c-Jun N-terminal kinase activation and adhesion molecule expression in endothelial cells. *Exp Cell Res*. 2004;292:1-10

32. Carter AB, Hunninghake GW. A constitutive active MEK --> ERK pathway negatively regulates NF-κB-dependent gene expression by modulating TATA-binding protein phosphorylation. *J Biol Chem*. 2000;275:27858-27864

33. Yeh PY, Yeh KH, Chuang SE, Song YC, Cheng AL. Suppression of MEK/ERK signaling pathway enhances cisplatin-induced NF-κB activation by protein phosphatase 4-mediated NF-κB p65 thr dephosphorylation. *J Biol Chem*. 2004;279:26143-26148

34. Maeng YS, Min JK, Kim JH, Yamagishi A, Mochizuki N, Kwon JY, Park YW, Kim YM, Kwon YG. ERK is an anti-inflammatory signal that suppresses expression of NF-κB-dependent inflammatory genes by inhibiting IKK activity in endothelial cells. *Cell Signal*. 2006;18:994-1005

35. Tonks NK. Protein tyrosine phosphatases: From genes, to function, to disease. *Nat Rev Mol Cell Biol*. 2006;7:833-846

36. Owens DM, Keyse SM. Differential regulation of MAP kinase signalling by dual-specificity protein phosphatases. *Oncogene*. 2007;26:3203-3213

37. Camps M, Nichols A, Arkinstall S. Dual specificity phosphatases: a gene family for control of MAP kinase function. *FASEB J*. 2000;14:6-16

38. Caunt CJ, Keyse SM. Dual-specificity MAP kinase phosphatases (MKPs): Shaping the outcome of MAP kinase signalling. *FEBS J*. 2013;280:489-504

39. Zhang Y, Blattman JN, Kennedy NJ, Duong J, Nguyen T, Wang Y, Davis RJ, Greenberg PD, Flavell RA, Dong C. Regulation of innate and adaptive immune responses by MAP kinase phosphatase 5. *Nature*. 2004;430:793-797

40. Masuda K, Shima H, Watanabe M, Kikuchi K. MKP-7, a novel mitogen-activated protein kinase phosphatase, functions as a shuttle protein. *J Biol Chem*. 2001;276:39002-39011

41. Karlsson M, Mathers J, Dickinson RJ, Mandl M, Keyse SM. Both nuclear-cytoplasmic shuttling of the dual specificity phosphatase MKP-3 and its ability to anchor MAP kinase in the cytoplasm are mediated by a conserved nuclear export signal. *J Biol Chem*. 2004;279:41882-41891

42. Wang X, Meng X, Kuhlman JR, Nelin LD, Nicol KK, English BK, Liu Y.

Knockout of *MKP-1* enhances the host inflammatory responses to gram-positive bacteria. *J Immunol*. 2007;178:5312-5320

43.   Frazier WJ, Wang X, Wancket LM, Li XA, Meng X, Nelin LD, Cato AC, Liu Y. Increased inflammation, impaired bacterial clearance, and metabolic disruption after gram-negative sepsis in *MKP-1*-deficient mice. *J Immunol*. 2009;183:7411-7419

44.   Jeffrey KL, Brummer T, Rolph MS, Liu SM, Callejas NA, Grumont RJ, Gillieron C, Mackay F, Grey S, Camps M, Rommel C, Gerondakis SD, Mackay CR. Positive regulation of immune cell function and inflammatory responses by phosphatase PAC-1. *Nat Immunol*. 2006;7:274-283

45.   Al-Mutairi M, Al-Harthi S, Cadalbert L, Plevin R. Over-expression of mitogen-activated protein kinase phosphatase-2 enhances adhesion molecule expression and protects against apoptosis in human endothelial cells. *Br J Pharmacol*. 2010;161:782-798

46.   Cornell TT, Rodenhouse P, Cai Q, Sun L, Shanley TP. Mitogen-activated protein kinase phosphatase 2 regulates the inflammatory response in sepsis. *Infect Immun*. 2010;78:2868-2876

47.   Qian F, Deng J, Gantner BN, Flavell RA, Dong C, Christman JW, Ye RD. MAP kinase phosphatase 5 protects against sepsis-induced acute lung injury. *Am J Physiol Lung Cell Mol Physiol*. 2012;302:L866-874

48.   Jeffrey KL, Camps M, Rommel C, Mackay CR. Targeting dual-specificity phosphatases: Manipulating MAP kinase signalling and immune responses. *Nat Rev Drug Discov*. 2007;6:391-403

49.   Zhou Z, Connell MC, MacEwan DJ. TNFR1-induced NF-κB, but not ERK, p38MAPK or JNK activation, mediates TNF-induced ICAM-1 and VCAM-1 expression on endothelial cells. *Cell Signal*. 2007;19:1238-1248

50.   Lee SE, Chung WJ, Kwak HB, Chung CH, Kwack KB, Lee ZH, Kim HH. Tumor necrosis factor-α supports the survival of osteoclasts through the activation of Akt and ERK. *J Biol Chem*. 2001;276:49343-49349

51.   Lenormand P, Sardet C, Pages G, L'Allemain G, Brunet A, Pouyssegur J. Growth factors induce nuclear translocation of MAP kinases (p42^{mapk} and p44^{mapk}) but not of their activator MAP kinase kinase (p45^{mapkk}) in fibroblasts. *J Cell Biol*. 1993;122:1079-1088

52.   Moreland JG, Fuhrman RM, Pruessner JA, Schwartz DA. CD11b and intercellular adhesion molecule-1 are involved in pulmonary neutrophil recruitment in lipopolysaccharide-induced airway disease. *Am J Respir Cell Mol Biol*. 2002;27:474-480

53.   Basit A, Reutershan J, Morris MA, Solga M, Rose CE, Jr., Ley K. ICAM-1 and

LFA-1 play critical roles in LPS-induced neutrophil recruitment into the alveolar space. *Am J Physiol Lung Cell Mol Physiol*. 2006;291:L200-207

54. Ekerot M, Stavridis MP, Delavaine L, Mitchell MP, Staples C, Owens DM, Keenan ID, Dickinson RJ, Storey KG, Keyse SM. Negative-feedback regulation of FGF signalling by DUSP6/MKP-3 is driven by ERK1/2 and mediated by ets factor binding to a conserved site within the *DUSP6/MKP-3* gene promoter. *Biochem J*. 2008;412:287-298

55. Teng CH, Huang WN, Meng TC. Several dual specificity phosphatases coordinate to control the magnitude and duration of JNK activation in signaling response to oxidative stress. *J Biol Chem*. 2007;282:28395-28407

56. Hung CF, Huang TF, Chen BH, Shieh JM, Wu PH, Wu WB. Lycopene inhibits TNF-α-induced endothelial ICAM-1 expression and monocyte-endothelial adhesion. *Eur J Pharmacol*. 2008;586:275-282

57. Maillet M, Purcell NH, Sargent MA, York AJ, Bueno OF, Molkentin JD. DUSP6 (MKP3) null mice show enhanced ERK1/2 phosphorylation at baseline and increased myocyte proliferation in the heart affecting disease susceptibility. *J Biol Chem*. 2008;283:31246-31255

58. Marchi L, Sesti-Costa R, Chedraoui-Silva S, Mantovani B. Comparison of four methods for the isolation of murine blood neutrophils with respect to the release of reactive oxygen and nitrogen species and the expression of immunological receptors. *Comparative Clinical Pathology*. 2014;23:1469-1476

59. Camps M, Chabert C, Muda M, Boschert U, Gillieron C, Arkinstall S. Induction of the mitogen-activated protein kinase phosphatase MKP3 by nerve growth factor in differentiating PC12. *FEBS Lett*. 1998;425:271-276

60. Springer TA. Traffic signals for lymphocyte recirculation and leukocyte emigration: the multistep paradigm. *Cell*. 1994;76:301-314

61. Sun SC, Ganchi PA, Ballard DW, Greene WC. NF-κB controls expression of inhibitor IκBα: Evidence for an inducible autoregulatory pathway. *Science*. 1993;259:1912-1915

62. Nichols A, Camps M, Gillieron C, Chabert C, Brunet A, Wilsbacher J, Cobb M, Pouyssegur J, Shaw JP, Arkinstall S. Substrate recognition domains within extracellular signal-regulated kinase mediate binding and catalytic activation of mitogen-activated protein kinase phosphatase-3. *J Biol Chem*. 2000;275:24613-24621

63. Cohen J. The immunopathogenesis of sepsis. *Nature*. 2002;420:885-891

64. Scott DW, Vallejo MO, Patel RP. Heterogenic endothelial responses to inflammation: role for differential N-glycosylation and vascular bed of origin. *J Am Heart Assoc*. 2013;2:e000263

65. Horgan MJ, Palace GP, Everitt JE, Malik AB. TNF-α release in endotoxemia contributes to neutrophil-dependent pulmonary edema. *Am J Physiol*. 1993;264:H1161-1165

66. Privratsky JR, Newman PJ. PECAM-1: Regulator of endothelial junctional integrity. *Cell Tissue Res*. 2014;355:607-619

67. Solan JL, Marquez-Rosado L, Sorgen PL, Thornton PJ, Gafken PR, Lampe PD. Phosphorylation at S365 is a gatekeeper event that changes the structure of Cx43 and prevents down-regulation by PKC. *J Cell Biol*. 2007;179:1301-1309

68. Ilan N, Cheung L, Pinter E, Madri JA. Platelet-endothelial cell adhesion molecule-1 (CD31), a scaffolding molecule for selected catenin family members whose binding is mediated by different tyrosine and serine/threonine phosphorylation. *J Biol Chem*. 2000;275:21435-21443

69. Marquez-Rosado L, Solan JL, Dunn CA, Norris RP, Lampe PD. Connexin43 phosphorylation in brain, cardiac, endothelial and epithelial tissues. *Biochim Biophys Acta*. 2012;1818:1985-1992

70. Tsang H, Leiper J, Hou Lao K, Dowsett L, Delahaye MW, Barnes G, Wharton J, Howard L, Iannone L, Lang NN, Wilkins MR, Wojciak-Stothard B. Role of asymmetric methylarginine and connexin 43 in the regulation of pulmonary endothelial function. *Pulm Circ*. 2013;3:675-691

71. Chang SF, Chen LJ, Lee PL, Lee DY, Chien S, Chiu JJ. Different modes of endothelial-smooth muscle cell interaction elicit differential β-catenin phosphorylations and endothelial functions. *Proc Natl Acad Sci U S A*. 2014;111:1855-1860

72. Eblaghie MC, Lunn JS, Dickinson RJ, Munsterberg AE, Sanz-Ezquerro JJ, Farrell ER, Mathers J, Keyse SM, Storey K, Tickle C. Negative feedback regulation of FGF signaling levels by Pyst1/MKP3 in chick embryos. *Curr Biol*. 2003;13:1009-1018

73. Kawakami Y, Rodriguez-Leon J, Koth CM, Buscher D, Itoh T, Raya A, Ng JK, Esteban CR, Takahashi S, Henrique D, Schwarz MF, Asahara H, Izpisua Belmonte JC. MKP3 mediates the cellular response to FGF8 signalling in the vertebrate limb. *Nat Cell Biol*. 2003;5:513-519

74. Van Lint J, Agostinis P, Vandevoorde V, Haegeman G, Fiers W, Merlevede W, Vandenheede JR. Tumor necrosis factor stimulates multiple serine/threonine protein kinases in swiss 3T3 and L929 cells. Implication of casein kinase-2 and extracellular signal-regulated kinases in the tumor necrosis factor signal transduction pathway. *J Biol Chem*. 1992;267:25916-25921

75. Hu MC, Tang-Oxley Q, Qiu WR, Wang YP, Mihindukulasuriya KA, Afshar R, Tan TH. Protein phosphatase X interacts with c-Rel and stimulates c-Rel/nuclear

factor κB activity. *J Biol Chem*. 1998;273:33561-33565

76. Zhou G, Mihindukulasuriya KA, MacCorkle-Chosnek RA, Van Hooser A, Hu MC, Brinkley BR, Tan TH. Protein phosphatase 4 is involved in tumor necrosis factor-α-induced activation of c-Jun N-terminal kinase. *J Biol Chem*. 2002;277:6391-6398

77. Wang Q, Chiang ET, Lim M, Lai J, Rogers R, Janmey PA, Shepro D, Doerschuk CM. Changes in the biomechanical properties of neutrophils and endothelial cells during adhesion. *Blood*. 2001;97:660-668

78. Wang Q, Doerschuk CM. Neutrophil-induced changes in the biomechanical properties of endothelial cells: Roles of ICAM-1 and reactive oxygen species. *J Immunol*. 2000;164:6487-6494

79. Doerschuk CM, Winn RK, Coxson HO, Harlan JM. CD18-dependent and -independent mechanisms of neutrophil emigration in the pulmonary and systemic microcirculation of rabbits. *J Immunol*. 1990;144:2327-2333

80. Qin L, Quinlan WM, Doyle NA, Graham L, Sligh JE, Takei F, Beaudet AL, Doerschuk CM. The roles of CD11/CD18 and ICAM-1 in acute *pseudomonas aeruginosa*-induced pneumonia in mice. *J Immunol*. 1996;157:5016-5021

81. Doerschuk CM, Mizgerd JP, Kubo H, Qin L, Kumasaka T. Adhesion molecules and cellular biomechanical changes in acute lung injury: Giles F. Filley lecture. *Chest*. 1999;116:37S-43S

82. Fraser CC. Exploring the positive and negative consequences of NF-κB inhibition for the treatment of human disease. *Cell Cycle*. 2006;5:1160-1163

83. Egan LJ, Toruner M. NF-κB signaling: Pros and cons of altering NF-κB as a therapeutic approach. *Ann N Y Acad Sci*. 2006;1072:114-122

84. Vogt A, Cooley KA, Brisson M, Tarpley MG, Wipf P, Lazo JS. Cell-active dual specificity phosphatase inhibitors identified by high-content screening. *Chemistry & Biology*. 2003;10:733-742

85. Molina G, Vogt A, Bakan A, Dai W, Queiroz de Oliveira P, Znosko W, Smithgall TE, Bahar I, Lazo JS, Day BW, Tsang M. Zebrafish chemical screening reveals an inhibitor of Dusp6 that expands cardiac cell lineages. *Nat Chem Biol*. 2009;5:680-687

86. Newman PJ, Newman DK. Signal transduction pathways mediated by PECAM-1: New roles for an old molecule in platelet and vascular cell biology. *Arterioscler Thromb Vasc Biol*. 2003;23:953-964

87. TenBroek EM, Lampe PD, Solan JL, Reynhout JK, Johnson RG. Ser364 of connexin43 and the upregulation of gap junction assembly by cAMP. *J Cell Biol*. 2001;155:1307-1318

APPENDIX

List of identified phosphoproteins altered in DUSP6-ablated HUVECs

Leading Proteins	Protein Names	Gene Names	Uniprot	PhosphoSTY (STY) Probabilities	PTM Score	Ratio H/L	Intensity
IPI00418471	Vimentin	VIM	P08670	S(1)RLGDLYEEEMR	78.875	7.9152	723180
IPI00010800	Nestin	NES	P48681	S(1)LDQEIARPLENENQEFLK	70.439	5.1826	477970
IPI00018195	MAPK3	MAPK3	P27361	IADPEHDHTGFLT(0.012)EY(0.986)VAT(0.002)R	105.65	3.8955	336450
IPI00003479	MAPK1	MAPK1	P28482	VADPDHDHTGFLT(0.002)EY(0.987)VAT(0.011)R	95.966	3.8053	1277700
IPI00220827	Thymosin beta-10	TMSB10	P63313	ADKPDMGEIAS(1)FDK	101.53	3.719	699840
IPI00215893	Heme oxygenase 1	HMOX1	P09601	DQS(0.954)PS(0.046)RAPGLR	69.667	3.5229	10886000
IPI00021812	Neuroblast differentiation-associated protein AHNAK	AHNAK	Q09666	LKS(1)EDGVEGDLGETQSR	121.34	2.7094	359820
IPI00171798	Metastasis-associated protein MTA2	MTA2	O94776	GHLSRPEAQS(0.121)LS(0.872)PY(0.003)T(0.001)T(0.001)S(0.001)ANR	82.295	2.5995	58680
IPI00044371	WD repeat-containing protein 44	WDR44	Q5JSH3-1	S(0.804)NS(0.155)GRELT(0.041)DEEILASVMIK	69.159	2.564	51817
IPI00008274	Adenylyl cyclase-associated protein 1	CAP1	Q01518-1	PFSAPKPQT(0.909)S(0.09)PS(0.001)PK	114.1	2.3664	59987
IPI00023503	Cell division protein kinase 3	CDK3	Q00526	IGEGT(0.001)Y(0.999)GVVYK	137.54	2.313	1015900
IPI00002804	Serine/threonine-protein kinase N2	PKN2	Q16513	AS(0.123)S(0.877)LGEIDESSELR	76.09	2.3019	173280
IPI00295618	Platelet endothelial cell adhesion molecule	PECAM1	P16284-1	DTETVY(0.995)S(0.005)EVRK	81.616	2.2931	212560
IPI00021267	Ephrin type-A receptor 2	EPHA2	P29317	QS(0.002)PEDVY(0.987)FS(0.011)K	62.998	2.2448	124430
IPI00784262	Serine/threonine-protein kinase receptor R3	ACVRL1	B4DPT9	GLHSELGES(0.948)S(0.052)LILK	114.1	2.2057	52715
IPI00010800	Nestin	NES	P48681	S(0.104)LRS(0.896)LEEQDQETLR	101.53	2.1597	1320000
IPI00015077	Eukaryotic translation initiation factor 1	EIF1	P41567	S(0.985)AIQNLHS(0.012)FDPFADAS(0.003)K	97.956	2.048	26018
IPI00021267	Ephrin type-A receptor 2	EPHA2	P29317	QSPEDVY(0.001)FS(0.999)K	62.998	2.0097	115440
IPI00942269	TBC1 domain family member 4	TBC1D4	C9JFI1	RSLTS(0.001)S(0.999)LENIFSR	104.43	2.0054	19898
IPI00012545	Trans-Golgi network integral membrane protein 2	TGOLN2	O43493-1	DS(0.115)PS(0.751)KS(0.019)S(0.115)AEAQTPEDTPNK	69.159	1.9625	44272
IPI00306840	Sphingosine-1-phosphate phosphatase 1	SGPP1	Q9BX95	RNS(0.994)LT(0.006)GEEGQLAR	82.955	1.9245	350330
IPI00744851	High mobility group protein HMG-I/HMG-Y	HMGA1	B4DWA0	KQPPVSPGT(0.004)ALVGS(0.995)QKEPS(0.001)EVPTPK	96.484	1.8938	2611200
IPI00295618	Platelet endothelial cell adhesion molecule	PECAM1	P16284-1	EPLNS(0.147)DVQY(0.823)T(0.029)EVQVSSAESHK	62.185	1.8389	299400
IPI00180404	Nexilin	NEXN	Q0ZGT2-1	RAEQIEDINNT(0.801)GT(0.033)ES(0.158)AS(0.007)EEGDDSLLITVVPVK	80.761	1.7835	101160
IPI00008274	Adenylyl cyclase-associated protein 1	CAP1	Q01518-1	PFSAPKPQT(0.003)S(0.968)PS(0.028)PK	114.1	1.7655	67995
IPI00010800	Nestin	NES	P48681	S(1)LGEEIQESLK	97.769	1.7339	717740
IPI00922610	Paxillin	PXN	B3KVL0	PGSQLDSMLGS(1)LQSDLNK	140.37	1.7083	260070
IPI00024579	E3 ubiquitin-protein ligase RAD18	RAD18	Q9NS91	NDLQDTEIS(1)PR	107.9	1.7064	191690
IPI00012434	MLN64 N-terminal domain homolog	STARD3NL	O95772-1	LLIVQDAS(1)ER	97.769	1.7036	124810
IPI00856116	Palladin	PALLD	Q8WX93-1	IAS(1)DEEIQGTK	104.29	1.7021	70898
IPI00008965	Transcription factor AP-1	JUN	P05412	NSDLLT(0.001)S(0.999)PDVGLLK	186.77	1.6877	546550
IPI00015077	Eukaryotic translation initiation factor 1	EIF1	P41567	SAIQNLHS(1)FDPFADASK	97.956	1.6859	82326
IPI00409590	LIM domain only protein 7	LMO7	Q8WWI1-1	VTTEIQLPS(0.107)QS(0.893)PVEEQSPASLSSLR	123.3	1.6371	2419990
IPI00295618	Platelet endothelial cell adhesion molecule	PECAM1	P16284-1	DTETVY(0.94)S(0.06)EVRK	81.616	1.6292	58315
IPI00044371	WD repeat-containing protein 44	WDR44	Q5JSH3-1	ELSDQAT(0.005)AS(0.995)PIVAR	101.53	1.6248	261830
IPI00647185	Centrosomal protein 170kDa	CEP170	B1ARM6	ARLGEAS(0.992)DS(0.008)ELADADK	101.53	1.6106	371160
IPI00737545	Tyrosine-protein kinase SgK269	SGK269	Q9H792	ANTLS(1)PVR	88.753	1.609	64919
IPI00743594	Actin-binding protein anillin	ANLN	B4DSL6	AAS(0.969)PPRPLLS(0.031)NASATPVGR	61.011	1.5967	562870
IPI00022349	Nuclear fragile X mental retardation-interacting protein 2	NUFIP2	Q72417	DYEIESQNPLAS(0.996)PT(0.004)NTLLGSAK	166.57	1.5883	270800
IPI00171636	Neuron navigator 1	NAV1	Q8NEY1-1	AVALDS(0.003)DNIS(0.997)LK	88.268	1.5869	1228840
IPI00023605	Cdc42 effector protein 1	CDC42EP1	Q00587-1	RSDS(1)LLSFR	110.05	1.5867	244110
IPI00007935	PDZ and LIM domain protein 5	PDLIM5	Q96HC4	YTEFY(1)HVPTHSDASK	87.563	1.5837	194530
IPI00185027	Arginine-glutamic acid dipeptide repeats protein	RERE	Q9P2R6-1	KQPAS(1)PDGRT(0.874)S(0.127)PINEDIR	71.758	1.5777	160940
IPI00185027	Arginine-glutamic acid dipeptide repeats protein	RERE	Q9P2R6-1	KQPAS(1)PDGRT(0.874)S(0.127)PINEDIR	71.758	1.5777	160940
IPI00902708	Phosphatase and actin regulator 2	PHACTR2	Q5T4W4	ASIANSDGPTAGSQT(1)PPFK	146.92	1.5769	128690
IPI00332106	Pre-B-cell leukemia transcription factor-interacting protein 1	PBXIP1	Q6AQ6-1	ALQAPHS(0.995)PS(0.005)K	74.948	1.5752	51163

1

List of identified phosphoproteins altered in DUSP6-ablated HUVECs (continuous)

Leading Proteins	Protein Names	Gene Names	Uniprot	PhosphoSTY (STY) Probabilities	PTM Score	H/L Normalized	Intensity
IPI00604620	Nucleolin	NCL	P19338	VVVS(0.993)PT(0.007)KK	88.753	1.5741	3335000
IPI00647185	Centrosomal protein 170kDa	CEP170	B1ARM6	LGSLSARS(0.914)DS(0.085)EATISR	80.533	1.5736	1129300
IPI00217467	Histone H1.4	HIST1H1E	P10412	SETAPAAPAAPAPAEKT(1)PVK	141.09	1.5599	632360
IPI00418169	Annexin A2	ANXA2	P07355-2	LSLEGDHSTPPS(0.054)AY(0.946)GSVK	140.37	1.5485	262900
IPI00009236	Caveolin-1	CAV1	Q03135-1	YVDS(0.002)EGHLY(0.897)T(0.101)VPIR	73.06	1.5394	133370
IPI00942869	Catenin delta-1	CTNND1	O60716-1	VGGS(0.002)S(0.998)VDLHR	74.948	1.5305	4674800
IPI00009946	Mitochondrial import receptor subunit TOM34	TOMM34	Q15785	NRVPS(1)AGDVEK	91.202	1.5227	148380
IPI00218487	Gap junction alpha-1 protein	GJA1	P17302	LAAGHELQPLAIVDQRPS(0.178)S(0.822)R	64.385	1.5225	360230
IPI00219841	DNA ligase 1	LIG1	P18858	RTIQEVIEEQS(1)EDEDREAK	86.649	1.5176	367310
IPI00924510	Telomere-associated protein RIF1	RIF1	C9JI70	RSQEDEIS(0.06)S(0.94)PVNK	94.905	1.51	47074
IPI00472160	Rho guanine nucleotide exchange factor 2	ARHGEF2	Q92974-2	ERPS(0.078)S(0.921)AIY(0.001)PSDSFR	78.251	1.5095	169740
IPI00014340	Protein phosphatase 1 regulatory subunit 12C	PPP1R12C	Q9BZL4-1	S(1)PVQLEEAPSR	104.29	0.7064	104110
IPI00028276	RING finger protein unkempt homolog	UNK	Q9C0B0	NSSLGSPSNLCGS(0.993)PPGS(0.007)IR	89.474	0.70545	110530
IPI00030131	Lamina-associated polypeptide 2, isoforms beta/gamma	TMPO	P42167-1	GPPDFSS(0.001)DEEREPT(0.995)PVLGS(0.004)GAAAAGR	109.69	0.70452	1279200
IPI00955022	cDNA FLJ53324, highly similar to Tight junction protein ZO-2	TJP2	B7Z2R8	DNS(1)PPPAFKPEPPK	91.447	0.70299	1454600
IPI00217051	Neuron navigator 3	NAV3	Q8IVL0-1	KT(0.064)S(0.935)LDGSQNQDDVVLHVSSK	175.05	0.70178	160850
IPI00399265	Tumor protein D52-like 2	TPD52L2	Q5IWU6	GLLS(0.006)DS(0.921)MT(0.073)DVPVDTGVAAR	111.07	0.70153	158490
IPI00797384	La-related protein 4	LARP4	Q71RC2-4	DGLNQTTIPVS(0.986)PPS(0.005)T(0.005)T(0.005)K	121.34	0.69828	212570
IPI00219301	Myristoylated alanine-rich C-kinase substrate	MARCKS	P29966	EAPAEGEAAEPGSPTAAEGEAASAAS(0.001)S(0.005)T(0.024)S(0.138)S(0.832)PK	103.42	0.69769	264160
IPI00022033	Rab11 family-interacting protein 5	RAB11FIP5	Q9BXF6	PLSAAPVEGS(1)PDRK	78.251	0.69754	507680
IPI00218845	Nitric oxide synthase, endothelial	NOS3	P29474	LQGRPS(1)PGPPAPEQLLSQAR	139	0.6961	196720
IPI00645608	Interferon regulatory factor 2-binding protein 1	IRF2BP1	Q8IU81	NVAEALGHS(1)PK	94.358	0.69573	133390
IPI00395463	Charged multivesicular body protein 7	CHMP7	Q8WUX9	IS(1)DAELEAELEK	138.98	0.69531	98946
IPI00008868	Microtubule-associated protein 1B	MAP1B	P46821	S(0.91)PS(0.087)LS(0.003)PSPPSPLEK	127.3	0.69448	181650
IPI00744851	High mobility group protein HMG-I/HMG-Y	HMGA1	B4DWA0	QPPVS(0.849)PGT(0.149)ALVGS(0.003)QK	96.484	0.69134	106510
IPI00152151	Protein FAM122B	FAM122B	Q7Z309-3	RIDFTPVS(1)PAPS(0.996)PT(0.004)R	117.63	0.69053	159150
IPI00152151	Protein FAM122B	FAM122B	Q7Z309-3	RIDFTPVS(1)PAPS(0.996)PT(0.004)R	117.63	0.69053	159150
IPI00941001	Phosphoacetylglucosamine mutase	PGM3	O95394	STIGVMVT(0.004)AS(0.996)HNPEEDNGVK	141.09	0.68993	1934600
IPI00515115	Putative uncharacterized protein ABLIM1	ABLIM1	A6NCD9	DCLCQLCAQPMSS(0.053)S(0.946)PK	127.24	0.68912	126030
IPI00915356	Cleavage and polyadenylation specificity factor subunit 7	CPSF7	Q8N684-3	DSSDS(0.031)ADGRAT(0.936)PS(0.031)ENLVPSSAR	66.648	0.68864	152110
IPI00377245	Histone-lysine N-methyltransferase MLL2	MLL2	O14686-3	ALS(1)PVIPLIPR	81.616	0.68702	56175
IPI00061087	Protein FAM122A	FAM122A	Q96E09	S(0.163)NS(0.837)APLIHGLSDTSPVFQAEAPSAR	96.484	0.68637	369240
IPI00641076	Mothers against decapentaplegic homolog 2	SMAD2	Q15796-1	SSILPFT(1)PPVVK	76.318	0.68614	38227
IPI00641076	cDNA FLJ56056	FAM65A	B4DEQ9	RFS(0.002)TYS(0.002)QS(0.995)PPDTPSLR	82.241	0.68581	412140
IPI00792422	Protein FAM21A	FAM21A	Q641Q2-1	RT(0.862)PS(0.138)DDEEDNLFAPPK	172.28	0.68452	166190
IPI00306087	Telomerase Cajal body protein 1	WDR79	Q9BUR4	VFPEPT(0.83)ES(0.17)GDEGEELGLPLLSTR	63.49	0.68301	142510
IPI00941977	ZYX protein	ZYX	Q9BUS0	LGHPEALS(0.113)AGT(0.113)GS(0.774)PQPPSFTYAQQR	96.484	0.68006	352090
IPI00398347	Protein Ag2 homolog	AG2	Q727L8	SFLQS(1)LECLR	87.769	0.67961	38524
IPI00211048	Myoferlin	MYOF	Q9NZM1-1	GPVGT(0.06)VS(0.94)EAQLAR	94.905	0.6771	311210
IPI00399265	Tumor protein D52-like 2	TPD52L2	Q5IWU6	MDSAGQDINLNS(1)PNK	147.5	0.67581	282700
IPI00792422	Protein FAM21A	FAM21A	Q641Q2-1	TVLS(1)LFDEEEDK	85.526	0.67444	28418
IPI00329147	Coiled-coil domain-containing protein 43	CCDC43	Q96MW1	AALLAQYADVT(1)DEEDEADEK	193.27	0.6744	137850
IPI00219301	Myristoylated alanine-rich C-kinase substrate	MARCKS	P29966	EEPAAAGSGAAS(0.946)PS(0.054)AAEK	140.37	0.67219	42191
IPI00749429	Protein tweety homolog 3	TTYH3	Q9C0H2-1	YLATSQPRPDS(0.006)S(0.068)GS(0.927)H	96.193	0.67176	306300
IPI00792743	SAFB-like transcription modulator	SLTM	Q9NWH9	AGAGMITQHSSNAS(1)PINR	104.52	0.67059	92946
IPI00410666	Protein LAP4	SCRIB	Q14160-3	RSEACPCQPDS(0.086)GS(0.914)PLPAEEEK	134.89	0.66915	139210

List of identified phosphoproteins altered in DUSP6-ablated HUVECs (continuous)

Leading Proteins	Protein Names	Gene Names	Uniprot	PhosphoSTY (STY) Probabilities	PTM Score	H/L Normalized	Intensity
IPI00216047	SWI/SNF complex subunit SMARCC2	SMARCC2	Q8TAQ2-1	DMDEPS(1)PVPNVEEVTLPK	176.78	0.66879	418480
IPI00337397	Nuclear pore complex protein Nup98-Nup96	NUP98	P52948-5	PAPPQS(0.06)QS(0.94)PEVEQLGR	121.34	0.66857	169810
IPI00514856	Ubiquitin-associated protein 2-like	UBAP2L	Q14157-2	SPAVATSTAAPPPS(0.093)S(0.896)PLPS(0.011)K	92.082	0.66776	*380000
IPI00396171	Microtubule-associated protein 4	MAP4	P27816-1	PTLLANGGHGVEGSDT(0.004)T(0.024)GS(0.948)PT(0.024)EFLEEK	97.159	0.66635	95575
IPI00217051	Neuron navigator 3	NAV3	Q8IVL0-1	IGS(0.003)GRS(0.113)S(0.884)PVTVNQTDK	102.8	0.66532	101280
IPI00030131	Lamina-associated polypeptide 2, isoforms beta/gamma	TMPO	P42167-1	S(0.09)S(0.043)T(0.867)PLTISSSAENTR	140.28	0.6626	1062200
IPI00017184	EH domain-containing protein 1	EHD1	Q9H4M9	DKPTYDEIFYT(0.011)LS(0.989)PVNGK	83.047	0.66238	18520
IPI00025428	B-cell lymphoma 3-encoded protein	BCL3	P20749	ATRPAS(0.015)T(0.015)SQPDPS(0.969)PDR	78.538	0.66212	55298
IPI00295502	Protein Wiz	WIZ	O95785-1	SPQLS(0.009)LS(0.991)PRPAS(1)PK	76.09	0.66194	76547
IPI00295502	Protein Wiz	WIZ	O95785-1	SPQLS(0.009)LS(0.991)PRPAS(1)PK	76.09	0.66194	76547
IPI00032064	A-kinase anchor protein 2	AKAP2	Q9Y2D5-4	VKPPPS(0.951)PT(0.024)T(0.024)EGPS(0.001)LQPDLAPEEAAGTQRPK	86.8	0.66185	435360
IPI00304589	182 kDa tankyrase-1-binding protein	TNKS1BP1	Q9C0C2-1	TEAQDLCRAS(1)PEPPGPESSSR	134.89	0.66076	285660
IPI00941170	E3 ubiquitin-protein ligase NEDD4-like	NEDD4L	Q96PU5-8	S(0.951)LS(0.045)S(0.004)PTVTLSAPLEGAK	100.32	0.66072	188460
IPI00001600	PAXIP1-associated protein 1	PA1	Q9BTK6	DLFSLDSEDPSPAS(1)PPLR	166.7	0.66012	91353
IPI00032970	Oxysterol-binding protein-related protein 11	OSBPL11	Q8NBX4	RPS(1)QNAISFFNVGHSK	135.71	0.65818	205200
IPI00171407	Syntaxin-binding protein 5	STXBP5	Q5T5C0-1	KLS(0.988)LPT(0.012)DLKPDLDVK	87.563	0.6509	139740
IPI00183118	MAP/microtubule affinity-regulating kinase 3	MARK3	P27448-1	LDT(0.997)FCGS(0.003)PPYAAPELFQGK	69.772	0.65061	62493
IPI00008868	Microtubule-associated protein 1B	MAP1B	P46821	DVMS(0.854)DET(0.145)NNEETESPSQEFVNITK	188.81	0.64977	82200
IPI00006865	Vesicle-trafficking protein SEC22b	SEC22B	O75396	NLGS(1)INTELQDVQR	127.3	0.64395	138280
IPI00289776	Probable E3 ubiquitin-protein ligase MYCBP2	MYCBP2	O75592-1	S(0.96)LS(0.04)PNHNTLQTLK	85.526	0.64244	227620
IPI00645192	Methyl-CpG-binding protein 2	MECP2	P51608-2	AETSEGGSAPAVPEASAS(1)PK	160.03	0.64085	1113150
IPI00006538	Phosphatidylserine synthase 2	PTDSS2	Q9BVG9	DAGGPRPES(1)PVPAGR	74.039	0.63959	190400
IPI00306369	tRNA (cytosine-5-)-methyltransferase NSUN2	NSUN2	Q08J23	AGEPNS(1)PDAEEANSPDVTAGCDPAGVHPPR	102.48	0.63586	294390
IPI00941001	Phosphoacetylglucosamine mutase	PGM3	O95394	STIGVMVT(0.868)AS(0.132)HNPEEDNGVK	141.09	0.63579	361850
IPI00145805	TRAF2 and NCK-interacting protein kinase	TNIK	Q9UKE5-1	QNS(1)DFTSENPPLPTR	147.5	0.63394	209190
IPI00792423	Mediator of RNA polymerase II transcription subunit 24	MED24	O75448	LLS(1)SNEDDANILSSPTDR	166.7	0.63374	65623
IPI00218035	Nuclear factor 1	NFIC	B5MDB4	S(0.999)PFNS(0.001)PSPQDSPR	145.18	0.63053	79323
IPI00418169	Annexin A2	ANXA2	P07355-2	LS(0.999)LEGDHS(0.001)TPPSAYGSVK	140.37	0.62972	122880
IPI00218696	Caldesmon	CALD1	Q05682-4	GNVFSSPTAAGT(1)PNK	120.67	0.62751	213440
IPI00955022	Tight junction protein ZO-2	TJP2	B7Z2R8	PSTPIPPQEGEEVGES(0.813)S(0.187)EEQDNAPK	71.274	0.62689	521910
IPI00289357	Serine/threonine-protein kinase ULK1	ULK1	O75385	T(0.017)PS(0.972)S(0.011)QNLLALLAR	80.535	0.62114	55544
IPI00954819	cDNA FLJ75213		A8K1U6	LQINS(1)PPFDQPMSR	101.53	0.61278	82444
IPI00292570	Rab effector MyRIP	MYRIP	Q8NFW9	S(0.962)VDRLDET(0.038)NLAPVLQSPDGNWVALK	73.385	0.60926	57065
IPI00290461	Eukaryotic translation initiation factor 3 subunit J	EIF3J	O75822	AAAAAAGDS(0.968)DS(0.032)WDADAFSVEDPVRK	157.03	0.60485	1033200
IPI00465123	KIAA0415 gene product	KIAA0415	A4D1Z4	S(0.999)APAS(0.913)PT(0.088)HPGLMSPR	74.039	0.60316	518230
IPI00465123	KIAA0415 gene product	KIAA0415	A4D1Z4	S(0.999)APAS(0.913)PT(0.088)HPGLMSPR	74.039	0.60316	518230
IPI00419979	Serine/threonine-protein kinase PAK 2	PAK2	Q13177	GTEAPAVVT(0.988)EEEDDDEET(0.012)APPVIAPRPDHTK	69.482	0.60188	45597
IPI00336047	Myosin-IXb	MYO9B	Q13459-1	RTS(1)FSTSDVSK	107.9	0.60065	335170
IPI00021766	Reticulon-4	RTN4	Q9NQC3-1	RRGS(0.12)S(0.12)GS(0.759)VDET(0.001)LFALPAASEPVIR	83.606	0.59763	355120
IPI00021812	Neuroblast differentiation-associated protein AHNAK	AHNAK	Q09666	GPSLDIDT(1)PDVNIEGPEGK	186.93	0.59315	190650
IPI00291800	Eukaryotic translation initiation factor 4E transporter	EIF4ENIF1	Q9NRA8-1	APS(1)PPLSQVFQTR	82.955	0.59258	98731
IPI00015805	Ras-interacting protein 1	RASIP1	Q5U651	GGS(0.998)PAPY(0.002)VDTFLNAPDILPR	166.3	0.5925	180920
IPI00019870	Caveolin-2	CAV2	P51636-1	ADVQLFMDDDS(0.028)Y(0.028)S(0.826)HHS(0.826)GLEY(0.292)ADPEK	63.932	0.591	253150
IPI00472160	Rho guanine nucleotide exchange factor 2	ARHGEF2	Q92974-2	EPALPLEPDSGGNT(0.02)S(0.98)PGVTANGEAR	105.14	0.5887	225530
IPI00179172	Liprin-beta-1	PPFIBP1	Q86W92-2	LT(0.011)PKPET(0.18)S(0.807)FFEENDGNILLGAT(0.001)VDTQLCDK	61.089	0.58768	135650
IPI00026317	Zinc finger and BTB domain-containing protein 7A	ZBTB7A	O95365	VRGGAPDPSPGATATPGAPAQPS(0.156)S(0.844)PDAR	78.006	0.57779	45864

3

List of identified phosphoproteins altered in DUSP6-ablated HUVECs (continuous)

Leading Proteins	Protein Names	Gene Names	Uniprot	PTM Score	PhosphoSTY (STY) Probabilities	H/L Normalized	Intensity
IPI00296485	Microtubule-associated protein 1S	MAP1S	Q66K74	62.185	FLREPVVTPQDLEGPGRAES(1)K	0.57778	434950
IPI00418471	Vimentin	VIM	P08670	98.788	SLYAS(0.107)S(0.893)PGGVYATR	0.57557	74422
IPI00742743	Tumor suppressor p53-binding protein 1	TP53BP1	Q12888-2	114.2	MVIQGPS(0.037)S(0.963)PQGEAMVT(0.001)DVLEDQK	0.57476	672240
IPI00102425	Regulation of nuclear pre-mRNA domain-containing protein 1A	RPRD1A	Q96P16-1	75.589	VDENENCS(0.001)S(0.001)LGS(0.967)PS(0.03)EPPQTLDLVR	0.56895	131160
IPI00012268	26S proteasome non-ATPase regulatory subunit 2	PSMD2	Q13200	122.57	APVQPQQS(1)PAAAPGGTDEK	0.5676	275690
IPI00336047	Myosin-IXb	MYO9B	Q13459-1	80.533	VSPPAPGS(0.999)APET(0.001)PEDK	0.56642	72142
IPI00032355	Pumilio homolog 1 (Drosophila)	PUM1	Q5T1Z8	76.318	RDS(0.918)LT(0.069)GS(0.006)S(0.006)DLYK	0.56088	227360
IPI00301609	Serine/threonine-protein kinase Nek9	NEK9	Q8TD19	67.915	VASEAPLEHKPQVEAS(0.169)S(0.831)PR	0.55734	312040
IPI00012462	Eukaryotic translation initiation factor 2A	EIF2A	C9JWR7	104.52	S(1)PDLAPTPAPQSTPR	0.5542	298770
IPI00643722	AT-rich interactive domain-containing protein 1A	ARID1A	O14497-1	76.632	GPS(0.906)PS(0.093)PVGSPASVAQSR	0.54894	207380
IPI00304589	182 kDa tankyrase-1-binding protein	TNKS1BP1	Q9C0C2-1	70.049	PAQLGT(0.859)QRS(0.141)QEADVQDWEFRK	0.54399	130730
IPI00339277	SAM domain-containing protein SAMSN-1	SAMSN1	Q9NSI8-1	87.769	RSSS(1)FGNFDR	0.54372	201960
IPI00855785	Fibronectin	FN1	P02751-15	101.03	TNTNVNCPIECFMPLDVQADREDS(1)RE	0.54201	170570
IPI00914890	Microtubule-associated serine/threonine-protein kinase 4	MAST4	O15021-5	104.29	S(1)AGNIPLSPLAR	0.53949	1222880
IPI00218035	Nuclear factor 1	NFIC	B5MDB4	145.18	SPFNSPS(1)PQDSPR	0.53947	174240
IPI00412441	Wings apart-like protein homolog	WAPAL	Q7Z5K2-3	118.75	VEEESTGDPFGFDS(0.998)DDES(0.002)LLPVSSK	0.53508	77988
IPI00328293	Serine/arginine repetitive matrix protein 1	SRRM1	Q8IYB3-2	128.36	VPKPEPIPEPKEPS(1)PEK	0.53147	1427500
IPI00410666	Protein LAP4	SCRIB	Q14160-3	70.232	QS(0.013)PAS(0.987)PPPLGGGAPVR	0.53045	114250
IPI00027258	Synaptopodin	SYNPO	Q8N3V7-2	100.94	RGS(1)LPAEASCTT	0.53004	353160
IPI00061087	Protein FAM122A	FAM122A	Q96E09	124.22	RIDFIPVS(1)PAPS(0.82)PT(0.18)R	0.52604	321430
IPI00061087	Protein FAM122A	FAM122A	Q96E09	124.22	RIDFIPVS(1)PAPS(0.82)PT(0.18)R	0.52604	321430
IPI00178072	Cytospin-A	CYTSA	Q69YQ0	82.955	RS(0.006)S(0.861)T(0.064)S(0.064)S(0.006)EPTPTVK	0.52517	196760
IPI00555833	Myelin expression factor 2	MYEF2	Q9P2K5-1	83.606	AEVPGAT(0.001)GGDS(0.999)PHLQPAEPPGEPR	0.51377	513640
IPI00552897	Mediator of DNA damage checkpoint protein 1	MDC1	Q14676-1	121.34	LILAEDS(1)EEEVDFLSER	0.50837	72677
IPI00743894	Zinc finger C3H1 domain-containing protein	ZFC3H1	O60293-1	81.616	RIS(0.887)IT(0.057)S(0.057)DILSEK	0.50729	117070
IPI00026156	Hematopoietic lineage cell-specific protein	HCLS1	P14317	154.14	RS(1)PEAPQPV1AMEEPAVPAPLPK	0.49863	107490
IPI00908578	cDNA FLJ51932	C1orf144	B4DQ06	114.1	RILGSAS(1)PEEEQEK	0.49787	56446
IPI00942450	Splicing factor, arginine/serine-rich 15	SFRS15	C9J1W7	98.094	IEIIQPLLDMAAGTSNAAPVAENVT(0.035)NNEGS(0.965)PPPPVK	0.48604	153110
IPI00307820	Heat shock 70 kDa protein 12B	HSPA12B	Q96MM6	132.91	TQESCGIAPLT(1)PS(0.01)QS(0.99)PKPEVR	0.486	149860
IPI00307820	Heat shock 70 kDa protein 12B	HSPA12B	Q96MM6	132.91	TQESCGIAPLT(1)PS(0.01)QS(0.99)PKPEVR	0.486	149860
IPI00296542	E-selectin	SELE	P16581	127.93	FVPASSCQS(1)LESDGSYQK	0.47459	381050
IPI00514311	CTTNBP2 N-terminal-like protein	CTTNBP2NL	Q9P2B4	120.16	FQSQADQDQQASGLQS(0.909)PPS(0.091)R	0.47063	127360
IPI00060181	EF-hand domain-containing protein D2	EFHD2	Q96C19	124.22	ADLNQGIGEPQS(0.995)PS(0.005)R	0.46505	1043300
IPI00007277	Leucine-rich repeat flightless-interacting protein 2	LRRFIP2	Q9Y608-1	65.53	RGS(0.859)GDT(0.047)S(0.047)S(0.047)LIDPDTSLSELRDIYDLK	0.45552	64809
IPI00022033	Rab11 family-interacting protein 5	RAB11FIP5	Q9BXF6	99.711	KY(0.005)DLES(0.029)AS(0.966)AILPSSAIEDPDLGSLGK	0.44665	154180
IPI00745406	C-jun-amino-terminal kinase-interacting protein 4	SPAG9	O60271-1	67.899	ERPISLGIFPLPAGDGLLT(1)PDAQK	0.43748	35076
IPI00794402	Rho GDP-dissociation inhibitor 1	ARHGDIA	P52565	66.929	AEQEPTAEQLAQIAAENEEDEHS(0.949)VNY(0.051)KPPAQK	0.39012	108940
IPI00853219	Rap guanine nucleotide exchange factor 2	RAPGEF2	Q9Y4G8	78.251	DLPPFGINS(1)PQALK	0.38809	77920
IPI00061087	Protein FAM122A	FAM122A	Q96E09	97.159	VSTTT(0.001)DS(0.004)PVS(0.994)PAQAASPFIPLDELSSK	0.36341	44565
IPI00294962	SH3 domain-containing kinase-binding protein 1	SH3KBP1	Q96B97-1	97.824	S(1)IEVENDFLPVEK	0.34508	664590
IPI00304589	182 kDa tankyrase-1-binding protein	TNKS1BP1	Q9C0C2-1	80.533	RFS(0.999)EGVLQS(0.001)PSQDQEK	0.27085	70915
IPI00219301	Myristoylated alanine-rich C-kinase substrate	MARCKS	P29966	140.37	EELQANGSAPAADKEEPA.AAGS(0.828)GAAS(0.145)PS(0.027)AAEK	0.26588	54599
IPI00009737	Ras-related GTP-binding protein D	RRAGD	Q9NQL2-1	141.14	MSPNETLFLES(0.04)IT(0.96)NK	0.20162	4853800
IPI00018889	Zinc finger protein GLI3	GLI3	P10071	60.097	S(0.969)PGRPT(0.031)QGALGEQQDLSNTTSK	0.067803	63511
IPI00186966	Myc box-dependent-interacting protein 1	BIN1	O00499-1	114.75	S(0.008)PS(0.992)PPDGSPAATPEIR	0.065432	330880